INDC(JPN)-166/U

NOT FOR PUBLICATION

PROGRESS REPORT

(July 1992 to June 1993 inclusive)

August 1993

Editor

Y. Nakajima

Japanese Nuclear Data Committee

Japan Atomic Energy Research Institute
Tokai Research Establishment
Tokai-mura, Ibaraki-ken, Japan

Editor's Note

This is a collection of reports which have been submitted to the Japanese Nuclear Data Committee at the committee's request. The request was addressed to the following individuals who might represent or be in touch with groups doing researches related to the nuclear data of interest to the development of the nuclear energy program.

Although the editor tried not to miss any appropriate addressees, there may have been some oversight. Meanwhile, contribution of a report rested with discretion of its author. The coverage of this document, therefore, may not be uniform over the related field or research.

In this progress report, each individual report is generally reproduced as it was received by the JNDC secretariat, and editor also let pass some simple obvious errors in the manuscripts if any.

This edition covers a period of July 1, 1992 to June 30, 1993. The information herein contained is of a nature of "Private Communication". Data contained in this report should not be quoted without the author's permission.

Table of Contents

ELEMENT S	A	QUANTITY	ENERGY MIN	MAX	LAB	TYPE	DOCUMENTATION REF VOL PAGE DATE	COMMENTS
BE	9	A EMISSION	1.4+7		OSA	EXPT-PROG	INDC(JPN)166/U AUG 93	TAKAHASHI+.P69.E-TOF METH.DA/DE,NDG
C	12	EVALUATION	2.0+7	5.0+7	JAE	EVAL-PROG	INDC(JPN)166/U AUG 93	CHIBA+.P28.SIG+DA/DE,OPTMDL+DWBA.NDG
C	12	DIFF ELASTIC	1.4+7		YOK	EXPT-PROG	INDC(JPN)166/U AUG 93	SHIRATO+.P73.DA/DE.OPT PARAMS IN TBL
C	12	DIFF INELAST	1.4+7		YOK	EXPT-PROG	INDC(JPN)166/U AUG 93	SHIRATO+.P73.DA/DE.OPT PARAMS IN TBL
C	12	(N,2N)	2.3+7	3.8+7	TOH	EXPT-PROG	INDC(JPN)166/U AUG 93	SOEWARSONO+.P83.LI7+P SOURCE,FIG
C	12	A EMISSION	1.4+7		OSA	EXPT-PROG	INDC(JPN)166/U AUG 93	TAKAHASHI+.P69.E-TOF METH.DA/DE,NDG
O	16	DIFF ELASTIC	1.4+7		YOK	EXPT-PROG	INDC(JPN)166/U AUG 93	SHIRATO+.P73.DA/DE.OPT PARAMS IN TBL
O	16	DIFF INELAST	1.4+7		YOK	EXPT-PROG	INDC(JPN)166/U AUG 93	SHIRATO+.P73.DA/DE.OPT PARAMS IN TBL
NA	23	(N,2N)	1.8+7	3.8+7	TOH	EXPT-PROG	INDC(JPN)166/U AUG 93	SOEWARSONO+.P83.LI7+P SOURCE,FIG
MG	24	(N,P)	FISS		KTO	EXPT-PROG	INDC(JPN)166/U AUG 93	KOBAYASHI.P42.U233 FISS,SIG=1.40MB
MG	26	(N,NP)	1.3+7	1.5+7	NAG	EXPT-PROG	INDC(JPN)166/U AUG 93	KASUGAI+.P65.ACT-SIG.NDG
AL	27	EVALUATION		1.0+9	JAE	EVAL-PROG	INDC(JPN)166/U AUG 93	FUKAHORI+.P18.PREEQ+STATMDL+SYST.NDG
AL	27	(N,P)	FISS		KTO	EXPT-PROG	INDC(JPN)166/U AUG 93	KOBAYASHI.P42.U233 FISS,SIG=3.87MB
S	32	(N,T)	1.3+7	1.5+7	NAG	EXPT-PROG	INDC(JPN)166/U AUG 93	KASUGAI+.P65.ACT-SIG.NDG
CA		EVALUATION	1.0-5	2.0+7	JAE	EVAL-PROG	INDC(JPN)166/U AUG 93	KOSAKO+.P29.FOR JENDL FUSION FILE
CA	40	DIFF ELASTIC	1.4+7		YOK	EXPT-PROG	INDC(JPN)166/U AUG 93	SHIRATO+.P73.DA/DE.OPT PARAMS IN TBL
CA	40	DIFF INELAST	1.4+7		YOK	EXPT-PROG	INDC(JPN)166/U AUG 93	SHIRATO+.P73.DA/DE.OPT PARAMS IN TBL
TI		EVALUATION	1.0-5	2.0+7	JAE	EVAL-PROG	INDC(JPN)166/U AUG 93	KOSAKO+.P29.FOR JENDL FUSION FILE
TI	46	(N,P)	FISS		KTO	EXPT-PROG	INDC(JPN)166/U AUG 93	KOBAYASHI.P42.U233 FISS,SIG=11.0MB
TI	47	(N,P)	FISS		KTO	EXPT-PROG	INDC(JPN)166/U AUG 93	KOBAYASHI.P42.U233 FISS,SIG=16.6MB

ELEMENT S	A	QUANTITY	ENERGY MIN	MAX	LAB	TYPE	DOCUMENTATION REF VOL PAGE	DATE	COMMENTS
TI	48	(N,P)	FISS		KTO	EXPT-PROG	INDC(JPN)166/U	AUG 93	KOBAYASHI.P42.U233 FISS,SIG=.272MB
CR	53	RESON PARAMS	4.2+3	2.9+4	JAE	EVAL-PROG	INDC(JPN)166/U	AUG 93	MENGONI.P24.E1 WG,VALENCE MDL.TBL
FE		EVALUATION	1.0-5	2.0+7	JAE	EVAL-PROG	INDC(JPN)166/U	AUG 93	KOSAKO+.P29.FOR JENDL FUSION FILE
FE		P EMISSION	1.4+7		OSA	EXPT-PROG	INDC(JPN)166/U	AUG 93	TAKAHASHI+.P69.E-TOF METH.DA/DE,NDG
FE		A EMISSION	1.4+7		TOH	EXPT-PROG	INDC(JPN)166/U	AUG 93	ITO+.P80.DA/DE.PUB JAERI-M93-046,334
FE		A EMISSION	7.1+6	1.1+7	JAE	EXPT-PROG	INDC(JPN)166/U	AUG 93	CHIBA+.P27.DA/DE.GRIDDED IC.NDG
FE		A EMISSION	1.4+7		OSA	EXPT-PROG	INDC(JPN)166/U	AUG 93	TAKAHASHI+.P69.E-TOF METH.DA/DE,NDG
FE	54	(N,P)	FISS		KTO	EXPT-PROG	INDC(JPN)166/U	AUG 93	KOBAYASHI.P42.U233 FISS,SIG=74.4MB
FE	56	DIFF ELASTIC	1.4+7		YOK	EXPT-PROG	INDC(JPN)166/U	AUG 93	SHIRATO+.P73.DA/DE.OPT PARAMS IN TBL
FE	56	DIFF INELAST	1.4+7		YOK	EXPT-PROG	INDC(JPN)166/U	AUG 93	SHIRATO+.P73.DA/DE.OPT PARAMS IN TBL
FE	56	(N,P)	FISS		KTO	EXPT-PROG	INDC(JPN)166/U	AUG 93	KOBAYASHI.P42.U233 FISS,SIG=1.04MB
CO	59	P EMISSION	1.4+7		OSA	EXPT-PROG	INDC(JPN)166/U	AUG 93	TAKAHASHI+.P69.E-TOF METH.DA/DE,NDG
NI		P EMISSION	1.4+7		OSA	EXPT-PROG	INDC(JPN)166/U	AUG 93	TAKAHASHI+.P69.E-TOF METH.DA/DE,NDG
NI		A EMISSION	7.1+6	1.1+7	JAE	EXPT-PROG	INDC(JPN)166/U	AUG 93	CHIBA+.P27.DA/DE.GRIDDED IC.NDG
NI		A EMISSION	1.4+7		TOH	EXPT-PROG	INDC(JPN)166/U	AUG 93	ITO+.P80.DA/DE.PUB JAERI-M93-046,334
NI	58	(N,P)	FISS		KTO	EXPT-PROG	INDC(JPN)166/U	AUG 93	KOBAYASHI.P42.U233 FISS,SIG=101.MB
ZN	64	(N,P)	FISS		KTO	EXPT-PROG	INDC(JPN)166/U	AUG 93	KOBAYASHI.P42.U233 FISS,SIG=33.8MB
GA	71	(N,ALPHA)	1.3+7	1.5+7	NAG	EXPT-PROG	INDC(JPN)166/U	AUG 93	KASUGAI+.P65.ACT-SIG TO META.NDG
ZR		EVALUATION	1.0-5	2.0+7	JAE	EVAL-PROG	INDC(JPN)166/U	AUG 93	KOSAKO+.P29.FOR JENDL FUSION FILE
ZR	90	(N,2N)	FISS		KTO	EXPT-PROG	INDC(JPN)166/U	AUG 93	KOBAYASHI.P42.U233 FISS,SIG=.0807MB

ELEMENT S	A	QUANTITY	ENERGY MIN	MAX	LAB	TYPE	DOCUMENTATION REF	VOL	PAGE	DATE	COMMENTS
NB	93	(N,2N)	FISS		KTO	EXPT-PROG	INDC(JPN)	166/U		AUG 93	KOBAYASHI.P42.U233 FISS,0.44MB TO MS
MO		EVALUATION	1.0-5	2.0+7	JAE	EVAL-PROG	INDC(JPN)	166/U		AUG 93	KOSAKO+.P29.FOR JENDL FUSION FILE
MO		N EMISSION	1.4+7		TOH	EXPT-PROG	INDC(JPN)	166/U		AUG 93	MATSUYAMA+.P79.PUB JAERI-M93-046,345
MO	100	(N,NP)	1.3+7	1.5+7	NAG	EXPT-PROG	INDC(JPN)	166/U		AUG 93	KASUGAI+.P65.ACT-SIG TO META.NDG
MO	98	(N,NP)	1.3+7	1.5+7	NAG	EXPT-PROG	INDC(JPN)	166/U		AUG 93	KASUGAI+.P65.ACT-SIG TO META.NDG
PD	106	(N,NP)	1.3+7	1.5+7	NAG	EXPT-PROG	INDC(JPN)	166/U		AUG 93	KASUGAI+.P65.ACT-SIG TO META.NDG
IN	115	DIFF INELAST	FISS		KTO	EXPT-PROG	INDC(JPN)	166/U		AUG 93	KOBAYASHI.P42.U233 FISS,190MB TO MS
SN	119	(N,P)	1.3+7	1.5+7	NAG	EXPT-PROG	INDC(JPN)	166/U		AUG 93	KASUGAI+.P65.ACT-SIG TO META.NDG
SB	121	RESON PARAMS		5.3+3	JAE	EXPT-PROG	INDC(JPN)	166/U		AUG 93	OHKUBO.P17.188LVLS,D=10.3+-0.5 EV
SB	121	STRNTH FNCTN		5.3+3	JAE	EXPT-PROG	INDC(JPN)	166/U		AUG 93	OHKUBO.P17.SO=(0.24+-0.03)E-4
SB	123	RESON PARAMS		5.3+3	JAE	EXPT-PROG	INDC(JPN)	166/U		AUG 93	OHKUBO.P17.202LVLS,D=20+-1 EV
SB	123	STRNTH FNCTN		5.3+3	JAE	EXPT-PROG	INDC(JPN)	166/U		AUG 93	OHKUBO.P17.SO=(0.25+-0.03)E-4
CS	137	(GAMMA,N)		6.0+7	TOH	EXPT-PROG	INDC(JPN)	166/U		AUG 93	YAMADERA+.P82.BREMSSTRAHLUNG
CE	140	RESON PARAMS		5.0+4	JAE	EXPT-PROG	INDC(JPN)	166/U		AUG 93	OHKUBO.P17.15LVLS,D=3.5+-0.8 KEV
CE	140	STRNTH FNCTN		5.0+4	JAE	EXPT-PROG	INDC(JPN)	166/U		AUG 93	OHKUBO.P17.SO=(1.6+-0.5)E-4
CE	142	RESON PARAMS		5.0+4	JAE	EXPT-PROG	INDC(JPN)	166/U		AUG 93	OHKUBO.P17.38LVLS,D=2.3+-0.2 KEV
CE	142	STRNTH FNCTN		5.0+4	JAE	EXPT-PROG	INDC(JPN)	166/U		AUG 93	OHKUBO.P17.SO=(2.7+-0.6)E-4
ND	144	DIFF INELAST	TR	2.0+7	JAE	EVAL-PROG	INDC(JPN)	166/U		AUG 93	KAWAI+.P30.DWBA AND CC CALC IN FIG
ND	150	DIFF INELAST	TR	2.0+7	JAE	EVAL-PROG	INDC(JPN)	166/U		AUG 93	KAWAI+.P30.DWBA AND CC CALC IN FIG
HF	181	(N,P)	1.3+7	1.5+7	NAG	EXPT-PROG	INDC(JPN)	166/U		AUG 93	KASUGAI+.P65.ACT-SIG.NDG

ELEMENT S	A	QUANTITY	ENERGY MIN	MAX	LAB	TYPE	DOCUMENTATION REF	VOL	PAGE	DATE	COMMENTS
TA	181	(N,2N)	1.3+7	1.5+7	NAG	EXPT-PROG	INDC(JPN)	166/U		AUG 93	KASUGAI+.P65.ACT-SIG.NDG
TA	181	N EMISSION	1.4+7		TOH	EXPT-PROG	INDC(JPN)	166/U		AUG 93	MATSUYAMA+.P79.PUB JAERI-M93-046,345
TA	181	(N,NP)	1.3+7	1.5+7	NAG	EXPT-PROG	INDC(JPN)	166/U		AUG 93	KASUGAI+.P65.ACT-SIG TO META.NDG
TA	181	(N,ALPHA)	1.3+7	1.5+7	NAG	EXPT-PROG	INDC(JPN)	166/U		AUG 93	KASUGAI+.P65.ACT-SIG TO META.NDG
W		N EMISSION	1.4+7		TOH	EXPT-PROG	INDC(JPN)	166/U		AUG 93	MATSUYAMA+.P79.PUB JAERI-M93-046,345
W	182	(N,P)	1.3+7	1.5+7	NAG	EXPT-PROG	INDC(JPN)	166/U		AUG 93	KASUGAI+.P65.ACT-SIG TO META.NDG
W	184	(N,P)	1.3+7	1.5+7	NAG	EXPT-PROG	INDC(JPN)	166/U		AUG 93	KASUGAI+.P65.ACT-SIG.NDG
W	184	(N,ALPHA)	1.3+7	1.5+7	NAG	EXPT-PROG	INDC(JPN)	166/U		AUG 93	KASUGAI+.P65.ACT-SIG.NDG
W	186	(N,2N)	1.3+7	1.5+7	NAG	EXPT-PROG	INDC(JPN)	166/U		AUG 93	KASUGAI+.P65.ACT-SIG.NDG
W	186	(N,P)	1.3+7	1.5+7	NAG	EXPT-PROG	INDC(JPN)	166/U		AUG 93	KASUGAI+.P65.ACT-SIG.NDG
W	186	(N,ALPHA)	1.3+7	1.5+7	NAG	EXPT-PROG	INDC(JPN)	166/U		AUG 93	KASUGAI+.P65.ACT-SIG.NDG
AU	197	(N,XN) X>2	2.8+7	3.8+7	TOH	EXPT-PROG	INDC(JPN)	166/U		AUG 93	SOEWARSONO+.P83.X=4.LI7+P SOURCE,FIG
PB		EVALUATION	1.0-5	2.0+7	JAE	EVAL-PROG	INDC(JPN)	166/U		AUG 93	KOSAKO+.P29.FOR JENDL FUSION FILE
PB		TOTAL	4.0+0	2.2+1	KTO	EXPT-PROG	INDC(JPN)	166/U		AUG 93	SHCHERBAKOV+.P44.LINAC+TOF.FIG GIVEN
PB	208	TOTAL	4.0+0	2.2+1	KTO	EXPT-PROG	INDC(JPN)	166/U		AUG 93	SHCHERBAKOV+.P44.LINAC+TOF.FIG GIVEN
BI		EVALUATION	1.0-5	2.0+7	JAE	EVAL-PROG	INDC(JPN)	166/U		AUG 93	KOSAKO+.P29.FOR JENDL FUSION FILE
U	233	ELASTIC	2.5-2		JAE	EVAL-PROG	INDC(JPN)	166/U		AUG 93	DERRIEN.P19.SIG=11.99 BARNS
U	233	(N,GAMMA)	2.5-2		JAE	EVAL-PROG	INDC(JPN)	166/U		AUG 93	DERRIEN.P19.SIG=45.27 BARNS
U	233	RES INT CAP	5.0-1		JAE	EVAL-PROG	INDC(JPN)	166/U		AUG 93	DERRIEN.P19.RI=130 BARNS
U	233	FISSION	2.5-2		JAE	EVAL-PROG	INDC(JPN)	166/U		AUG 93	DERRIEN.P19.SIG=531.29 BARNS

ELEMENT S	A	QUANTITY	ENERGY MIN	MAX	LAB	TYPE	DOCUMENTATION REF	VOL	PAGE	DATE	COMMENTS
U	233	RES INT FISS	5.0-1		JAE	EVAL-PROG	INDC(JPN)	166/U		AUG 93	DERRIEN.P19.RI=775 BARNS
U	233	RESON PARAMS		1.5+2	JAE	EVAL-PROG	INDC(JPN)	166/U		AUG 93	DERRIEN.P19.R-M ANAL OF TOT, NF, NG
U	235	FISS PROD GS	PILE		NAG	EXPT-PROG	INDC(JPN)	166/U		AUG 93	SHIBATA+.P66.35 GAMMAS FROM PR152
U	235	FISS PROD GS	PILE		NAG	EXPT-PROG	INDC(JPN)	166/U		AUG 93	SHIBATA+.P66.93 GAMMAS FROM PR147
U	237	EVALUATION	1.0-5	2.0+7	JAE	EVAL-PROG	INDC(JPN)	166/U		AUG 93	NAKAGAWA.P21.FOR JENDL-3.2.FIG GIVEN
U	237	TOTAL	1.0-5	2.0+7	JAE	EVAL-PROG	INDC(JPN)	166/U		AUG 93	NAKAGAWA.P21.FOR JENDL-3.2.FIG GIVEN
U	237	ELASTIC	1.0-5	2.0+7	JAE	EVAL-PROG	INDC(JPN)	166/U		AUG 93	NAKAGAWA.P21.FOR JENDL-3.2.FIG GIVEN
U	237	TOT INELAST	TR	2.0+7	JAE	EVAL-PROG	INDC(JPN)	166/U		AUG 93	NAKAGAWA.P21.FOR JENDL-3.2.FIG GIVEN
U	237	(N,GAMMA)	1.0-5	2.0+7	JAE	EVAL-PROG	INDC(JPN)	166/U		AUG 93	NAKAGAWA.P21.FOR JENDL-3.2.FIG GIVEN
U	237	(N,2N)	TR	2.0+7	JAE	EVAL-PROG	INDC(JPN)	166/U		AUG 93	NAKAGAWA.P21.FOR JENDL-3.2.FIG GIVEN
U	237	(N,XN) X>2	TR	2.0+7	JAE	EVAL-PROG	INDC(JPN)	166/U		AUG 93	NAKAGAWA.P21.X=3.FOR JENDL-3.2.FIG
U	237	FISSION	1.0-5	2.0+7	JAE	EVAL-PROG	INDC(JPN)	166/U		AUG 93	NAKAGAWA.P21.FOR JENDL-3.2.FIG GIVEN
U	238	LVL DENSITY	NDG		JAE	EVAL-PROG	INDC(JPN)	166/U		AUG 93	MENGONI.P23.PUB IN JAERI-M92-046,92
NP	236	EVALUATION	1.0-5	2.0+7	JAE	EVAL-PROG	INDC(JPN)	166/U		AUG 93	NAKAGAWA.P21.FOR JENDL-3.2.FIG GIVEN
NP	236	TOTAL	1.0-5	2.0+7	JAE	EVAL-PROG	INDC(JPN)	166/U		AUG 93	NAKAGAWA.P21.FOR JENDL-3.2.FIG GIVEN
NP	236	ELASTIC	1.0-5	2.0+7	JAE	EVAL-PROG	INDC(JPN)	166/U		AUG 93	NAKAGAWA.P21.FOR JENDL-3.2.FIG GIVEN
NP	236	TOT INELAST	TR	2.0+7	JAE	EVAL-PROG	INDC(JPN)	166/U		AUG 93	NAKAGAWA.P21.FOR JENDL-3.2.FIG GIVEN
NP	236	(N,GAMMA)	1.0-5	2.0+7	JAE	EVAL-PROG	INDC(JPN)	166/U		AUG 93	NAKAGAWA.P21.FOR JENDL-3.2.FIG GIVEN
NP	236	(N,2N)	TR	2.0+7	JAE	EVAL-PROG	INDC(JPN)	166/U		AUG 93	NAKAGAWA.P21.FOR JENDL-3.2.FIG GIVEN
NP	236	(N,XN) X>2	TR	2.0+7	JAE	EVAL-PROG	INDC(JPN)	166/U		AUG 93	NAKAGAWA.P21.X=3.FOR JENDL-3.2.FIG

ELEMENT S A	QUANTITY	ENERGY MIN	ENERGY MAX	LAB	TYPE	DOCUMENTATION REF VOL PAGE	DATE	COMMENTS
NP 236	FISSION	1.0-5	2.0+7	JAE	EVAL-PROG	INDC(JPN)166/U	AUG 93	NAKAGAWA.P21.FOR JENDL-3.2.FIG GIVEN
NP 237	(N,GAMMA)	2.5-2		KTO	EXPT-PROG	INDC(JPN)166/U	AUG 93	KOBAYASHI+.P47.154.7+-2.9B,CFD OTHS
NP 237	RES INT CAP	5.0-1		KTO	EXPT-PROG	INDC(JPN)166/U	AUG 93	KOBAYASHI+.P47.646+-55B,CFD OTHS
NP 237	FISSION	1.0+0	5.0+3	KTO	EXPT-PROG	INDC(JPN)166/U	AUG 93	YAMANAKA+.P46.TBP IN JNST
NP 238	EVALUATION	1.0-5	2.0+7	JAE	EVAL-PROG	INDC(JPN)166/U	AUG 93	NAKAGAWA.P21.FOR JENDL-3.2.FIG GIVEN
NP 238	TOTAL	1.0-5	2.0+7	JAE	EVAL-PROG	INDC(JPN)166/U	AUG 93	NAKAGAWA.P21.FOR JENDL-3.2.FIG GIVEN
NP 238	ELASTIC	1.0-5	2.0+7	JAE	EVAL-PROG	INDC(JPN)166/U	AUG 93	NAKAGAWA.P21.FOR JENDL-3.2.FIG GIVEN
NP 238	TOT INELAST	TR	2.0+7	JAE	EVAL-PROG	INDC(JPN)166/U	AUG 93	NAKAGAWA.P21.FOR JENDL-3.2.FIG GIVEN
NP 238	(N,GAMMA)	1.0-5	2.0+7	JAE	EVAL-PROG	INDC(JPN)166/U	AUG 93	NAKAGAWA.P21.FOR JENDL-3.2.FIG GIVEN
NP 238	(N,2N)	TR	2.0+7	JAE	EVAL-PROG	INDC(JPN)166/U	AUG 93	NAKAGAWA.P21.FOR JENDL-3.2.FIG GIVEN
NP 238	(N,XN) X>2	TR	2.0+7	JAE	EVAL-PROG	INDC(JPN)166/U	AUG 93	NAKAGAWA.P21.X=3.FOR JENDL-3.2.FIG
NP 238	FISSION	1.0-5	2.0+7	JAE	EVAL-PROG	INDC(JPN)166/U	AUG 93	NAKAGAWA.P21.FOR JENDL-3.2.FIG GIVEN
PU 241	RESON PARAMS		3.0+2	JAE	EVAL-PROG	INDC(JPN)166/U	AUG 93	DERRIEN.P20.TBP AS JAERI-M
AM 241	FISSION	5.0-2	1.0+4	KTO	EXPT-PROG	INDC(JPN)166/U	AUG 93	KOBAYASHI+.P49.REL U235NF.SIG IN FIG
MANY	EVALUATION	NDG		JAE	EVAL-PROG	INDC(JPN)166/U	AUG 93	KAWAI+.P30.FP'S FOR JENDL-3.2
MANY	LVL DENSITY	NDG		JAE	EVAL-PROG	INDC(JPN)166/U	AUG 93	MENGONI+.P25.FERMI-GAS PARS,A=41-253

The content table in the CINDA format was compiled by the JNDC CINDA group:
S.Chiba(JAERI), M.Kawai(Toshiba), H.Kitazawa(Tokyo Inst. of Tech.),
T.Nakagawa(JAERI), R.Nakasima(Hosei Univ.)

I. Electrotechnical Laboratory

A. Quantum Radiation Division

I-A-1 Characteristics of a Reference 2.413 MeV Neutron Field Measured by Using a Well-defined ^{3}He Gas Proportional Counter

K.Kudo, N.Takeda and A.Fukuda

In measurements of neutron response functions and energy calibration of spectrometers, reference energy points of monoenergetic neutrons which are independent of the bombarding particle energy, target thickness, its age and composition are needed particularly in the case of a low energy accelerator like a Cockcroft-Walton type accelerator. Seagrave first suggested the idea of production of the monoenergetic DD and DT neutrons[1]. Ryves et al. calibrated a Si-SSD and Zr/Nb activation foils with 14.00 MeV neutrons emitted at a special "magic angle" of 96°[2],[3]. We also developed the reference energy of 14.00 MeV and extended this technique to DD neutron field in order to establish another reference energy of 2.413 MeV, emitted to the direction of 100° for the maximum bombarding deuteron energy of 0.3 MeV[4],[5].

For the precise energy measurements of monoenergetic neutrons produced by several nuclear reactions of ^{7}Li(p,n)^{7}Be, T(p,n)^{3}He and D(d,n)^{3}He, ^{3}He gas proportional counters were calibrated at the reference energy of 2.413 MeV. Pulse height spectra corresponding to the monoenergetic neutrons of 2.413 MeV were calculated by a modified NRESP code[6]. Calculated spectrum was folded with a Gaussian distribution and fitted to the experimental response function as shown in Fig.1. While agreement was good in the region of the full energy peak produced by the ^{3}He(n,p)T reaction, both in form and magnitude, it is less satisfactory in the vicinity of a valley just following closely to the lower tail of the full energy peak(see Fig.3).

To improve this discrepancy, we took into account the angular straggling of incident deuterons in a Ti-D target, which may result in an energy spread of the neutrons emitted at a reference angle of 100°, and the effect of secondary neutrons produced in the target assembly. Furthermore, we carefully studied the position dependency of gas multiplication along the central axis in a cylindrical detector (H1819 type manufactured by Reuter-Stokes, USA) by using a thermal neutron beam collimated with 2 mm width. Especially attention was paid to measure the gas multiplication near the both edge parts of the anode wire, since the electric field may be extremely distorted in the vicinity of edge parts and this may affect the shape of the response function. A set of relative gas gain obtained by the experiments was used as input data for the NRESP calculation, as shown in Fig.2. The measured gas

multiplication factor has been normalized to that in the case of the whole area irradiation perpendicular to the detector by a thermal neutron beam.

The response functions have been calculated with the modified NRESP Monte Carlo code for the ^{3}He gas proportional counter having an nominal active length of 15 cm with a diameter of 2.54 cm and containing mixture of ^{3}He gas at 400 kPa and Ar gas at 200 kPa. The neutron source, which is on the axis of the cylindrical detector, was placed at 30 cm apart from the top flat end of the counter.

Calculations were performed by changing the input conditions:

(a)constant gas multiplication within the nominal effective length and no gas multiplication outside the effective length, monoenergetic neutron source of 2.413 MeV and no contribution of secondary neutrons from the target assembly,

(b)position dependent gas multiplication measured by the thermal neutron beam experiments, monoenergetic neutron source of 2.413 MeV and contribution of secondary neutrons from the target assembly calculated by the MCNP Monte Carlo code,

(c)same as the conditions described in (b) except taking into accounts the angular straggling and solid angle spread subtended by the detector.

To illustrate the direct comparison of the agreement between the experiment and the calculation, a simple parameter of χ^2 is introduced to check whether the calculated spectrum is consistent with the experimental one in the fitted region. It is defined as

$$\chi^2 = \sum_{i=1}^{M} \left(N_i^{exp} - N_i^{cal}\right)^2 / N_i^{exp}$$

The pulse height spectra obtained near the full energy peak produced by the ^{3}He(n,p)T reaction are illustrated in Figs.3–5. Figure 3 shows the experimental spectrum(individual points) and the fitted spectrum(solid line) calculated under the condition of (a). While the agreement seems to be not so bad in the region of the full energy peak, the disagreement in the vicinity of a valley can be seen as described previously.

Figure 4 shows the results in the case of taking position dependent gas multiplication, and the secondary neutron effect described in the condition of (b). A remarkable improvement can be seen in the value of χ^2 from 625 to 217.

The final results taking into account all considerable effects including the angular straggling show the fairly good agreement as shown in Fig.5. The χ^2 was further reduced from 217 to 168.

From these comparisons in the referece energy field, we conclude that the angular straggling effect of accelerated deuterons in a target has become observable to some extent by using χ^2 fitting, since the position dependency of gas multiplication along the central axis in the ^{3}He proportional counter has been determined carefully.

References

(1) J.D.Seagrave, LAMS–2162 (1958).

(2) T.B.Ryves et al., Nucl. Instr. and Meth., **167** (1979) 449.

(3) V.E.Lewis et al., Metrologia, **20** (1984) 49.

(4) K.Kudo et al., Nucl. Eng. and Design/Fusion, **10** (1989) 145.

(5) K.Kudo et al., Proceedings of Nuclear Data for Science and Technology held at the Forschungzentrum Jülich, (1991).

(6) X.Yang et al., Bull. of the Electrotechnical Laboratory, **56** (1992) 863.

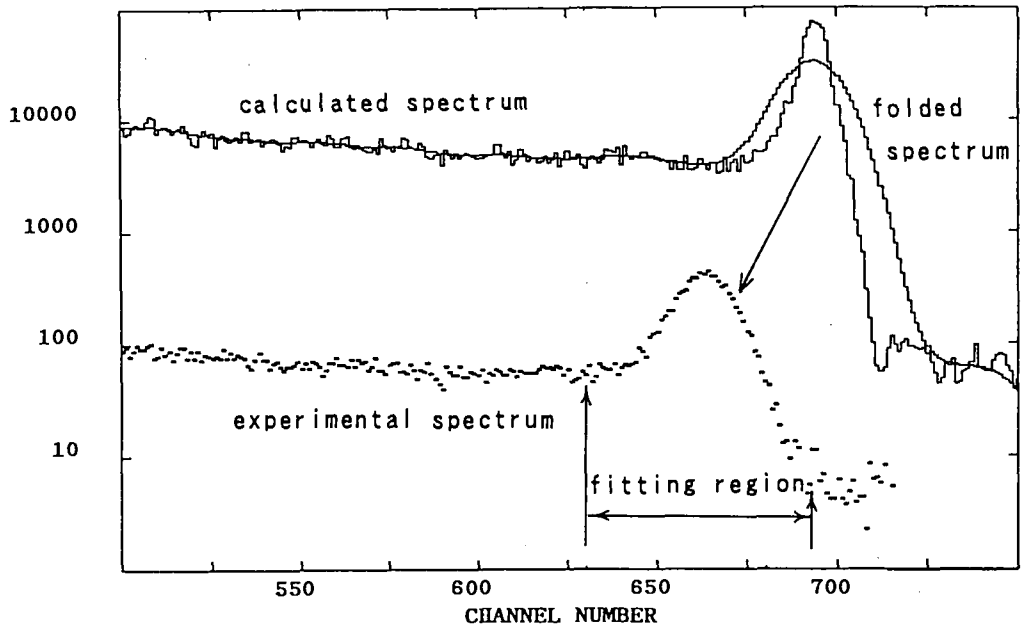

Fig.1 Procedures of folding and fitting of calculated spectrum to experimental spectrum.

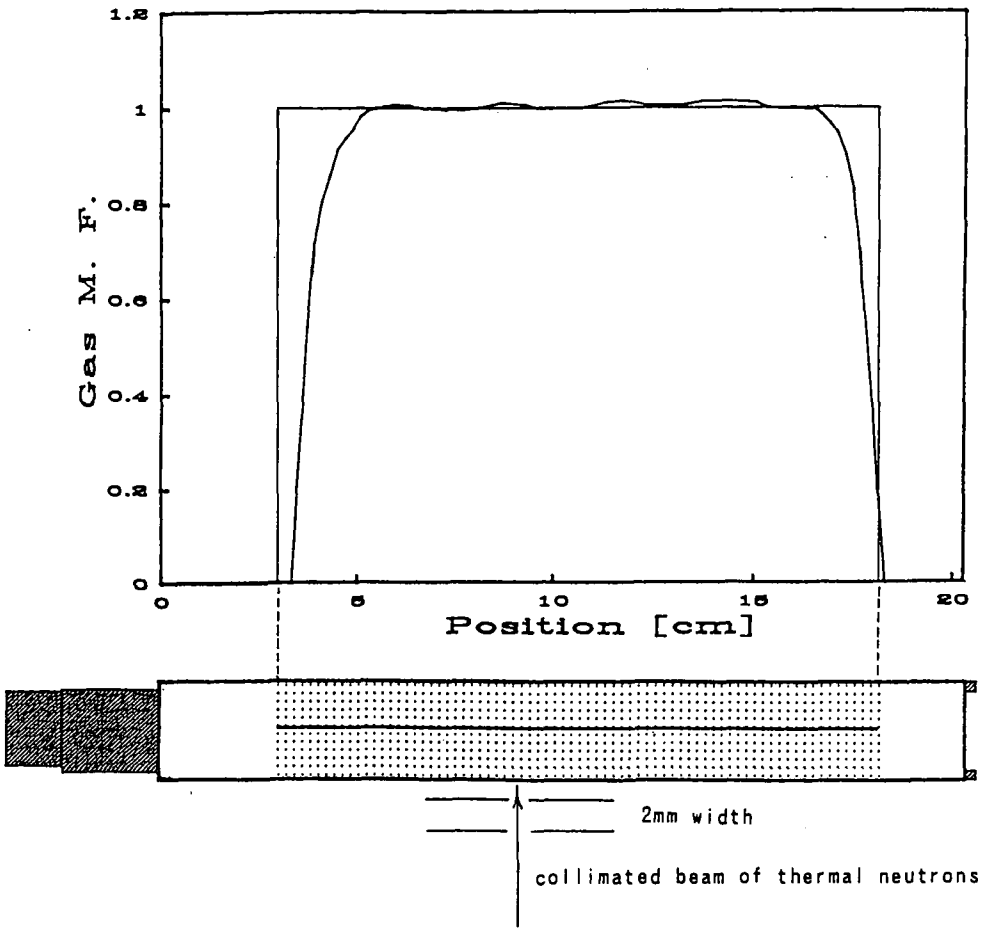

Fig.2 Gas multiplication factor, relative to the factor for the whole area irradiation of the detector, as a function of position along the central axis of a ^{3}He gas counter.

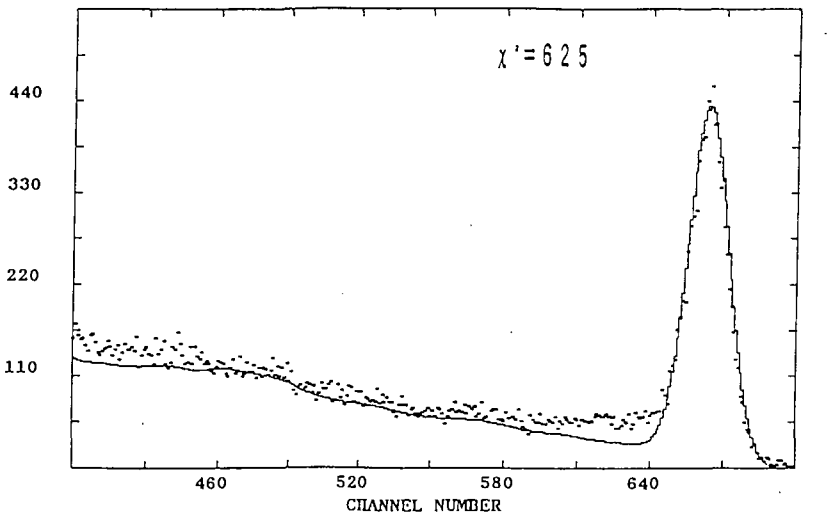

Fig.3 Comparison of measured (individual points) and calculated (solid line) pulse height spectra under the conditions of constant gas multiplication, 2.413 MeV incident energy and no secondary neutron effect.

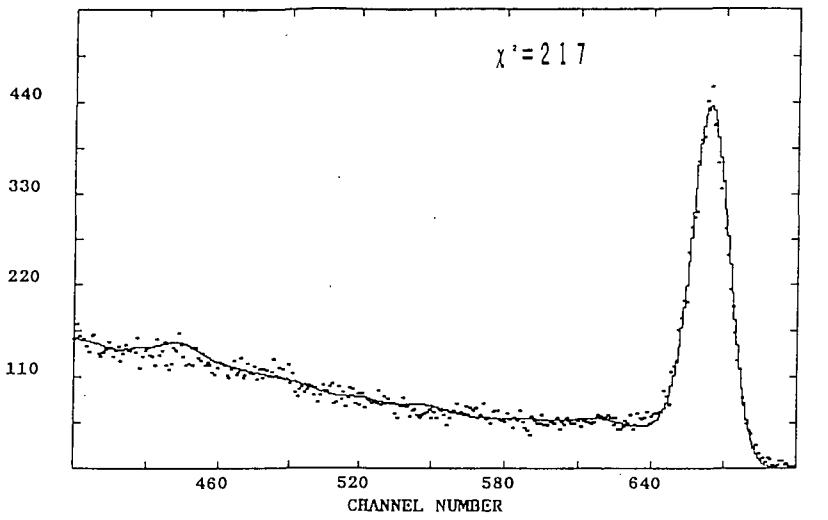

Fig.4 Comparison of measured (individual points) and calculated (solid line) pulse height spectra under the conditions of measured gas multiplication, 2.413 MeV incident energy and secondary neutron effect.

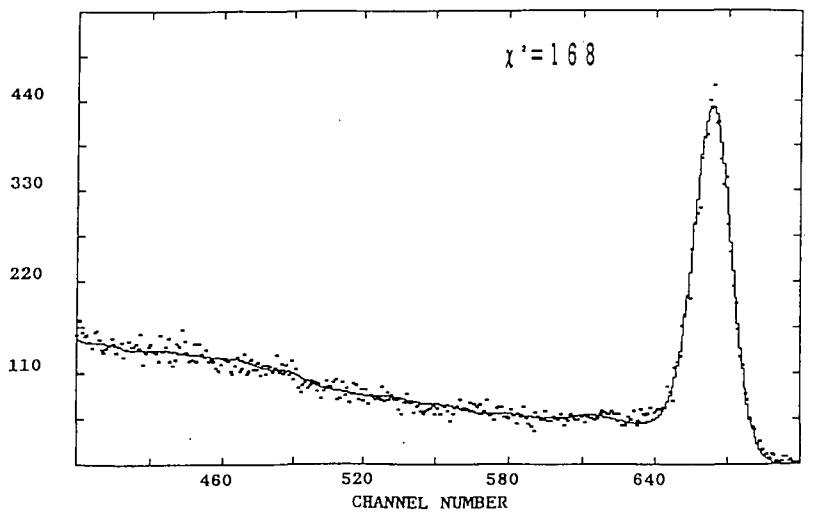

Fig.5 Comparison of measured (individual points) and calculated (solid line) pulse height spectra under the conditions of measured gas multiplication, angular straggling effect and secondary neutron effect.

II. JAPAN ATOMIC ENERGY RESEARCH INSTITUTE

A. Fast Reactor Physics Laboratory

II-A-1 Measurement of Doppler Effect up to 2000 °C at FCA

S. OKAJIMA, H. OIGAWA, T. MUKAIYAMA

Introduction

Most Doppler effect measurements at various fast critical facilities around the world have been made in the temperature range from 20 to 800 °C. The Doppler effect at higher temperature plays an important role in the transient behavior of the FBR.

New experimental devices were developed and used to measure Doppler effect to 2000 °C at the Fast Critical Assembly (FCA) of JAERI. These measurements should improve the Doppler effect calculation accuracy in this high temperature range.

Measurement of the high temperature Doppler effect

Two methods were combined to extend the temperature range of Doppler measurements to higher temperatures. The first method involves sample reactivity measurements and is used for temperatures up to 1500 °C. The other method uses foil activation measurements with laser heating and is used for temperatures up to 2000 °C.

A UO_2 Doppler sample is placed in the core center and kept at a desired high temperature for a certain period. The Doppler effect is derived from the difference between the reactivities measured for the unheated Doppler sample and the heated sample placed at the core center. The reactivity difference is determined by the position difference of a fine control rod which maintains the reactor at a constant power level.

Figure 1 shows a schematic view of the experimental device for the sample reactivity measurement. The depleted UO_2 Doppler sample is 20 mm in diameter, 150 mm in length and contains 390 g of uranium. The sample is contained in a tungsten holder which is surrounded by a tungsten electric heater. The sample and heater are surrounded by several layers of tungsten thermal-reflector. This assembly is placed in an evacuated stainless steel inner tube. This tube is positioned inside a stainless steel outer tube. Cooling air flows through the space between the inner and outer tubes. This removes heat escaping from the heated Doppler sample and prevents any significant increase in temperature of adjacent core materials.

To compensate for the reactivity drift of the core caused by the slight temperature rise of the core materials, reactivity measurements are performed by alternately placing a reference sample and the Doppler sample at the core center. Both samples are loaded in a 5 cm square drawer, and the drawer is repetitively oscillated in and out so that one of samples is at the core center while the other is out of the core.[1),2)] The accuracy of the reactivity measurement is $\pm 3 \times 10^{-7}$ $\Delta k/k$.

The sample reactivity measurement is impractical for the temperature range above 1500 °C because the limited space does not allow adequate thermal insulation for a massive Doppler sample at higher temperatures. A foil activation method is used to measure the Doppler effect in the temperature range up to 2000 °C.

A UO_2 foil placed at the core center is kept at a given high temperature (up to 2000 °C) by exposure to a Nd-YAG laser beam. After several hours of irradiation, the irradiated foil is removed from the core and the γ rays (106, 210 and 277 keV) from ^{239}Np, which is the neutron capture product of ^{238}U, are counted. The experimental Doppler effect is expressed as the *Doppler ratio*, the ratio of the increase in foil activity caused by the temperature rise compared to the activity of the unheated foil:

$$\textit{Doppler ratio} \equiv \frac{R(T) - R(T_0)}{R(T_0)} .$$

where $R(T)$: γ ray count rate of a foil irradiated at temperature T
T_0 : room temperature

A schematic view of the experimental device for this method is also shown in Fig. 1. A depleted UO_2 foil 12.7 mm in diameter and 0.5 mm thick is wrapped in a tungsten cover. These elements are suspended in the center of a vacuum capsule which has silica glass windows at both ends along the longitudinal direction of the drawer. One side of the foil is exposed to a Nd-YAG laser beam. The laser beam, transmitted by an optical fiber cable from a laser oscillator, enters the capsule through one window. The temperature of the other side of the foil is monitored, through the other window, with a monochromatic radiation thermometer. The thermal insulation for this device is similar to the device described previously.

The Doppler effect measurement to 2000 °C was made in the FCA assembly XVII-1, which is a mockup core for a prototype MOX-fueled FBR. Figure 2 shows the experimental results obtained by both measurement techniques.

Analysis of the higher temperature Doppler effect measurement

From the standpoint of neutron cross section, tungsten has many resonance peaks. Some of the resonance peaks for tungsten overlap with those for ^{238}U. It is, therefore, important to evaluate the resonance overlapping effect between the ^{238}U of the Doppler sample and the tungsten structural material in the devices. In analyzing this resonance overlapping effect, a new collision probability code, PEACO-X[3], was used. The code calculates the regional neutron flux with ultra-fine group structure ($\Delta u = 0.25 \sim 4\times10^{-4}$) based on the RABBLE method[4] and generates effective cross sections with the JFS-3 type group structure ($\Delta u = 0.25$)[5].

The Doppler reactivity worth was calculated by first order perturbation theory. The effective cross section of the Doppler sample was obtained from PEACO-X. The real and adjoint fluxes were obtained from a two-dimensional diffusion calculation. The calculated *Doppler ratio* in the foil activation method was obtained from the combination of PEACO-X results in the energy range below 100 keV and the conventional cell code's results above 100 keV. JENDL-3 data[6] were used in these calculations.

The calculated resonance overlapping effect between the ^{238}U of the Doppler sample and the tungsten structural material contributed only 1.0% to the measured Doppler reactivity, and 2.1% to the *Doppler ratio* in the foil activation measurement.

The calculated results are also shown in Fig. 2. The ratios of the calculated value to the experiment (C/E values) are 0.86 for the Doppler reactivity worth for the temperature change from 20 °C to 1500 °C and 0.98 for the *Doppler ratio* at 2000 °C.

Conclusion

The Doppler effect was measured up to 2000 °C at FCA using newly developed experimental devices. A cell calculation code with ultra-fine groups was developed and used for the analysis of the resonance overlapping effect between the ^{238}U of the Doppler sample and the tungsten structural material of the experimental devices. The calculation showed a relatively small overlapping effect. The calculation of the Doppler effect was 15-20% lower than the measured values for the sample reactivity method, and was in good agreement with the results of foil activation method.

These types of measurements are being performed in various cores at FCA to obtain the neutron spectrum dependence of the very high temperature Doppler effect.

References

1) Okajima S. and Mukaiyama T.: JAERI-M 84-086 (1984) (in Japanese).
2) Mukaiyama T. and Okajima S.: J. Nucl. Sci. and Technol., 22, 243 (1985).
3) Okajima S., Oigawa H. and Mukaiyama T.: JAERI-M 92-185 (1992) (in Japanese).
4) Kier P.H. and Robba A.A.: ANL-7326 (1967).
5) Takano H. and Ishiguro Y.: JAERI-M 82-135 (1982).
6) Shibata K., et al.: JAERI-1319 (1990).

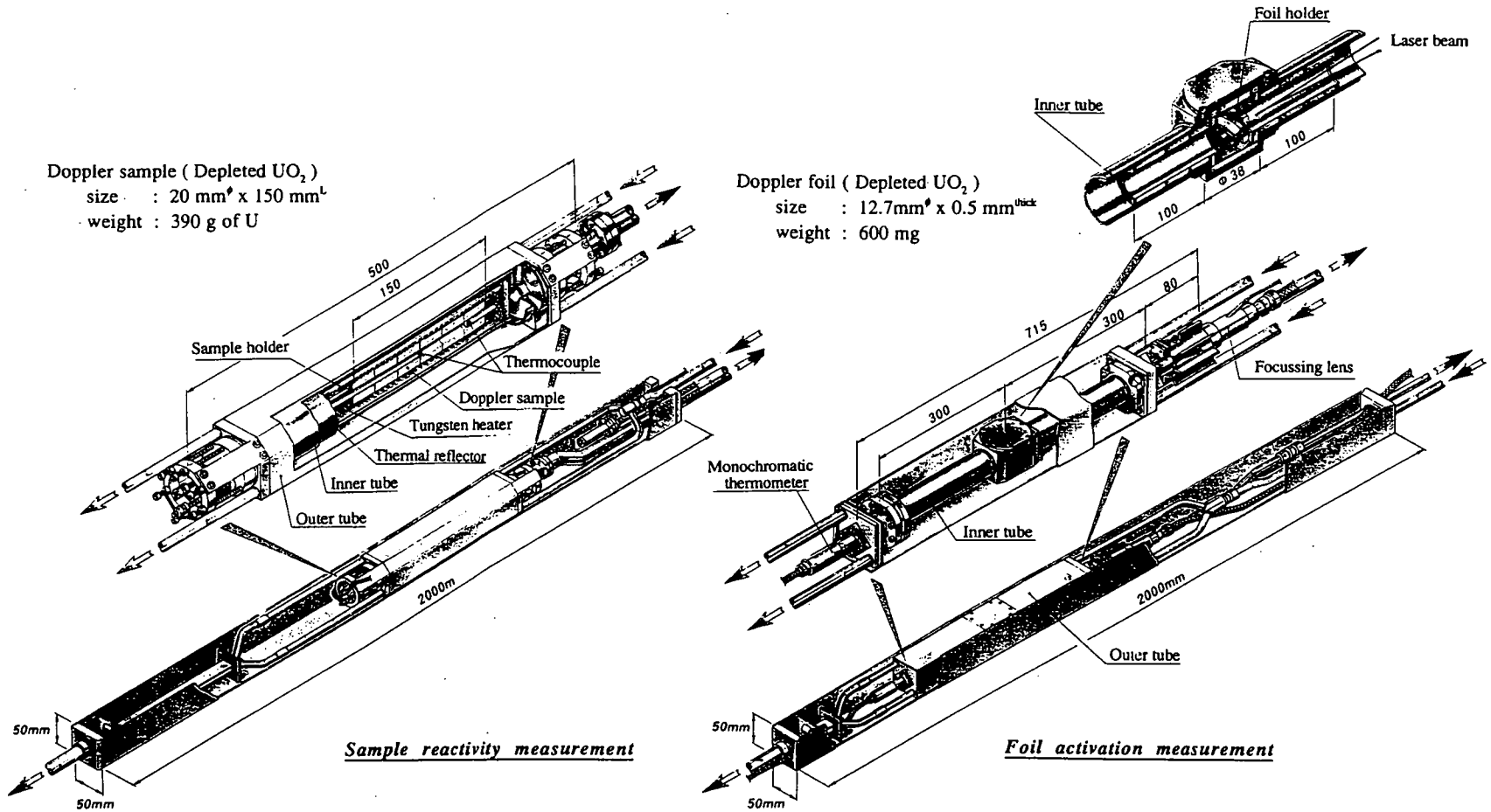

Fig. 1 Schematic view of experimental devices used in FCA Doppler effect experiment

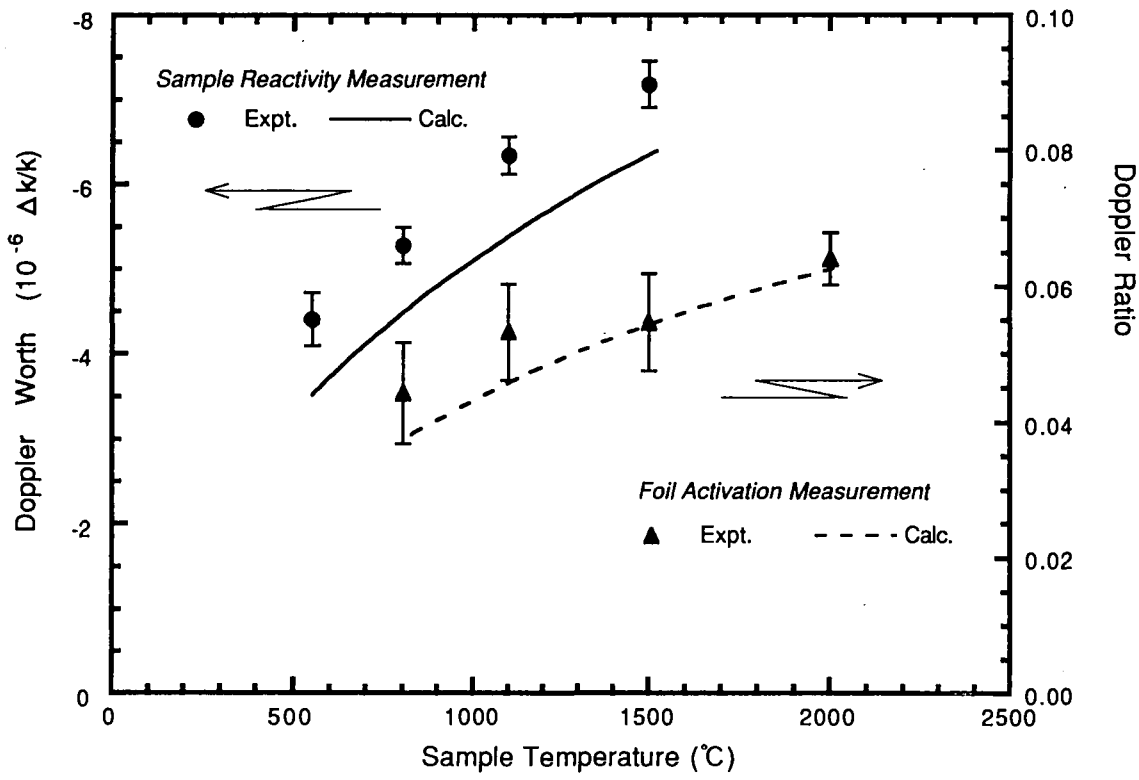

Fig. 2 Experimental and calculated results of ^{238}U Doppler effect measured in mockup core of MOX-fueled FBR at FCA

B. Thermal Reactor Physics Laboratory

II-B-1

Characterization of the Neutrons Produced from $^{1}H(^{11}B,n)^{11}C$ Reaction

S. Meigo, S. Chiba* and T. Fukahori*

Properties of the neutrons produced from the $^{1}H(^{11}B,n)^{11}C$ reaction[1], which was proved to be suitable for producing mono-energetic neutrons in the region of 7 to 13 MeV[2),3),4)] were measured. The energy spectrum of the neutrons was determined by the time-of-flight(TOF) method with a flight path longer than previous measurements. For the precise measurements of neutron cross-sections using $^{1}H(^{11}B,n)^{11}C$ neutron source, it is required to know the characterization of produced neutron.

A calculation code program was developed which simulated the neutron production inside the H_2 gas target by the Monte-Carlo method. This program takes account of the mean energy loss and the energy straggling of the ^{11}B incident beam by the Mo entrance foil and H_2 gas. The mean energy loss is calculated by the integral of the stopping power[5)]. The energy straggling is calculated by both Landau-Vavilov and Bohr models. The neutron spectrum at the detector point is calculated by taking the energy dependence and kinematics of $^{1}H(^{11}B,n)^{11}C$ reaction into account. The TOF spectrum was calculated by folding the neutron spectrum with the resolution function which was determined from the prompt gamma-ray peak of the measurements.

The measurements of the produced neutron via $^{1}H(^{11}B,n)^{11}C$ reaction were carried out with the NE-213 scintillator at JAERI tandem accelerator. The detector had 5"ϕx2" size and was located 6~8 m from the target. The FWHM of the gamma-ray peak had typically 4nsec.

At various incident energies(57.3,60.0,62.7 MeV) and emission angles(0,20,30,35-deg.), the measured and the calculated TOF spectra are shown in Fig 1. and Fig2. The folding calculated results reproduced the measured spectra quite favorably at various incident energies and emission angles. Then, various characteristics on the "real" energy spectrum(those without folding) of this reaction,i.e, the mean energy, standard deviation, skewness and kurtosis, have been calculated. The results showed a characteristic fluctuation which reflects the energy dependence of this reaction. These results will be employed in designing future experiments.

---

*: Nuclear Data Center, JAERI.

1. S. Chiba, M. Mizumoto, K. Hasegawa, Y. Yamanouti, M. Sugimoto, Y. Watanabe and M. Drosg, Nucl. Instr. Method A281,581(1989).
2. S.Chiba, M.Sugimoto, Y. Ikeda and Y. Yamanouti,"Study of Fast Neutron Cross Sections at JAERI Tandem Accelerator", Proc. of Beijing Int. Symposium on Fast Neutron Physics, Beijing, China, 9th–13th 1991, World Scientific, p.226(1982)
3. Y. Ikeda, C.Konno, M. Mizumoto, K.Hasegawa, S.Chiba, Y. Yamanouti and M. Sugimoto, "Activation Cross Section Measurement at Neutron Energies of 9.5,11.0,12.0 and 13.2 MeV Using $^{1}H(^{11}B,n)^{11}C$ Neutron Source at JAERI", Proc. of Int. Conf. of Nuclear Data for Science and Technology, 13th–17th May, 1991, Springer–Verlag, p.294(1992).
4. K. Hasegawa, M.Mizumoto, S. Chiba, M. Sugimoto, Y. Yamanouti, M. Igashira and H. Kitazawa, "Gamma–ray Production Cross Section Measurements of Some Structural Materials Between 7.8 and 13.0 MeV", Proc. of Int. Conf. of Nuclear Data for Science and Technology, 13th–17th May, 1991, Springer–Verlag, p.329(1992).
5. F.Hubert, R.Bimbot and H. Gauvin, "Range and Stopping–Power Tables for 2.5–500 MeV/Nucleon Heavy Ion In Solids", Atomic and Nuclear Data Tables 46, 1–213(1990).

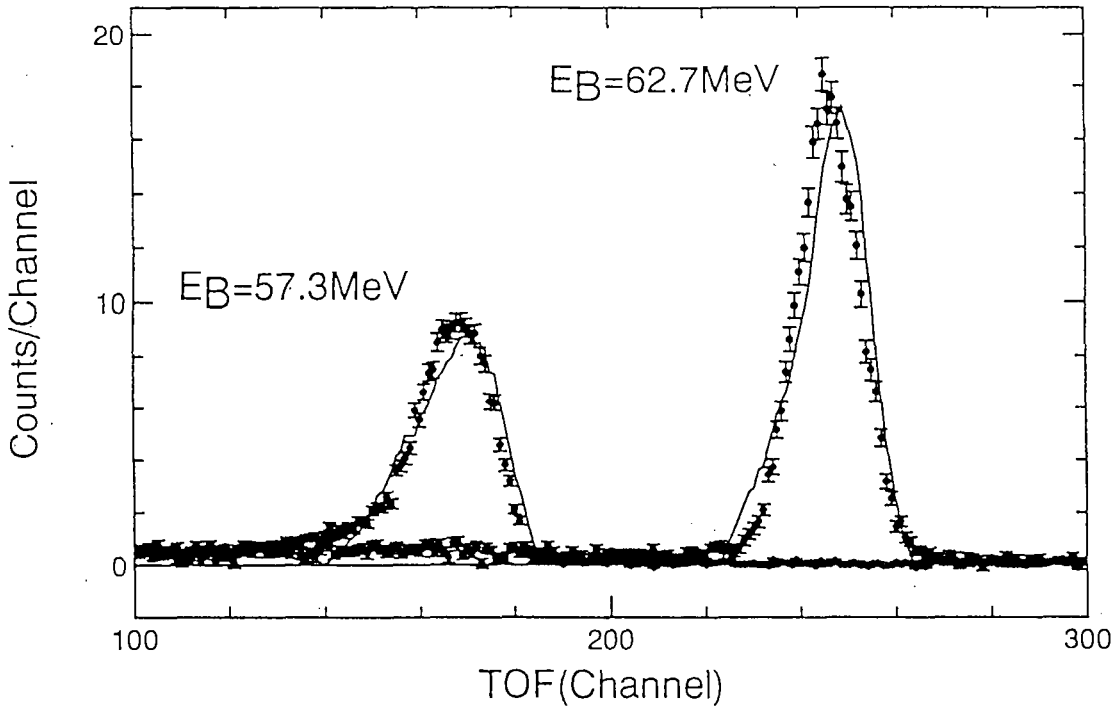

Fig. 1. Measured and calculated TOF spectra at various ^{11}B incident energies(one channel equals 0.4 nsec).

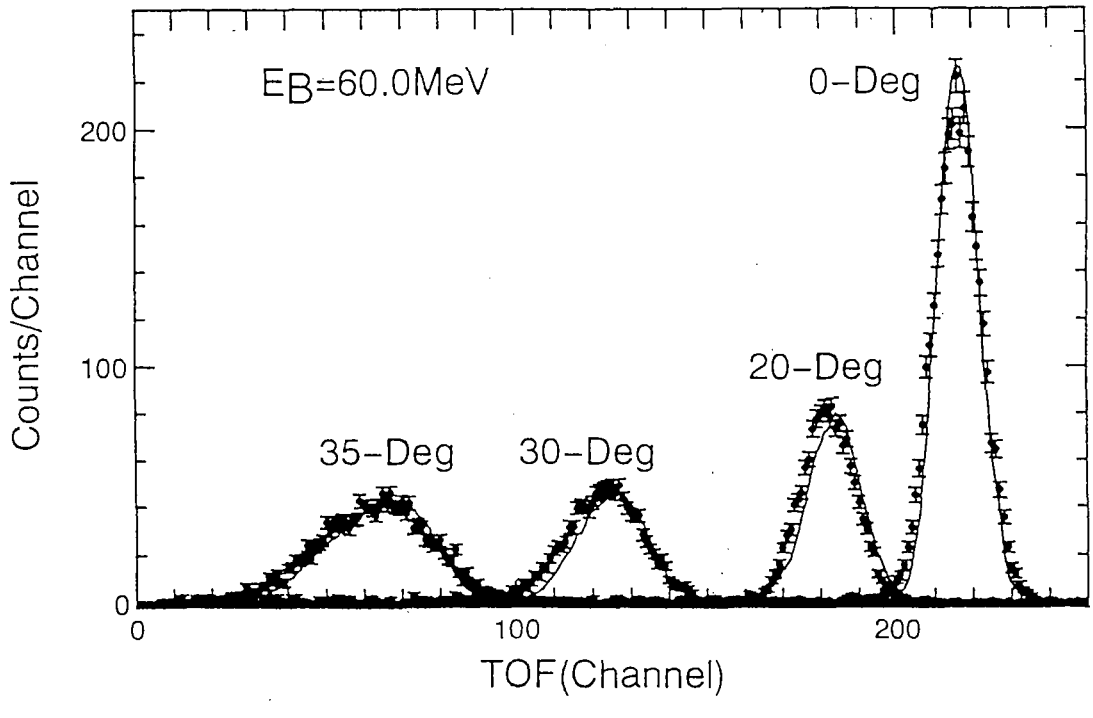

Fig. 2. Measured and calculated TOF spectra at several emission angles (one channel equals 0.4 nsec).

C. Free Electron Laser Laborastory

II-C-1 Neutron Transmission Measurements on ^{121}Sb, ^{123}Sb, ^{140}Ce and ^{142}Ce in the Resonance Region

Makio Ohkubo, Motoharu Mizumoto and Yutaka Nakajima

A paper on this subject was published in JAERI-M 93-012 with the following abstract:

Neutron transmission measurements have been made on natural antimony, natural cerium, separated isotopes Sb-121, Sb-123 and Ce-142 at the TOF facility of the Japan Atomic Energy Research Institute linear accelerator. Resonance parameters are determined on many levels of Sb-121 and Sb-123 up to 5.3 keV, and Ce-140 and Ce-142 up to 50 keV. S-wave strength function S_0, and average s-wave level spacing D were deduced as follows:

^{121}Sb: $S_0 = (0.24 \pm 0.03) \times 10^{-4}$ for 188 levels below 5.3 keV,
D = 10.3 ± 0.5 eV below 0.6 keV,

^{123}Sb: $S_0 = (0.25 \pm 0.03) \times 10^{-4}$ for 202 levels below 5.3 keV,
D = 20 ± 1 eV below 1.3 keV,

^{140}Ce: $S_0 = (1.6 \pm 0.5) \times 10^{-4}$ for 15 levels below 50 keV,
D = 3.5 ± 0.8 keV below 50 keV,

^{142}Ce: $S_0 = (2.7 \pm 0.6) \times 10^{-4}$ for 38 levels below 50 keV,
D = 2.3 ± 0.2 keV below 10 keV.

D. Nuclear Data Center and Working Groups of Japanese Nuclear Data Committee

II-D-1 Evaluation of Intermediate Energy Nuclear Data for Accelerator System; A Case Study, Neutron- and Proton-Induced Reactions in ^{27}Al

T. Fukahori, Y. Nakajima and Y. Kikuchi

A paper on this subject will be published in Proc. of Seventh International Conference on Emerging Nuclear Energy Systems (ICENES '93), September 20–24, 1993, at Makuhari, Chiba, Japan with the following abstract:

Nuclear data in the intermediate energy range up to several GeV are necessary to many applications, especially for accelerator-driven radioactive waste transmutation systems. Such systems need the neutron- and proton-induced reaction data as fundamental data for calculations of system and shielding design, spallation target characteristics, transmutation rate, etc. However, evaluated intermediate energy nuclear data are not available except for a few isotopes, while neutron nuclear data below 20 MeV are well established for wide range of nuclei.

Evaluation works were reported only for ^{56}Fe by Pearlstein and for ^{208}Pb and ^{209}Bi by Fukahori. In this paper, methods and results of evaluation for neutron- and proton-induced reactions up to 1.0 GeV in ^{27}Al are described so as to fill a lack of lighter mass range and to show the feasibility of the some evaluation methods employed for the heavier nuclei. The isotope of ^{27}Al is one of the important nuclides as a candidate material for accelerator tubes and many equipments.

Evaluated quantities were total, elastic, total reaction, particle production and isotope production cross sections, and double differential particle emission spectra for neutron, proton, deuteron, triton, ^{3}He and alpha. The total (only for neutron), elastic and total reaction cross sections were calculated with an empirical formula which was derived by Pearlstein to reproduce the experimental data of these cross sections for the elements from carbon to uranium. The particle and isotope production cross sections were mainly obtained by the ALICE-F code which is based on the multistep compound decay model including the preequilibrium process. The calculations of double differential cross sections were performed by the semi-empirical formulas of Pearlstein for neutron and of Kalbach for charged particles. The evaluated results can reproduce the overall trend of the experimental data.

II-D-2 R-Matrix Analysis of Neutron Effective Total Cross Section, Fission Cross Section and Capture Cross Section of ^{233}U in the Energy Range from Thermal to 150 eV

Herve Derrien

A paper on this subject has been submitted to J. Nucl. Sci. Technol. with the following abstract:

The Reich-Moore approximation of the R-matrix theory was applied to the analysis of selected measurements of neutron effective total cross sections, fission cross sections and capture cross sections of ^{233}U in the energy range from thermal to 150 eV. The resonance parameters were obtained by fitting the experimental data by the Bayesian code SAMMY. Results of the calculated cross sections are compared with the corresponding experimental data in graphs and tables. The statistical properties of the resonance parameters were examined and the average parameters were obtained. The resonance parameters are given in an ENDF-6 format file available from JAERI Nuclear data Center and from the NEA Data Bank (OECD, Paris).

Thermal cross sections and resonance integral are compared in Table 1.

Table 1 Thermal cross sections and resonance integral

	present	JENDL-3	ENDF/B-VI	JEF-2
resonance integral (b)				
capture	130.08	138.42	136.37	134.74
fission	774.63	774.79	754.43	762.47
thermal cross section(b)				
capture	45.27	45.3	45.8	45.9
fission	531.29	529.9	528.5	525.1
scattering	11.99	12.7	12.6	14.4

II-D-3 Revision of the ^{241}Pu Reich-Moore Resonance Parameters by Comparison with Recent Fission Cross Section Measurements

Herve Derrien

A paper on this subject will be submitted as a JEARI-M report with the following abstract:

The fission cross section of ^{241}Pu was re-measured recently by Wagemans et al. They found that the shape of the cross section in the thermal energy range was compatible with the 1/v law, in contradiction with the previously reported data. As a consequence, the re-normalization of the experimental data used for evaluation purpose is needed. In order to take into account this re-normalization, the resonance parameters of ENDF/B-VI were revised, resulting in a decrease of the fission cross section by about 3 % on average, in the energy range from thermal to 300 eV. The present results will be adopted in JENDL-3.2.

II-D-4 Bibliographic Index to Photonuclear Reaction Data (1955-1992)

Tetsuo ASAMI and Tsuneo NAKAGAWA

A paper on this subject will be submitted as a JEARI-M report with the following abstract:

This report contains the bibliographic index data on photonuclear reactions and on their inverse ones, in the format similar to CINDA for neutron nuclear data. As photonuclear reactions the electron-induced reaction data are also included. As the inverse reactions considered are those induced by neutron, proton, deuteron, triton, helion and alpha particles. The index covers major journals on nuclear data published in 1955 to 1992, for all nuclides through hydrogen (H) to einsteinium (Es). The bibliographic index contains information on target nucleus, incident beam, type of reaction and quantity, energy range of incident beam, laboratory, type of work, reference citations, first author's name, and short comment. The index also contains the indication for information on cross-section data. All the index data are listed in the order of target element, target mass and incident particle, and in the chronological order of reference data. Also a brief description is given on the data format, the abbreviations used and the journals surveyed.

II-D-5 Nuclear data Evaluation for ^{237}U, ^{236}Np and ^{238}Np

Tsuneo Nakagawa

Neutron-induced reaction cross section data of ^{237}U, ^{236}Np and ^{238}Np have been evaluated in the energy range from 10^{-5} eV to 20 MeV. The quantities considered are the total, elastic and inelastic scattering, fission, capture, (n,2n) and (n,3n) reaction cross sections. The angular and energy distributions of neutrons were also estimated. Available experimental data for these nuclides are limited to fission cross sections of a small range of energy. Therefore, theoretical calculations and systematics of cross sections are widely applied. Results are shown in Figs. 1 to 3. They will be stored in JENDL-3.2 and JENDL Actinide File.

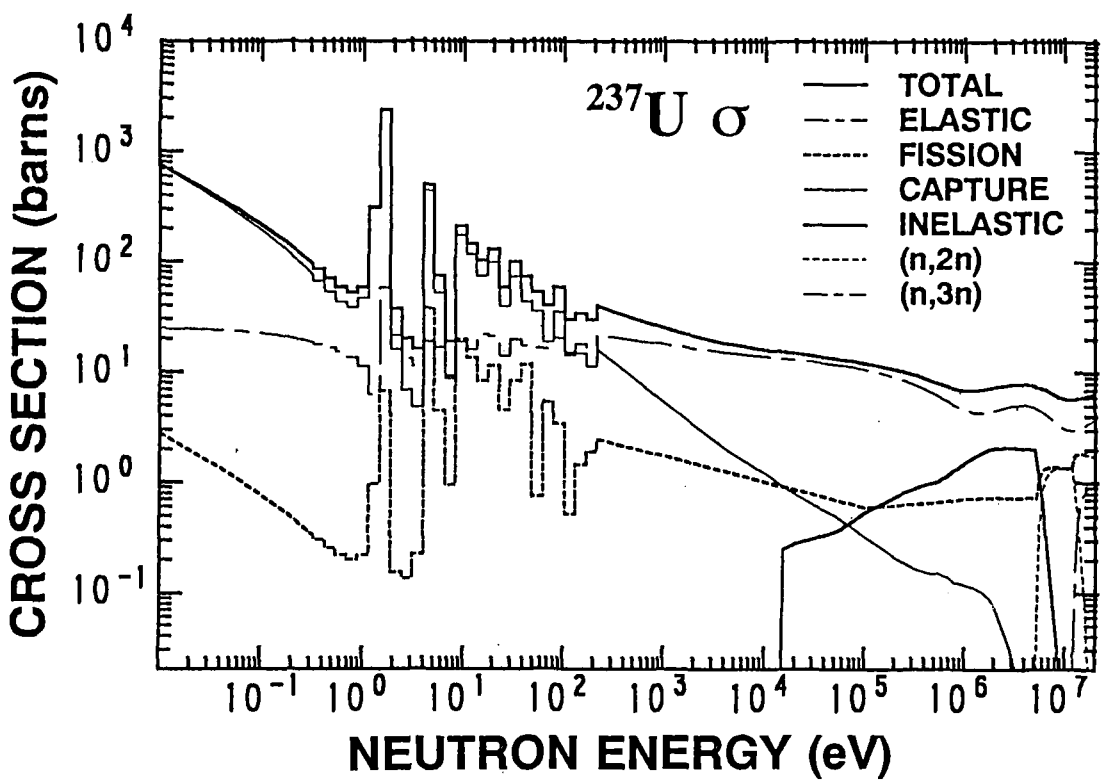

Fig. 1 Evaluated cross sections of ^{237}U. The cross sections in the resolved resonance region below 200 eV are averaged in suitable energy intervals only for this figure.

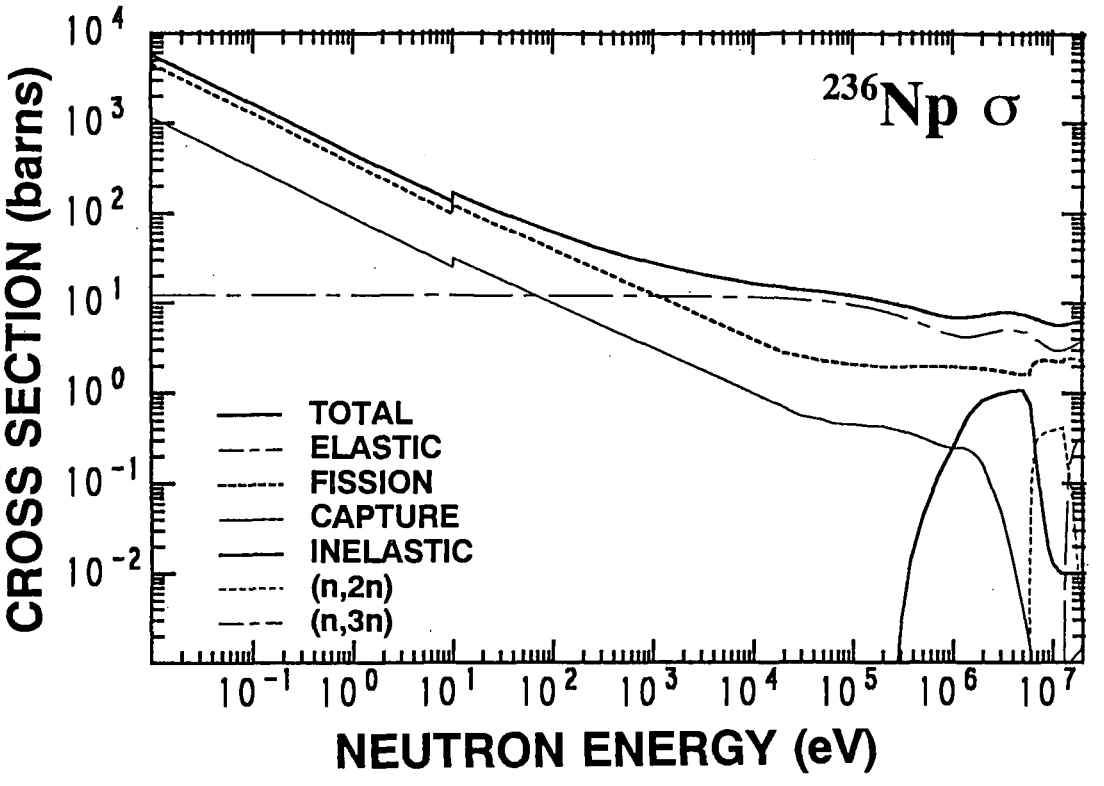

Fig. 2 Evaluated cross sections of ^{236}Np

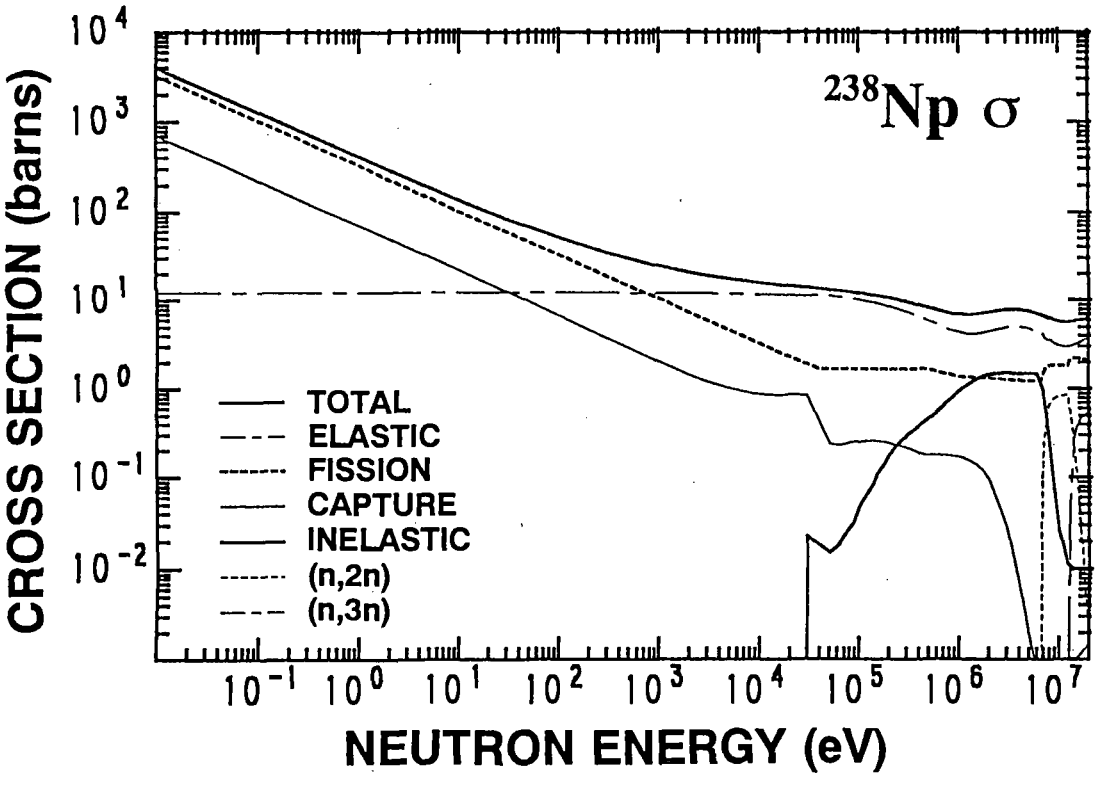

Fig. 3 Evaluated cross sections of ^{238}Np

II-D-6 Collective Enhancement of Nuclear Level Density in the Frame of the Interacting Boson Model [a)]

A. Mengoni*

Paper published in the *Proceedings of the 1992 Symposium on Nuclear Data*, JAERI-M 93-046, March 1993, pag. 92.

The Interacting Boson Model (IBM) has been applied to the calculation of the collective enhancement of nuclear level density. The problem of including collective excitation into the Fermi-Gas model has been reviewed. The technique for estimating the enhancement due to collective excitations has been applied to the calculation of the level densities of ^{238}U. The collective enhancement factor as a function of the nuclear temperature, calculated using different prescriptions, is shown in the figure. The first set of calculation was done using a simple rigid-rotor expression for the rotational energy (empty dots). The second set has been made using the full IBM spectrum (triangles) but with a *constant* number of bosons. Finally, the third and more realistic calculation was done using the IBM spectrum (full dots), with the number of bosons allowed to vary with the temperature, as suggested in the calculations of the reference[1)].

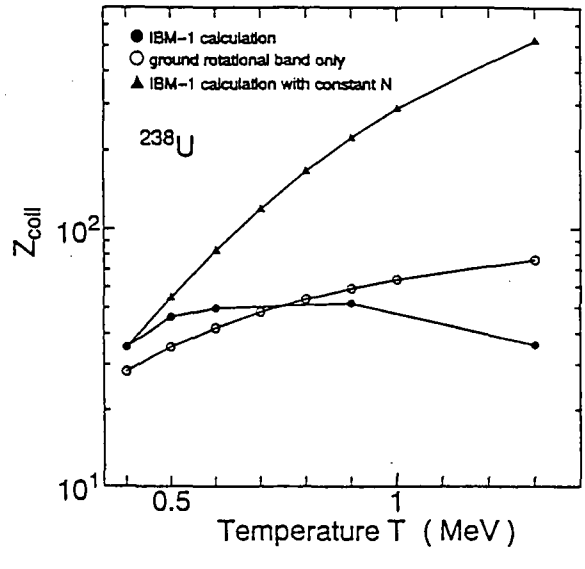

Reference:

1) Maino G., Mengoni A., and Ventura A., 1990, *Phys. Rev.* C **42**, pag. 988.

a) Work partially supported by the Commission of the European Communities under the EC-STF Programme in Japan

*Permanent address: ENEA, Bologna, Italy.

II-D-7 Resonance capture gamma-ray emission mechanism in n + ^{53}Cr [a)]

A. Mengoni*, C. Coceva** and H. Kitazawa***

Paper to be published in the *Proceedings of the 8th International Symposium on Capture Gamma Ray Spectroscopy and Related Topics*, Fribourg, Switzerland, September 20-24, 1993.

A recent measurement of capture gamma rays from the neutron resonances in ^{53}Cr provided a wide set of data for investigating the capture mechanisms. The observed gamma-ray emission intensities for E1 radiation are compared with the theoretical calculations based on the valence model. The results show that the valence mechanism, though accounting for a considerable porion of the emission strength, is not sufficient to fully describe the fluctuations of the observed data. The results of the calculations, in comparison with the experimental data are shown in the Table.

Table. Energies, spins and reduced neutron widths are given in columns 1 to 3. Experimental transition widths and their errors leading to three final states in ^{54}Cr with $J^{\pi} = 2^{+}$ are on columns 4, 6 and 8. The corresponding calculated valence widths are on columns 5, 7 and 9.

			E_f = 2.6195 MeV		E_f = 3.074 MeV		E_f = 3.437 MeV	
E_n KeV	J	Γ^0_n eV	$\Gamma^{exp}_{\gamma f}$ meV	$\Gamma^{VM}_{\gamma f}$ meV	$\Gamma^{exp}_{\gamma f}$ meV	$\Gamma^{VM}_{\gamma f}$ meV	$\Gamma^{exp}_{\gamma f}$ meV	$\Gamma^{VM}_{\gamma f}$ meV
4.21	1	21.8	286.6± 91.2	344.4	289.1±92.2	222.9	111.8±36.1	115.0
5.67	2	2.92	159.1± 47.1	29.1	0.0± 1.9	18.8	49.1±14.6	9.7
6.75	1	13.6	93.2± 24.6	227.1	156.3±39.7	146.9	166.1±43.0	75.8
8.18	2	12.4	756.9±397.5	113.2	10.9±13.3	73.3	103.4±55.3	37.8
19.71	2	0.74	6.7± 3.4	7.3	138.5±20.8	4.7	3.3± 4.1	2.4
25.92	2	1.21	2.7± 4.1	11.9	2.4± 5.8	7.7	13.3± 7.5	4.0
27.26	1	4.12	13.7± 11.6	69.8	41.5±28.5	45.1	48.0±20.7	23.2
29.49	2	2.04	12.1± 6.7	18.5	145.4±33.2	11.9	52.7±15.4	6.2
average			166.4	102.7	98.0	66.8	68.4	34.3

a) Work partially supported by the Commission of the European Communities under the EC-STF Programme in Japan.

*Permanent address: ENEA, Bologna, Italy.

**ENEA, Bologna, Italy.

***Tokyo Institute of Technology, Tokyo.

II-D-8 Fermi-Gas Model Parametrization of Nuclear Level Density [a)]

A. Mengoni* and Y. Nakajima

Paper accepted for publication in the *Journal of Nuclear Science and Technology*, 1993.

Abstract: we furnish here a new parametrization of the Fermi-Gas model description of nuclear level densities at excitation energies corresponding to the neutron binding energy. The model adopted is the standard Fermi-Gas model with pairing and shell-effect corrections. Particular care has been devoted to the inclusion of shell effects and to their parametrization. The procedure for the evaluation of level density parameters has been applied to a data-base of 217 nuclei covering a mass range $41 \leq A \leq 253$. A global systematics parametrization has been derived which allows for a derivation of level density parameters for nuclei where experimental information is not available.

II-D-9 HERMES: a personal-computer program for calculation of the Fermi-Gas model parameters of nuclear level density [b)]

A. Mengoni* and Y. Nakajima

Paper to be published as JAERI-M report, 1993.

A computer program, HERMES, that provides the quantities usually needed in nuclear level density calculations, has been developed. The applied model is the standard Fermi Gas Model (FGM) in which paring correlations and shell effects are opportunely taken into account. The effects of additional nuclear structure properties together with their inclusion into the computer program are also considered. Using HERMES, a level density parameter systematics has been constructed for mass range $41 \leq A \leq 253$. HERMES is available for distribution upon request to the authors.

a,b) Work partially supported by the Commission of the European Communities under the EC-STF Programme in Japan

*Permanent address: ENEA, Bologna, Italy.

II-D-10

Neutron Scattering and Optical Model Potentials of Several Fission Produce Nuclei

S. Chiba and A.B. Smith*

A paper on this subject was published in the Proceedings of a Specialists' Meeting on Fission Product Nuclear Data, held at Tokai, Japan on 25th-27th May 1992, NEA/NSC/DOC(92)9, p. 162, with the following abstract:

Some remarks on the neutron scattering experiments and optical model potentials in the fission product mass region are described. Status on the recent measurements is briefly summarized, and some systematic trends of the empirically determined optical model potential and deformation parameters are addressed. In this mass region, effects of the Z=50 and N=50 and 82 magic numbers play an important role in neutron scattering, and those effects are embedded in the phenomenological model parameters. It is shown that blind use of the global parameters will in some cases introduce differences in he calculated total, elastic and reaction cross sections as much as 20%, while for inelastic scattering the differences can be much larger. An example of the application of the dispersion relationship which relates the bound-state shell model potential and the positive energy optical model potential is also presented. Emphasis is placed in neutron scattering from Zr for which the most recent data are available.

---

* : Argonne National Laboratory

II-D-11

Impacts of Isomorphic Transformations and Truncations of Data Spaces on the Least-Squares Solutions

S. Chiba

A paper on this subject was published in the Proceedings of a Specialists' Meeting on Evaluation and Processing of Covariance Data, held at ORNL, USA on 7th-9th October, 1992, NEA/NSC/DOC(93)3, p.81, with the following abstract:

The least-squares method (LSM) is most commonly used as a tool of statistical inference in nuclear data evaluation and data analyses because its solution (the least-squares solution, LSS) has such desirable properties as indicated by Gauss-Markov theorem. However, in applying the LSM in actual data analyses, the LSSs obtained before and after a transformation of the data are often different from each other. Sometimes the impact is very serious, and an example of such anomaly is know as Peelle's Pertinent Puzzle (PPP). In this paper, criterion to obtain the same LSS before and after transformations of data which conserves dimensionality are established, i.e., in order to obtain the same least-squares solution before and after this type of transformation, the data covariance matrix and the design matrix must be transformed in a covariant manner. It is also shown that the Least-Squares solution is NOT generally invariant under a truncation of data spaces. This fact also results in the same type of anomaly as PPP. According to these results, the origin of PPP was traced to an improper truncation of a data space and a neglect of the invariance criterion.

II-D-12

Perspectives on Peelle's Pertinent Puzzle and Its Significance in Data Fitting and Evaluation

S. Chiba and D.L. Smith*

A paper on this subject was submitted to Symposium on Nuclear Data Evaluation Methodology, held at BNL on 12th-16th October, 1992 with the following abstract:

The least-squares method is widely used as a method of statistical inference. In applying this method to analysis of actual data, however, the least-squares method sometimes yields strange results which is strongly against our intuition. For example, the average of the two data (1.5, 1.0) becomes 0.88 in a certain combination of the elements of the covariance matrix, an answer outside the range of the input data! This problem, as it was introduced by R.W. Peelle in 1987, is called the "Peelle's Pertinent Puzzle". The purposes of this paper are to explain what the PPP is, what its origins are and what the correct answer is. However, whether or not such an answer is correct depends strongly on the history how the data were derived. An approximate but practical method to achieve the correct answer in actual data evaluation will be also described.

---

* : Argonne National Laboratory

II-D-13 **Measurement of the Double-Differential (n,xα) Reaction Cross Sections of Elemental Iron and Nickel in the Energy Region of 7 to 11 MeV**

S. Chiba, N. Ito* and M. Baba*

A paper on this subject was submitted to the First IAEA Research Co-ordination Meeting on "Improvement of Measurements, Theoretical Computations and Evaluations of Neutron Induced Helium Production Cross Sections", held at Kossuth Lajos University, Debrecen, Hungary on 17th-19th November, 1992 with the following abstract:

The double-differential (n,xα) reaction cross sections of elemental Fe and Ni were measured at incident neutron energies of 7.1, 7.9, 9.7 and 10.6 MeV. The secondary α-particles were detected by a specially designed gridded ionization chamber (GIC) developed at Tohoku University in mono-energetic neutron fields produced by the D(d,n)3He reaction at the JAERI tandem facility. Because of the extraordinarily high geometrical efficiency (nearly 1) of the GIC, high statistical accuracy was obtained in short experimental periods, and the whole counting system could be kept to be reasonably stable during each period. This was useful in avoiding unrecognized "drift" or "systematic errors". The present data give, when combined with those measured at Tohoku University, a comprehensive and unique information on the (n,xα) reaction channel from threshold to 15 MeV in a systematic manner. Some remarks on the evaluated data and computational methods were drawn from comparisons with the present data.

---

* : Tohoku University

II-D-14

Calculation of Neutron Cross Sections of ^{12}C up to 50 MeV

S. Chiba, Y. Watanabe* and Y. Koyama*

Calculations of the neutron-induced reaction cross sections of ^{12}C are in progress in the energy region from 20 to 50 MeV upon request from ESNIT group. The total, elastic and inelastic scattering cross section, angular distributions of elastic and inelastic scattering to the first 2^+ state are calculated by the optical model and DWBA. The potential was calculated from the microscopic JLM (Jeukenne-Lejeune-Mahaux) theory[1], with realistic nucleon (different for neutron and proton) density distributions obtained from Skyrme-Hartree-Fock calculation. The real and imaginary spin-orbit terms of Walter-Guss global potential[2] were employed, since different choices of the spin-orbit term did not yield considerable difference in calculated results. The strengths of the real and imaginary central potentials were adjusted to reproduce the (n,n) data measured at Michigan State University. The results are identical with those obtained by Petler et al.[3]

The double-differential cross sections (DDX) of various secondary particles were calculated by the Monte-Carlo method with SCINFUL/DDX code system[4], which is a modified version of ORNL SCINFUL code[5]. Starting from the primary 9 reactions, i.e.,

$$
\begin{aligned}
n + {}^{12}C \quad &\rightarrow \quad n + {}^{12}C \\
&\rightarrow \quad n' + {}^{12}C^*(2^+) \\
&\rightarrow \quad n' + 3\alpha \\
&\rightarrow \quad 2n + {}^{11}C \\
&\rightarrow \quad p + {}^{12}B \\
&\rightarrow \quad d + {}^{11}B \\
&\rightarrow \quad t + {}^{10}B \\
&\rightarrow \quad {}^{3}He + {}^{10}Be, \\
&\rightarrow \quad \alpha + {}^{9}Be
\end{aligned}
$$

decay of the each unstable nucleus was traced by the sequential two-body break-up model up to 5 subsequent steps. Angular distributions of these primary reactions are taken from experimental information if available, while those of the subsequent two-body decay are assumed to be isotropic with respect to the center-of-mass of the decaying system. All the kinematical calculations are carried out relativistically, and the final results are converted to laboratory system. By this modeling, DDXs of recoiled particles, e.g., ^6Li, ^7Li, ^9Be, ^{10}B, ^{11}B, are obtained fairly accurately as well as those of n, p, d, t, ^3He and α.

References:

1) J.P. Jeukenne, A. Lejeune and C. Mahaux, Phys. Rev. C16, 80(1977).
2) R.L. Walter and P.P. Guss, "A Global Optical Model for Neutron Scattering for A>53 and 10 MeV < E < 80 MeV", Proc. of Int. Conf. on Nuclear Data for Basic and Applies Scienses, Santa Fe, New Mexico, USA, p.1079 (1985).
3) J.S. Petler, M.S. Islam, R.W. Finlay and F.S. Dietrich, Phys. Rev. C32, 673(1985).
4) H. Kashimoto, Y. Watanabe, Y. Koyama, H. Shinohara and S. Chiba, "Study of ^{12}C Breakup Processes and Carbon Kerma Factors", JAERI-M 93-046, 287(1993).
5) J.K. Dickens, "SCINFUL", ORNL-6463 (1988).

* : Kyushu University

II-D-15

Evaluation of JENDL Fusion File

K. Kosako* and S. Chiba

Evaluation of JENDL Fusion File is on-going. The double-differential cross section (DDX) of secondary neutrons is given by the Kumabe's systematics[1], while DDX's of p, d, t, ^{3}He and α are given by Kalbach's systematics[2] in a composite form. The MSD/MSC ratio needed in these systematics was taken to be equal to the pre-equilibrium/equilibrium ratio calculated by the SINCROS-II code system[3]. Recently Chadwick and Young[4] showed that the MSC contribution is much smaller than was considered previously at 14 MeV, and that the MSD spectrum very close to that of pre-equilibrium component. This result seems to favorably justify the approximation taken in this project. The deformation parameters used in calculation of the direct inelastic components and the normalization for internal transition rate in the pre-equilibrium model were carefully adjusted to reprodece the energy differential cross section measured at Osaka and Tohoku Universities. The method of evaluation is described in more detail in Ref. 5. Evaluations for Ca, Ti, Fe, Zr, Mo, Pb and Bi have been finished in fiscal year 1992, and the results were compiled in ENDF-6 format files. In the fiscal year 1993, evaluation for the rest of the nuclei, i.e., F, Ge, As, Sn, Sb and W will be carried out.

References:

1) I. Kumabe, Y. Watanabe, Y. Nohtomi and M. Hamada, Nucl. Sci. Eng. 104, 280(1990).
2) C. Kalbach, Phys. Rev. C37, 2350(1988).
3) N. Yamamuro, "SINCROS-II", JAERI-M 90-006(1990).
4) M. Chadwick and P.G. Young, Phys. Rev. C47 (1993).
5) S. Chiba, B. Yu and T. Fukahori, "Evaluation of JENDL Fusion File", JAERI-M 92-027, p.35(1992).

* : Nuclear Energy Data Center

II-D-16

Activities of Fission Product Nuclear Data Evaluation in JNDC FP Nuclear Data Working Group

JNDC Fission Product Nuclear Data Working Group
M. Kawai[1], S. Chiba, H. Matsunobu[2], T. Nakagawa, Y. Nakajima, T. Sugi
T. Watanabe[3] and A. Zukeran[4]

1. Reevaluation of FP Cross Sections for JENDL-3.2

JENDL-3 Fission Product Nuclear Data Library(1) was released in December of 1990. Its integral test for the STEK sample reactivities and the capture rates measured at EBR-II and CFRMF has clarified that the JENDL-3 data reproduce well the integral data for important nuclides within 10% accuracy, and that it has a tendency underestimating sample worths of nuclides in the heavier mass region than 130(2). Additionally, after the evaluation for JENDL-3, new experimental data were measured at ORNL, KFK, FEI of Russia and JAERI. Corresponding to the opportunity of revision of JENDL-3 general purpose file, we make reevaluation of the resonance parameters and cross sections for about 50 fission product nuclides given in Table 1 by taking into consideration of the new experimental data. As for themal cross sections of long lived nuclides, JRR-4 measurements at JAERI were adopted. Major part of the revision of the resonance parameters are made according to the renormalization of the experimental capture area data of ORNL. Capture cross sections were renormalized so as to reduce the contradiction between the differential and the integral data. For some nuclides, the optical model parameters were revised to improve the energy dependence of total and capture cross sections in the higher energy region than 1 MeV. Direct components were added to the inelastic scattering cross sections of the even mass number isotopes of Zr and Mo. As for deformed nuclides such as Sm and Nd isotopes, the coupled channel calculation is in progress.

2. Study on Evaluation Method of Inelastic Scattering Cross Sections

The evaluation method of inelastic scattering cross sections for weakly absorbing FP nuclides is studied as one of the activities of NEANSC Evaluation Cooperation SG10. In JENDL-3, the direct inelastic scattering cross sections were evaluated on the basis of the DWBA calculation, of which reliability is issue of discussion in the subgroup. As far as the Zr and Mo isotopes, we have made assure that DWBA is applicable within the acceptable accuracy(3). In the present period, the coupled channel theory was applied to the inelastic scattering calculations for vibrational levels of ^{90}Zr, ^{144}Nd and ^{150}Nd by using the ECIS code according to the recommendation at the specialists' meeting(4). As is shown in Fig. 1 for ^{144}Nd, the excitation functions for vibrational levels calculated with

1. Toshiba Corporation.
2. Sumitomo Atomic Energy Industries, Ltd.
3. Kawasaki Heavy Industries, Ltd.
4. Hitachi Ltd.

the coupled channel theory using slightly reduced imaginary potential strength, Ws, gave a general agreement with the DWBA results denoted with JENDL-3 in the wide energy range up to 20 MeV. Accordingly, we nearly reach the conclusion that the DWBA is applicable to the direct inelastic scattering cross sections for the vibrational levels. However, further study is desirable for Pd and/or Ru in the mass range around 100 to confirm the conclusion. The investigation for rotational level band is also in progress. The latest result for ^{150}Nd is shown in Fig. 2: coupled channel theory calculations were made by considering the 0^+-2^+-4^+-6^+-coupling and using β_2=0.2848. As for the 2^+ level at 1.77 MeV, the result of the coupled channel calculation with Ws = 4.5 MeV agrees well with the DWBA calculation (JENDL-3) with Ws=9.13MeV.

For the second priority nuclides such as Ru, Cd, Ba, Ce and Sm, the status review of the inelastic scattering cross sections has been started and it is now in progress. Graphical intercomparison of the evaluated data with experimental data was made for Cd and Sm. The nuclear model and their parameters were surveyed for these nuclides and the direct inelastic scattering cross sections were estimated with DWBA.

3. Spectrum Calculation of STEK Cores with Monte Carlo Method

In order to investigate the accuracy of neutron fluxes used for the integral test, neutron spectra of the STEK cores were calculated with the vectorized pointwise Monte Carlo code, MVP, using a three dimensional homogeneous model of the STEK reactor and corrected for a heterogeneous effect according to the diffusion calculations. The results were compared with the original spectra reported by Dekker et al.[5] and employed to the sample worth calculations. Figure 3 shows the comparison of neutron spectra in the test region of the STEK-4000 core calculated with the various models with the original spectrum (ECN-ADJUSTED). The Monte Carlo method gives appreciable improvement of sample reactivity worth of the weak absorbers, although some discrepancies are still remaining between the calculations and the measurements. In a lower energy range of which neutrons much contribute to worth of the strong absorbers in a large core, the Monte Carlo calculation corrected for a heterogeneous effect supports the original spectra which were obtained through the adjustment of a diffusion theory calculation spectrum to reproduce the reactivity worth of standard samples. Tables 2 and 3 give the results for standard samples and strongly absorbing nuclides, respectively. Further investigation about plate heterogeneity effects and the review of the C/E values of sample worth are in progress.

References:

1) M. Kawai, et al., J. Nucl. Sci. Technol., 29, 195 (1992).
2) T. Watanabe, et al., Proc. of Specialists' Meet. on Fission Product Nuclear Data, Tokai, 25th-27th May 1992, NEA/NSC/DOC(92)9, p.411 (1992)
3) M. Kawai, et al., ibid., p.39 (1992).
4) M. Kawai, ibid., p.495 (1992).
5) J.W.M. Dekker, et al., ECN-35 (1978).

Table 1 Contents of Modification of JENDL-3 FP Nuclear Data Library

Themal Cross Sections and Resonance Integral:

^{90}Sr, ^{137}Cs, ^{154}Eu, ^{155}Eu

Resonance Parameters:

^{88}Sr, ^{89}Y, ^{90}Zr, ^{111}Cd, ^{122}Te, ^{124}Te, ^{125}Te, ^{126}Te, ^{137}Cs, ^{139}La, ^{141}Pr, ^{142}Nd, ^{143}Nd, ^{144}Nd and ^{145}Nd.

Reducing the Upper Limits of Resolved Resonance Region:

^{80}Se, ^{107}Pd, ^{107}Ag, ^{109}Ag, ^{113}Cd, ^{127}I, ^{139}La, ^{147}Sm and ^{154}Sm.

Renormalization of Capture Cross Sections:

^{79}Br, ^{81}Br, ^{111}Cd, ^{115}In, ^{117}Sn, ^{124}Sn, ^{121}Sb, ^{123}Sb, ^{122}Te, ^{123}Te, ^{124}Te, ^{138}Ba and ^{142}Ce.

Energy Dependence of Total and Capture Cross Sections:

^{98}Mo, ^{100}Mo, ^{101}Ru and ^{103}Rh.

Inelastic Scattering Cross Sections:

^{90}Zr, ^{92}Zr, ^{94}Zr, ^{96}Zr, ^{92}Mo, ^{94}Mo, ^{96}Mo, ^{98}Mo, ^{100}Mo, ^{150}Nd, ^{144}Sm, ^{148}Sm, ^{150}Sm, ^{152}Sm and ^{154}Sm.

Table-2 C/E values of reactivity worth for standard samples

Nuclides	Monte-Carlo+Hetero Effect Flux		Original(ECN Adjusted) Flux
	<C/E>	δ (C/E)	<C/E>
^{10}B	0.963	0.018	0.981
C	0.823	0.020	0.829
N	0.847	0.085	0.850
O	0.753	0.030	0.729
Al	0.871	0.037	0.817
Pb	0.823	0.025	0.662
^{235}U	0.962	0.021	0.946

Table-3 C/E values of reactivity worth for strongly absorbiing FP nuclides

Nuclides	Monte-Carlo+Hetero Effet Flux		Original(ECN Adjusted) Flux
	<C/E>	δ (C/E)	<C/E>
^{95}Mo	0.969	0.045	0.998
^{99}Tc	0.859	0.026	0.872
^{105}Pd	0.883	0.027	0.894
^{107}Pd	0.888	0.019	0.899
^{149}Sm	0.841	0.018	0.851
^{153}Eu	0.888	0.020	0.899
^{159}Tb	1.009	0.024	1.017

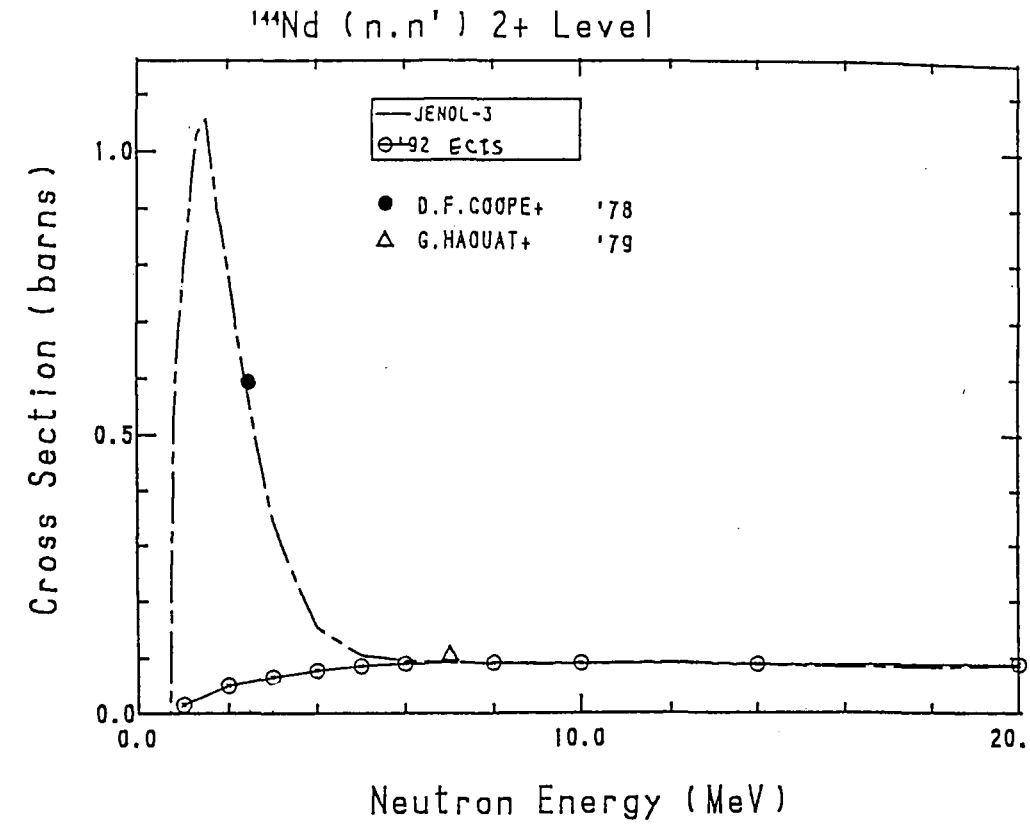

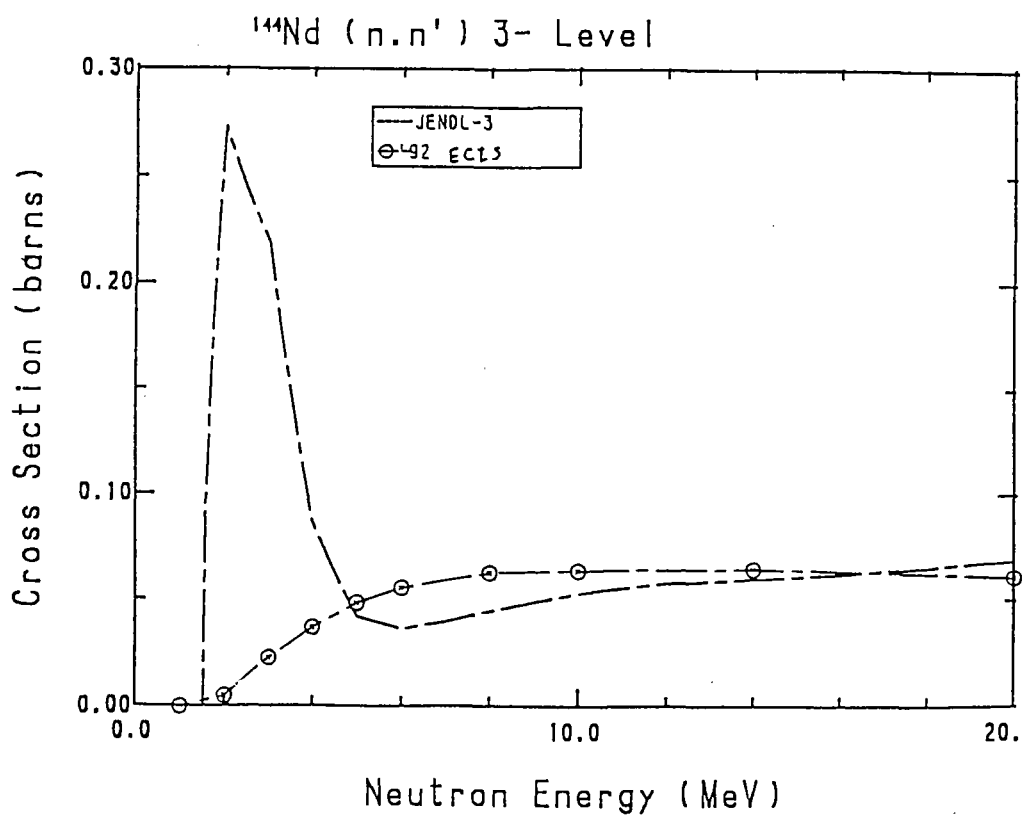

Fig. 1 Comparison of calculated and measured level excitation functions for ^{144}Nd.
JENDL-3 (DWBA calculation) with Ws=9.1MeV,
ECIS (coupled channel calculation) with Ws=7.0MeV.

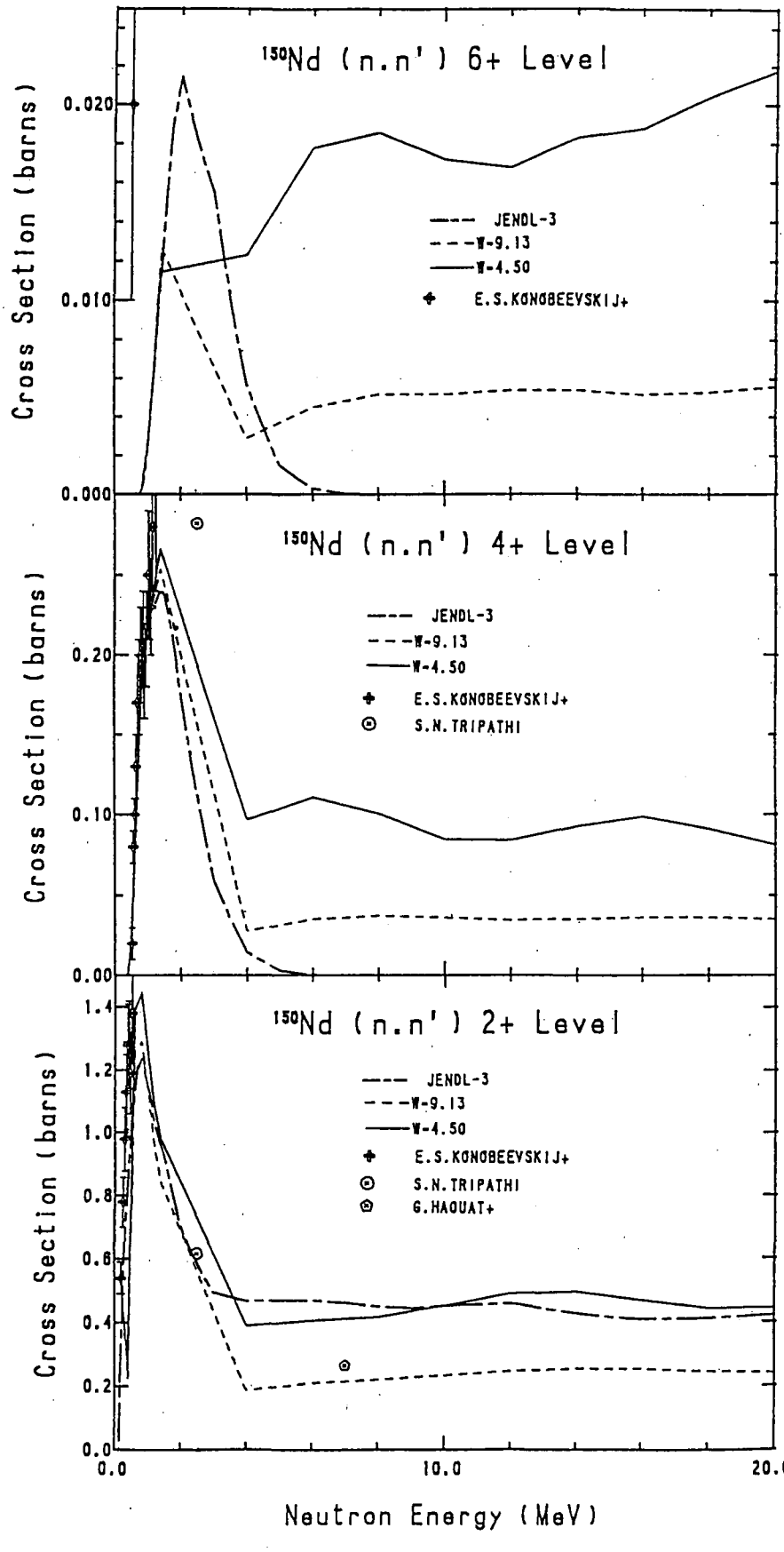

Fig. 2 Comparison of calculated and measured level excitation functions for ^{150}Nd.
JENDL-3 (DWBA calculation) with Ws=9.13MeV,
ECIS (coupled channel calculation) with Ws=9.13MeV and 4.5MeV.

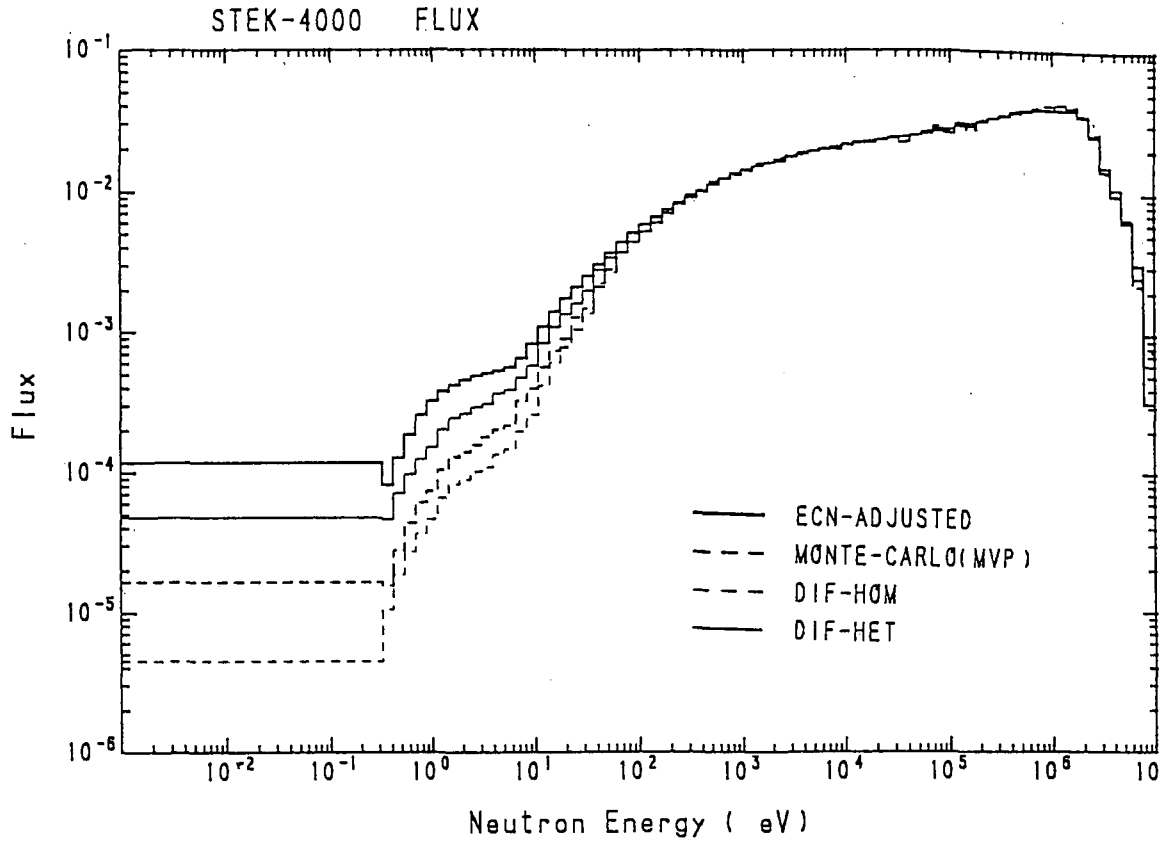

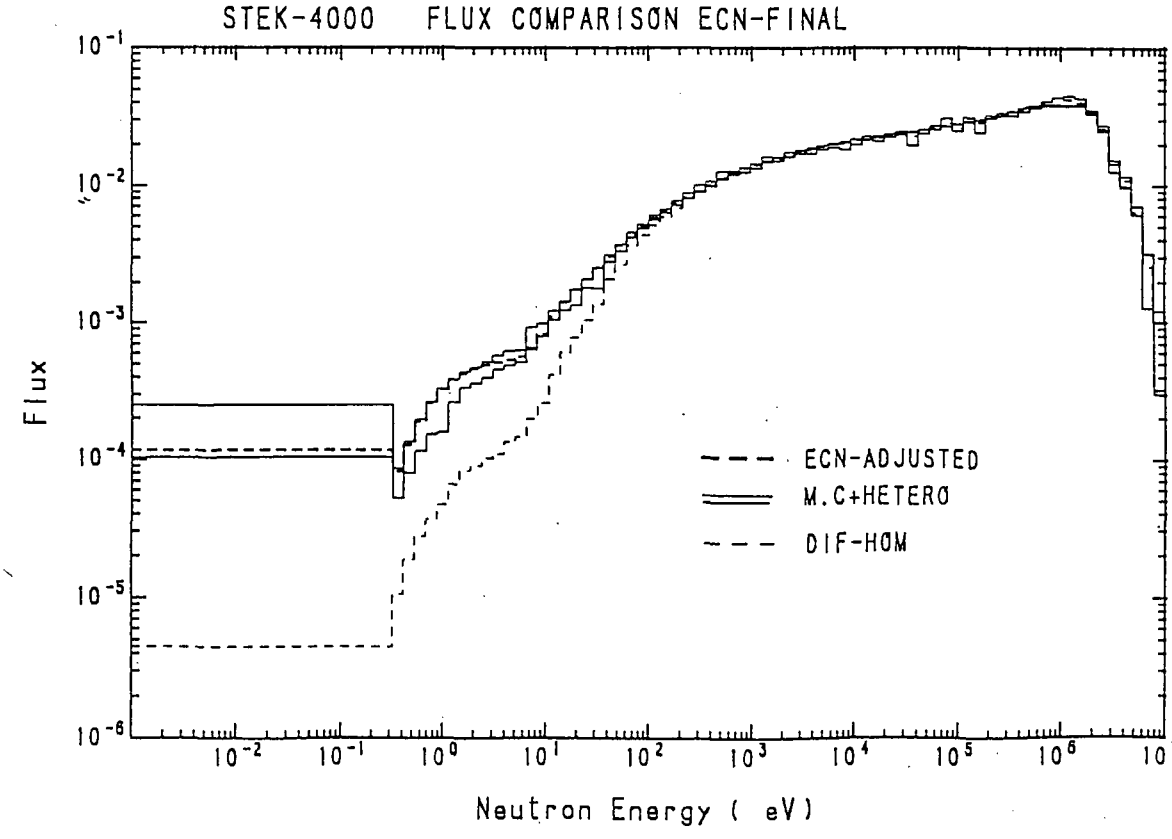

Fig. 3 Comparison of neutron spectra calculated with various models in case of STEK-4000 core.

III. KYOTO UNIVERSITY

A. Research Reactor Institute

III-A-1

Efficiency Correction for Disk Sources Using Coaxial High-Purity Ge Detectors

Hiroshi Chatani

A paper on this subject was published in KURRI-TR-370 (1992), (in Japanese) with the following abstract:

Efficiency correction factors for disk sources were determined by making use of closed-ended coaxial High-Purity Ge (HPGe) detectors, their relative efficiencies for a 3" x3" NaI(Tl) with the 1.3 MeV γ-rays were 30 % and 10 %, respectively. Parameters for the correction by mapping method were obtained systematically, using several monoenergetic (i.e. no coincidence summing loses) γ-ray sources produced by irradiation in the Kyoto University Reactor (KUR) core.

Those were found out that (1) the systematics of the Gaussian fitting parameters, which were calculated using the relative efficiency distributions of HPGe, to the γ-ray energies are recognized, (2) the efficiency distributions deviate from the Gaussian distributions, on the outside of the radii of HPGe, (3) mapping method is a practical use in satisfactory accuracy, as the results of in comparison with the disk source measurements.

III-A-2 Characteristic Behavior of Neutrons in the Lead Slowing-down Spectrometer Coupled to Electron Linac

K.Kobayashi, Y.Nakagome, A.Yamanaka*, S.Yamamoto, Y.Fujita, T.Tamai, S.Kanazawa* and I.Kimura*

A lead slowing-down spectrometer was installed coupling to the 46 MeV electron linear accelerator (linac) at the Research Reactor Institute, Kyoto University (KURRI). With the Kyoto University Lead Slowing-down Spectrometer(KULS), as seen in Fig. 1, characteristics for (1) the relation between neutron slowing-down time and energy, (2) energy resolution, and (3) neutron energy spectrum were obtained by the experiments using neutron resonance filters and/or the linac time-of-flight (TOF) method, and by the continuous energy Monte Carlo code MCNP including time-dependent process. Detailed specific features of the KULS are described elsewhere[1-4].

We have measured the relation between neutron slowing-down time and energy in the bismuth hole and the lead hole. A BF_3 counter (12 mm in diam., 50 mm long, 1 atm.) covered with resonance filter was employed for the measurement of dip structure observed in the time spectrum corresponding to the resonance energy. Since the resonance energies for these filters are well known, we can calibrate the relation between the slowing-down time t and energy E, as an equation of $E=K/(t+t_o)^2$, where K is slowing-down constant and t_o is zero time correction constant. An Ar gas counter (0.5" in diam., 2.5" long, 1 atm.) covered with resonance filter was also used for the measurement of the capture peak corresponding to the slowing-down time. Figure 2 shows the curves which were obtained, by the least squares method, from the neutron slowing-down time and the resonance energy using the BF_3 and the Ar gas counters.

The time spectra which were measured with BF_3 and Ar gas counters were used to derive energy resolution of the KULS. A dip structure by the BF_3 counter and a resonance structure by the Ar gas counter in the time spectrum were fitted to obtain the energy resolution as full width at half maximum (FWHM) with a Gaussian function. These results are shown in Fig. 3.

As one of the characteristic behavior of neutrons in the KULS, the neutron spectrum has been measured by the linac TOF method using the 22 m station. We have measured angular neutron fluxes emitted to 90 degree direction from the bottom of the reentrant hole made at 15 cm distant from the photoneutron target in the KULS. The results are displayed in Fig. 4, comparing with the MCNP calculations.

As summary, the slowing-down constant K in the relation of $E=K/(t+t_o)^2$ has experimentally

* Department of Nuclear Engineering, Kyoto University

been determined to be 190±2 (keV μsec^2) for bismuth and 156±2 (keV μsec^2) for lead hole. The energy resolution of the KULS are around 40 % in the relevant energy region for bismuth and lead holes.

The neutron energy spectra from a few eV to about 10 MeV were also measured by the TOF method and compared with those calculated by the MCNP code using the ENDF/B-IV, JENDL-3 and ENDL-85 cross section data.

References: 1) Y.Nakagome, et al.: JAERI-M 92-027, p.369 (1992). 2) A.Yamanaka, et al.: JAERI-M 92-027, p.375 (1992). 3) K.Kobayashi, et al.: JAERI-M 92-027, p.384 (1992). 4) K.Kobayashi, et al.: JAERI-M 93-046, p.360 (1993).

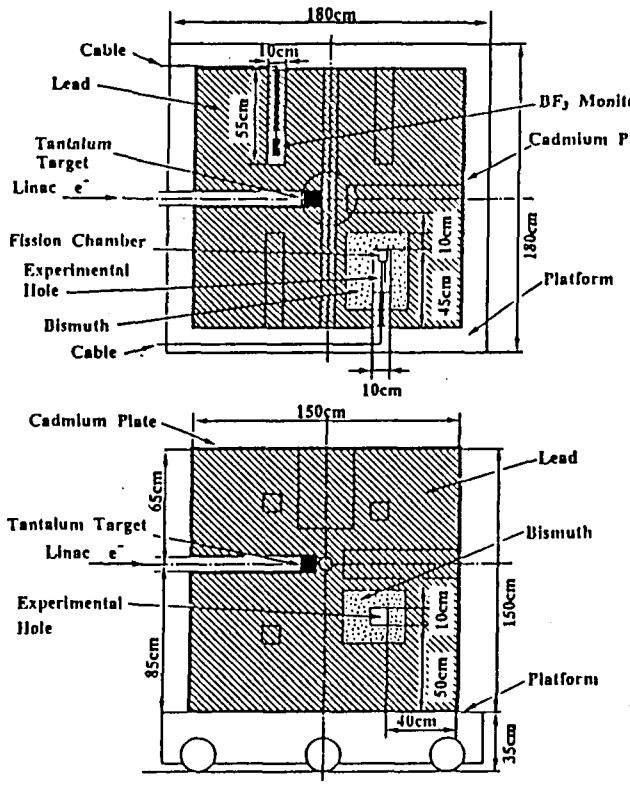

Fig.1 Cross sectional view of the Kyoto University Lead Slowing-down Spectrometer, KULS.

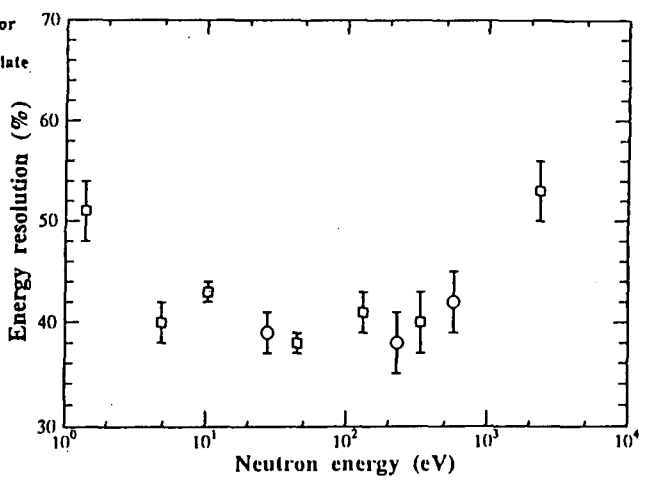

Fig.3 Energy resolution as a function of neutron energy measured with
□ BF_3 counter
○ Ar gas counter.

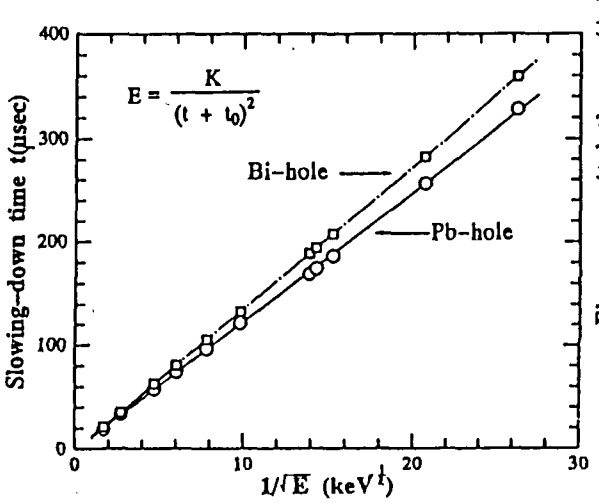

Fig.2 Relation between slowing-down time and energy in the Bi and Pb holes.

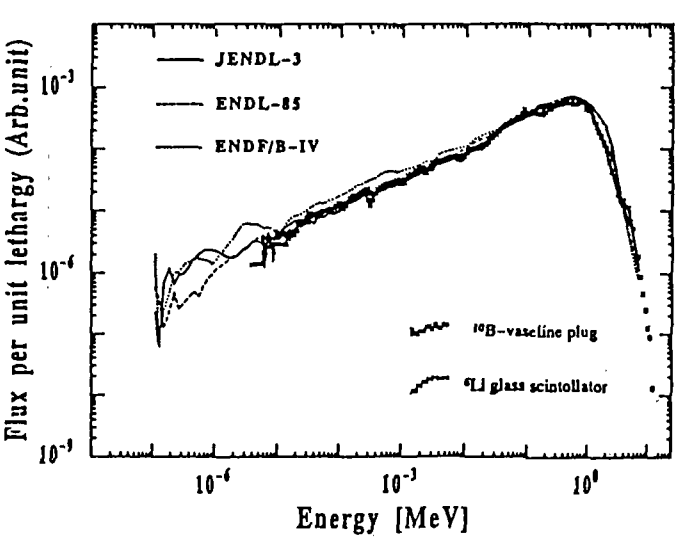

Fig.4 Measured and calculated neutron spectra in the KULS.

III-A-3 Measurement of ^{233}U Fission Spectrum-Averaged Cross Sections for Some Threshold Reactions

Katsuhei Kobayashi

The ^{233}U fission spectrum-averaged cross sections for twelve threshold reactions were measured with a pair of $^{233}U_3O_8$-Al alloy fission foils, which were set at the heavy water thermal neutron facility of the Kyoto University Reactor, KUR. The size of the uranium foils was 12.7 x 12.7 mm^2 and 2 or 1 mm in thickness. Quantity of ^{233}U was about 0.18 g in each 2 mm thick foil. Two or three kinds of sample foils were sandwiched with the uranium foils and irradiated for 24 to 50 hours. Each sample foil is 12.7 mm in diameter and less than 0.5 mm in thickness. Induced activities were measured with HPGe detector whose detection efficiencies had been calibrated. The measured cross sections were normalized to the calculated average cross section for the $^{27}Al(n,\alpha)^{24}Na$ reaction, whose value of 0.688 ± 0.040 mb was obtained with the energy dependent cross section in JENDL Dosimetry File and the Watt-type fission neutron spectrum of ^{233}U appearing in ENDF/B-VI. Present results are shown in Table 1.

In Table 2, the measured average cross sections are compared with the calculated ones making use of the JENDL Dosimetry File and the Watt-type fission spectrum. Most of the calculated average cross sections show good agreement with the measured ones within the experimental uncertainties, except for the $^{24}Mg(n,p)^{24}Na$, $^{47}Ti(n,p)^{47}Sc$ and $^{64}Zn(n,p)^{64}Cu$ reactions.

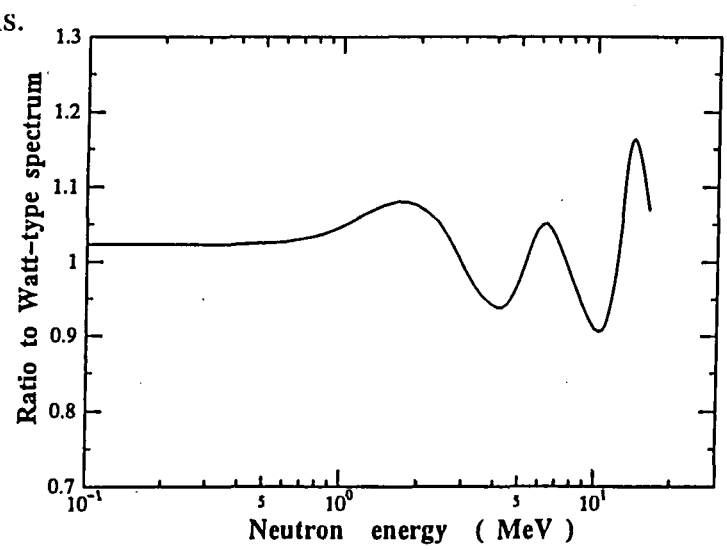

Fig. 1 Ration spectrum of ^{233}U fission neutrons to Watt type-spectrum adjusted with NEUPAC code.

The measured average cross sections were also applied for the spectrum adjustment of the ^{233}U fission neutrons using the NEUPAC code. The adjusted spectrum is displayed in Fig. 1, as a ration spectrum to the Watt-type spectrum. Although there exist some fluctuations in the ratio spectrum, it is recognized that the adjusted spectrum is rather close to the Watt-type spectrum of ^{233}U within the spectrum uncertainty.

Table 1 Present measurement for the ^{233}U fission spectrum-averaged cross sections and the correlation matrix.

Reaction	Measured (mb)	Correlation matrix (x 100)											
24Mg(n,p)24Na	1.40 ± 0.084	100											
27Al(n,p)27Mg	3.87 ± 0.231	95	100										
27Al(n,a)24Na	.688 ± 0.040	97	98	100									
46Ti(n,p)46Sc	11.0 ± 0.65	96	97	98	100								
47Ti(n,p)47Sc	16.6 ± 1.01	97	97	98	98	100							
48Ti(n,p)48Sc	.272 ± 0.0177	97	97	99	98	98	100						
54Fe(n,p)54Mn	74.4 ± 4.24	93	95	96	94	94	95	100					
56Fe(n,p)56Mn	1.04 ± 0.062	94	97	97	96	96	96	96	100				
58Ni(n,p)58Co	101. ± 6.0	96	98	99	98	98	98	95	97	100			
64Zn(n,p)64Cu	33.8 ± 2.04	94	96	97	94	95	96	93	96	97	100		
90Zr(n,2n)89Zr	.0807 ± 0.0054	83	85	86	85	85	85	85	85	86	84	100	
92Nb(n,2n)92mNb	.440 ± 0.0263	95	96	97	96	96	97	94	95	98	95	84	100
115In(n,n')115mIn	190. ± 11.5	94	95	96	96	97	96	92	94	96	94	83	94	100

Table 2 Comparison of measured and calculated ^{233}U fission spectrum-averaged cross sections.

Reaction	Measured (U-233)	Calculated (U-233)	C / M (U-233)
24Mg(n,p)24Na	1.40(6.00)*	1.64(4.69)	1.172
27Al(n,p)27Mg	3.87(5.98)	4.29(6.17)	1.109
27Al(n,a)24Na	.688(5.81)	.688(5.81)	1.000
46Ti(n,p)46Sc	11.0(5.96	11.2(12.8)	1.027
47Ti(n,p)47Sc	16.6(6.07)	19.3(11.4)	1.161
48Ti(n,p)48Sc	.272(6.51)	.278(10.7)	1.025
54Fe(n,p)54Mn	74.4(5.97)	80.7(4.08)	1.085
56Fe(n,p)56Mn	1.04(6.03)	1.06(5.00)	1.019
58Ni(n,p)58Co	101.(5.93)	107.(6.90)	1.061
64Zn(n,p)64Cu	33.8(6.04)	43.1(7.71)	1.277
90Zr(n,2n)89Zr	.0807(6.69)	.0830(3.27)	1.030
92Nb(n,2n)92mNb	.440(5.96)	.440(4.54)	1.001
115In(n,n')115mIn	190.(6.05)	185.(3.03)	.9755

* Numerical values with ( ) show experimental error in %.

III-A-4 Precise Measurement of Neutron Total Cross Section of Pb-208 and Pb-nat

O. Shcherbakov+, S. Yamamoto, K. Kobayashi and Y. Fujita

Neutron total cross sections for enriched Pb-208 and natural Pb have been measured by the time-of-flight (TOF) method using 46 MeV electron linear accelerator (linac) at the Research Reactor Institute, Kyoto University (KURRI). In the present experiment, a resonance capture detector with capture samples of Ta and Sb was used for the neutron transmission measurement, as the neutron detection system. The detector gives high counting peaks in the TOF spectrum corresponding to the resonance energy of the capture sample. In the off-resonance energy region, the event signals are quite low compared to those at the resonances. For the background measurement, Ta and Sb samples, which were same materials as the capture samples, were placed in the TOF beam to black-out neutrons at the resonance. With careful background measurement and by performing a good signal-to-noise ratio transmission measurements for Pb-208 and Pb-nat samples, we can obtain the precise neutron total cross sections, which are expected for the study of electric polarizability of neutrons[1,2].

The experimental geometry is shown in Fig.1, as we had measurements before[3]. The transmission samples were metallic plates of Pb-208 (enrichment:97.65%, Pb-207:1.48%, Pb-206:0.87%), 3.6 cm in thickness with impurities less than 0.003% and of natural Pb (purity: 99.9993%), 4 cm in thickness. Data taking was carried out as we did before[3], using four 2048-channel analyzers which corresponded to each sample (Pb-208, Open, Pb-nat, Open) position on the automatic sample changer. The linac operating conditions and the data reduction process were also almost same as those in the previous measurement[3].

The present preliminary results are shown in Fig.2, with the experimental uncertainties within about 1 %. Both results of Pb-208 and Pb-nat are almost constant with energy, and the Pb-208 values are larger by about 0.4 barns than the Pb-nat. The previous measurements[3] with Pb-nat samples agree well with those measured in this experiment. Concerning the Pb-208 measurements, recent values by Alexandrov[1] and Schmiedmayer[2] are in good agreement with the preliminary data.

References:

1) Y.A.Alexandrov, et al.: Proc. Nucl. Data for Sci. Technol., Springer-Verlag, p.160 (1992).

+ Visiting Scientist from Petersburg Nuclear Physics Institute, Gatchina, Russia

2) J.Schmiedmayer, et al.: ibid., p.163 (1992).
3) K.Kobayashi, et al.: Nucl. Instr. Meth., A287, 570 (1990).

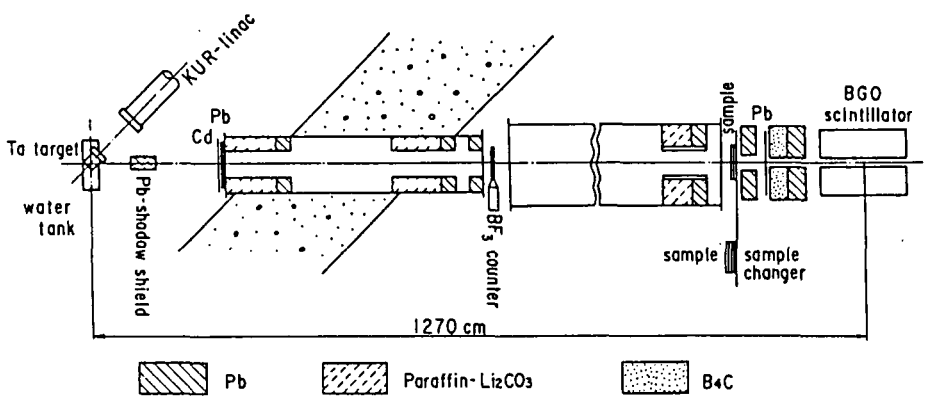

Fig.1 Experimental arrangement for the transmission measurement.

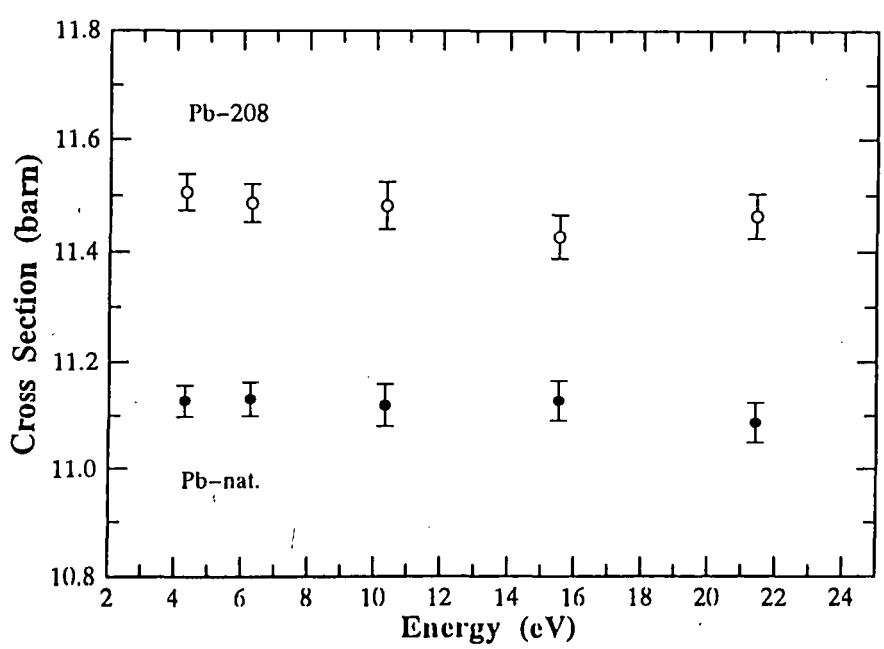

Fig.2 Present results of neutron total cross sections of Pb-208 and Pb-nat measured by the transmission method using a resonance capture detector.

III-A-5 Measurement of Fission Cross Section of Neptunium-237 in Resonance Region with Electron Linac-Driven Lead Spectrometer

A.Yamanaka*, I.Kimura*, S.Kanazawa*K.Kobayashi, S.Yamamoto, Y.Nakagome, Y.Fujita and T.Tamai

A paper on this subject will be published with the following abstract in Journal of Nuclear Science and Technology, soon.

Making use of a lead neutron slowing-down spectrometer combined with an electron linear accelerator and back-to-back type double fission chamber, we measured the fission cross section of neptunium-237 relative to that of uranium-235 from about 1 eV to about 5 keV with energy resolution of about 40 %. The experimentally obtained result has been compared with two newly evaluated data files, JENDL-3 and ENDF/B-VI, and with previously measured values by Plattard et al. and by Hoffman et al. Although the shape of the present energy dependent cross section agrees with that of ENDF/B-VI, that of JENDL-3 below 130 eV and that of Plattard et al., the absolute values of above three are from 3 to 4 times smaller than those of the present data. However the Hoffman et al.'s data are rather closer to the present data.

* Department of Nuclear Engineering, Kyoto University

III-A-6 Measurements of Thermal Neutron Cross Section and Resonance Integral for the $^{237}Np(n,\gamma)^{238}Np$ Reaction

K. Kobayashi, A. Yamanaka[*,+] and I. Kimura[*]

Thermal neutron cross section for the $^{237}Np(n,\gamma)^{238}Np$ reaction was measured at the heavy water thermal neutron facility of the Kyoto University Reactor, KUR. The resonance integral for the same reaction was also measured with the 1/E standard neutron spectrum field in the cavity of graphite reflector of the Research Reactor, UTR-KINKI. The neptunium samples were prepared in the form of dried filter-paper with a drop of the sloution, and the amount of ^{237}Np atoms was determined to be 10^{16} to 10^{17} for each sample. Induced activities of ^{238}Np were simultaneously measured with the ^{233}Pa activities which were in radioactive equilibrium to ^{237}Np making use of a calibrated HPGe detector.

Thermal neutron flux was monitored with gold foil of 3 mm in diameter and 50 μm thick and/or with AuAl alloy wire, 0.0314 percent in weight of gold, 0.5 mm in diameter. The thermal neutron cross section for the $^{237}Np(n,\gamma)^{238}Np$ reaction was measured relative to the reference value of 98.65 $\pm$ 0.09 b for the $^{197}Au(n,\gamma)^{198}Au$ reaction. The experiment was independently repeated six times, and reproducibility of the measurement was good. The thermal neutron cross section is summarized in Table 1. The present value is lower by about 10 % than that with the ENDF/B-V data. The data given by Mughabghab and obtained from JENDL-3 are larger more than 10 % than the present measurement.

The resonance integral for the $^{237}Np(n,\gamma)^{238}Np$ reaction was measured relative to 1550 $\pm$ 28 b for the $^{197}Au(n,\gamma)^{198}Au$ reaction. Gold foil, which was put in the Cd-cover of 0.5 mm in thickness, was 12.7 mm in diameter and 50 μm thick, and the correction factor for the neutron resonance self-shieldings in the foil was derived by the Monte Carlo code VIM. The measured result is shown in Table 2, comparing with earlier data. Defining the Cd cut-off energy as 0.5 eV, present resonance integral is 646 b, which is in good agreement with the JENDL-3, ENDF/B-V and Mughabghab data.

---

[*] Department of Nuclear Engineering, Kyoto University,
[+] Present address: Hitachi Works, Hitachi, Ltd.
Saiwai-cho, Hitachi-shi, Ibaraki 317, Japan

Table 1 Thermal neutron cross section for the $^{237}Np(n,\gamma)^{238}Np$ reaction

Present	154.7 ± 2.9 b
JENDL-3	181.0
ENDF/B-V	169.1
Mughabghab('84)	175.9 ± 2.9
IAEA handbook('87)	169 ± 3
Eberle('71)	187 ± 6
Hellstrand('70)	172

Table 2 Resonance integral for the $^{237}Np(n,\gamma)^{238}Np$ reaction

Present (without Cd cut-off correction)	920 ± 78 b
Present (with Cd cut-off correction)	646 ± 55
JENDL-3	663.0
ENDF/B-V	662.6
Mughabghab('84)	640 ± 50
IAEA handbook('87)	821.5 ± 58.0

III-A-7

Fission Cross Section Measurement of ^{241}Am with Lead Slowing-Down Spectrometer

K.Kobayashi, M.Miyoshi*, S.Yamamoto, I.Kimura*,
I.Kanno*, S.Kanazawa* and Y.Fujita

A lead slowing-down spectrometer was installed beside the 46 MeV electron linear accelerator (linac) at the Research Reactor Institute, Kyoto University (KURRI). The characteristics of this Kyoto University Lead Slowing-down Spectrometer (KULS) have been obtained in the previous work[1,2]. By making use of the KULS, we have measured the cross section for the ^{241}Am(n,f) reaction relative to that for the ^{235}U(n,f) reaction in the energy region from 0.05 eV to about 10 keV. In the present measurement, the experimental arrangement and the procedures are same as the previous experiment[2]. A back-to-back type double fission chambers[3] were employed, and electrodeposited films of ^{241}Am and ^{235}U were put into the chambers filled with a mixed gas of 97 % Ar and 3 % N_2 at 1 atm.

Operating the KURRI linac for about 200 hours, the ^{241}Am(n,f) reaction cross section has been obtained as displayed in Fig.1, where the statistical uncertainty is within the size of the mark. The present preliminary data are normalized to the ENDF/B-VI value at 1 keV. From the figure, it is seen that (1) although the gross shape of the preliminary result is close to those in ENDF/B-VI and JENDL-3, (2) the JENDL-3 data underestimates the present result between 10 to 200 eV and (3) the JENDL-3 and ENDF/B-VI data overestimates at energies from 0.3 to 2 eV, respectively. Next, we are going to have absolute values of the preliminary result by the measurement of number of atoms for the ^{241}Am and ^{235}U samples using the alpha spectrometry.

References:

1) K.Kobayashi, et al.: JAERI-M 93-046, p.360 (1993).
2) A.Yamanaka, et al.: J. Nucl. Sci. Technol., in print.
3) M.Obu: JAERI-M 9757 (1981).

* Department of Nuclear Engineering, Kyoto University

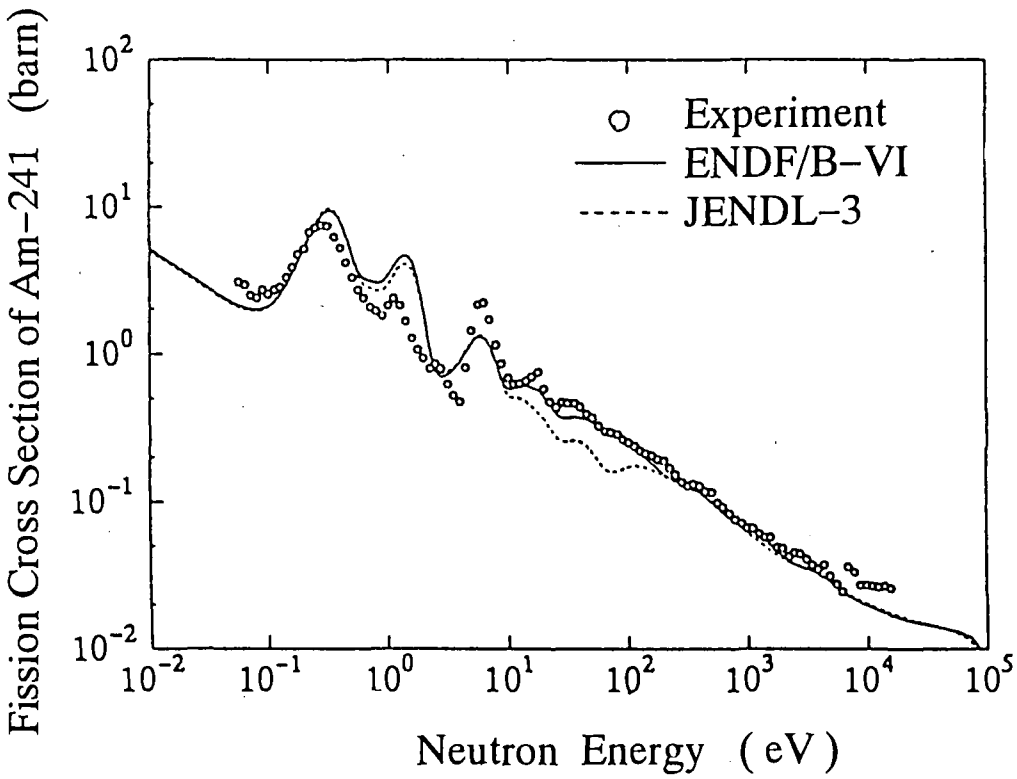

Fig. 1 Preliminary result for the ^{241}Am(n,f) reaction cross section, comparing with the evaluated cross sections.

IV. KYUSHU UNIVERSITY

A. Department of Nuclear Engineering

IV-A-1 Spallation Neutron Measurement at Incident Proton Energies of 0.8 to 3 GeV

K. Ishibashi, T. Nakamoto, N. Matsufuji, K. Maehata,
Y. Wakuta, Y. Watanabe*, M. Numajiri**, H. Takada+,
S. Meigo+, S. Chiba+ and T. Nakamura++

A paper on this subject was presented at the 12th International Collaboration on Advanced Spallation Sources, May 24-28, 1993, Abingdon, U.K.

It has been experimentally confirmed that the high-energy nucleon (proton or neutron) spectra from the nuclear spallation reaction are in good agreement with the results of the cascade calculation. However, low-energy nucleon spectra below several 10 MeV have not been measured for the spallation reaction for incident protons of GeV range. The experiment on the neutron-emission double-differential cross section was carried out at proton energies of 0.8, 1.5 and 3 GeV at KEK. The neutrons were measured by the time-of-flight method with a typical flight path of 1 m. The experiment for C and Pb targets was completed in November 1992. Neutrons having energies of 1 to 300 MeV were successfully measured with acceptable uncertainty. Some results are shown in Figs. 1 and 2. The calculated results deviate from the experimental data below 100 MeV in the case of 3 GeV proton incidence. Measurements for targets of Al, Fe and In will be continued during the summer of 1993.

* Interdisciplinary Graduate School of Engineering Sciences, Kyushu University.
** National Laboratory for High Energy Physics (KEK).
+ Japan Atomic Energy Research Institute.
++ Cyclotron and Radioisotope Center, Tohoku University.

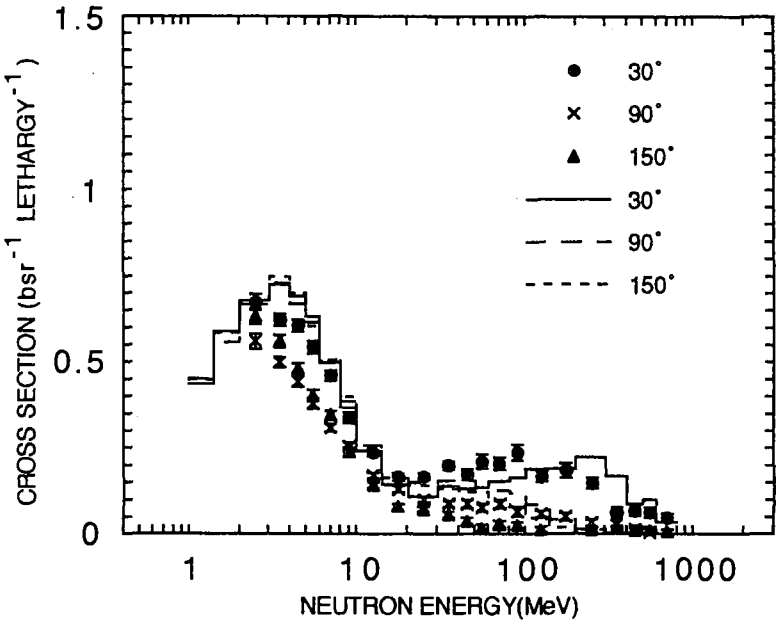

Fig. 1 Experimental (p,xn) cross sections for 0.8 GeV proton incidence on Pb. Lines show the results of HETC calculation (cascade-evaporation model). The lethargy of $\ln(E_{n+1}/E_n)$ is used for linearizing the vertical axis.

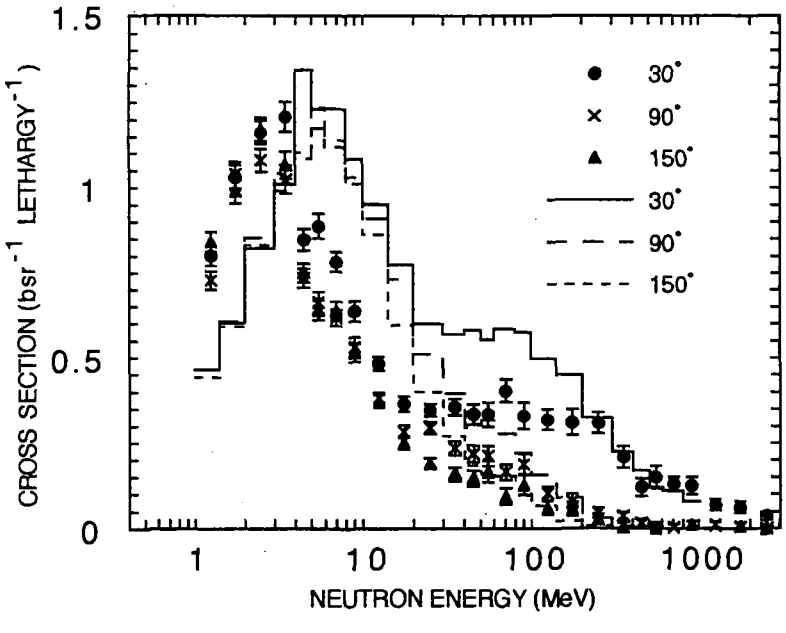

Fig. 2 Experimental (p,xn) cross sections for 3.0 GeV proton incidence on Pb. Lines show the results of HETC calculation (cascade-evaporation model). The lethargy of $\ln(E_{n+1}/E_n)$ is used for linearizing the vertical axis.

IV-A-2 Inclusion of Preequilibrium Calculation into High Energy Transport Code

K. Ishibashi, H. Takada*, Y. Yoshizawa**, N. Matsufuji, T. Nakamoto,
Y. Wakuta and Y. Nakahara*

A paper on this subject was presented at the 12th International Collaboration on Advanced Spallation Sources, May 24-28, 1993, Abingdon, U.K.

The High Energy Transport Code (HETC) has been widely used for engineering purposes in the incident energy region of a hundred to several thousand MeV. We incorporate the preequilibrium calculation into the HETC with a smooth connection to the cascade process. The preequilibrium process is introduced to retain a clear physical meaning both in the connection method and in the initial number of particles and holes. The calculation results are compared with the experimental preequilibrium spectra which have been decomposed[1] from experimental data by the moving source model, as shown in Fig. 1. The computation results by the cascade-preequilibrium-evaporation model (three-step model) are shown by solid lines in Figs. 2 to 4, where experimental data[2-4] are plotted by marks. The present calculation results successfully reproduce the backward neutron spectra particularly at incident energies of 25.5 and 113 MeV. The cascade-preequilibrium-evaporation model is confirmed to be applicable to the incident proton energies from 20 MeV to 1 GeV.

References:

1) K. Ishibashi et al.: J. Nucl. Sci. Technol. 29 (1992) 499.
2) M.M. Meier et al.: Nucl. Sci. Eng. 102 (1989) 310.
3) K. Harder et al.: Hamburg University HH87-01 (1987).
4) W. Amian et al.: Nucl. Sci. Eng. 112 (1992) 78.

* Japan Atomic Energy Research Institute
** Mitsubishi Research Institute, Co.

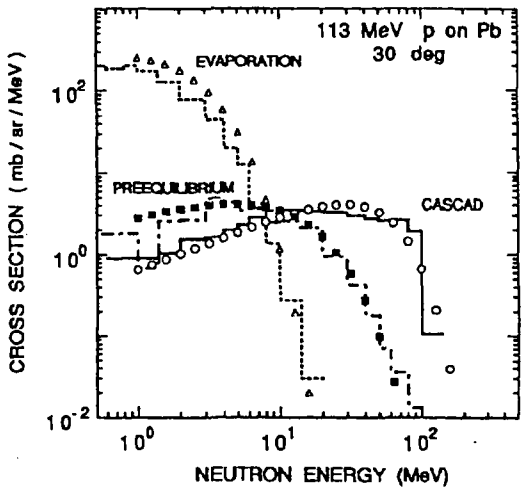

Fig. 1 Decomposed neutron spectra. Marks stand for the experimental data separated by the moving source model.[1)]

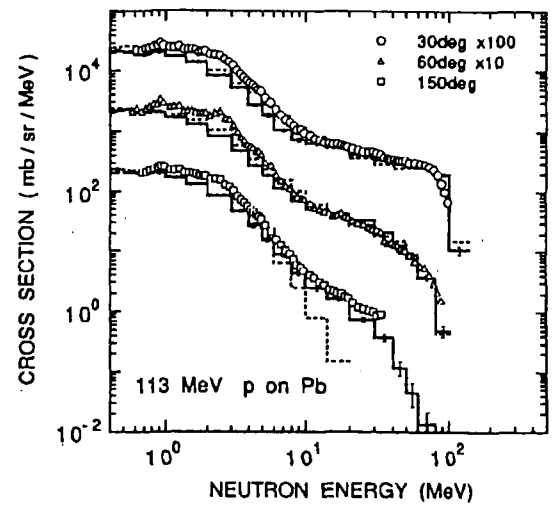

Fig. 2 Experimental[2)] and calculational (p,xn) cross section. Dashed and solid lines show two- and three-step calculations, respectively.

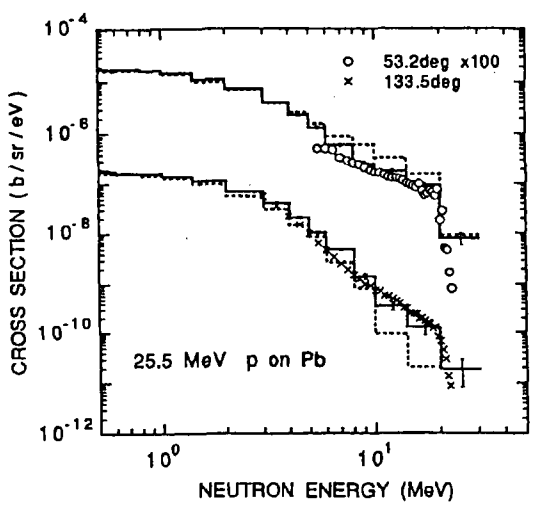

Fig. 3 Experimental[3)] and calculational (p,xn) cross section. Dashed and solid lines show two- and three-step calculations, respectively.

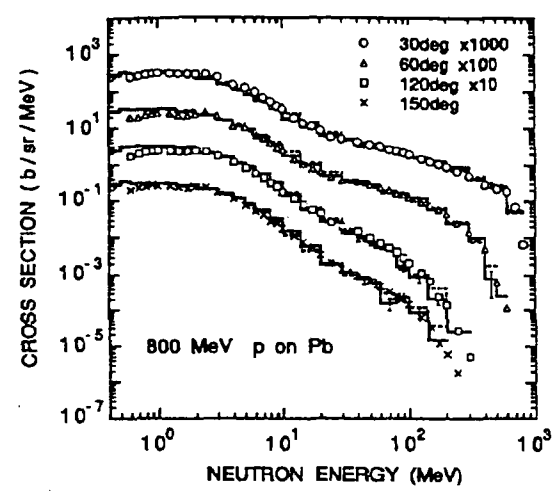

Fig. 4 Experimental[4)] and calculational (p,xn) cross section. Dashed and solid lines show two- and three-step calculations, respectively.

B. Department of Energy Conversion Engineering

IV-B-1 Estimation of Real Surface Term of Optical Potential for ^{209}Bi in Low Energy Region

T. Kawano, K. Kamitsubo, T. Iwamoto, N. Fujikawa and Y. Kanda

A paper on this subject was presented at the 1992 Symposium on Nuclear Data, and published in JAERI-M 93-046, P.222, with the following abstract:

An imaginary part of the optical potential is consisted of both volume and surface absorption types. When a dispersion relation between real and imaginary potential is considered, the contribution of the volume type imaginary potential is embedded in the real potential while the surface type imaginary potential causes the surface peaked component in the real potential. We attempt to estimate this surface peaked real potential of ^{209}Bi. In addition, we fit a Brown-Rho parametrization to the imaginary potential of a conventional optical model analysis, and we estimate the energy dependencies of the optical potential parameters due to the dispersion relation.

IV-B-2 Methods of Covariance Generation for Nuclear Data

Y. Kanda

A paper on this subject was presented at the 1992 Symposium on Nuclear Data, and published in JAERI-M 93-046, P.110, with the following abstract:

Covariances for evaluated cross sections are generated with the methods based on the uncertainties of experimental data or estimated by combining experimental and theoretical information. The former methods are in principle preferred but are limited in application because a lack of experimental information. The latter methods are available in many cases. However, they have been generated with the procedures which are adopted by individual evaluators as to adapt to their understanding for covariances. The values of the estimated covariances which decisively depend on the adopted procedures are too different at every evaluation to be agree by other evaluators and be accepted by users of them. In order to arrive at an agreement about the definitive understanding of the covariance generation we must discuss on this problem. It is another problem to solve the one mentioned above that the method to visualize the covariance must be developed to quantitatively compare it with the other.

IV-B-3 Generation of Covariance Data from Combined Experimental and Theoretical Data

Y. Kanda

A paper on this subject was presented at the NEANSC Specialists' Meeting on Evaluation and Processing of Covariance Data, 7–9 Oct., Ork Ridge, USA, and published in NEA/NSC/DOC(93)3, p.119, (Ed. M. Wagner), with the following abstract:

Covariances for evaluated nuclear data can be usefully estimated by combining experimental and theoretical information. In this report, the covariances generated on various assumptions are compared to search their significance by using neutron-induced reactions of ^{56}Fe and ^{54}Fe as examples. The theoretical information used to calculate their cross sections are the Hauser-Feshbach formulae and the parameters required in it. Only level density parameters are considered as the sources of the theoretical uncertainly and the other parameters used in the cross section calculation such as optical model parameters are fixed. A reference correlation (a covariance matrix is factored to a correlation matrix and a standard deviation vector) is the resultant one calculated with prior level density parameters which originate in Gilbert-Cameron. The prior level density parameters are adjusted to make the calculated cross sections fitting to the experimental encounters as possible, and then the new covariance estimated with the adjusted level density parameters is obtained, called the posterior covariance. Comparing the posterior with the prior, the effect of the experimental information to the resultant covariance can be estimated. This makes it clear that the posterior correlation is finely changed as that correlation at the further distance is smaller than the prior (the reference). It is reasonably understood i.e. short rang correlation is strengthen through the experimental data. In addition, the effects of the correlation between level density parameters and between experimental points in the identical set are studied. They are small. On the basis of these works, the useful method of the covariances estimation from combined experimental and theoretical data can be developed.

IV-B-4 Measurement of double differential charged-particle emission cross sections for reactions induced by 26 MeV protons

Y. Watanabe, H. Kashimoto, H. Sakaki, Y. Koyama, H. Shinohara, T. Michibata, Y. Kanda, N. Koori* , S. Chiba**, T. Fukahori**, K. Hasegawa**, M. Mizumoto**, and S. Meigo**

A paper on this subject was submitted to Tandem ANNUAL REPORT 1992, Japan Atomic Energy Research Institute, with the following abstract:

Double differential charged-particle emission cross sections have been measured for proton-induced reactions on ^{12}C, ^{27}Al, ^{106}Pd, ^{159}Tb, and ^{181}Ta at 26 MeV, in order to investigate preequilibrium process and multiparticle breakup process. The measured (p,xp) and (p,α) energy spectra are compared with those calculated using a code EXIFON based on the statistical multistep direct and compound (SMC/SMD) model.

* The University of Tokushima, Tokushima 770
** Japan Atomic Energy Research Institute

IV-B-5 A semiclassical distorted wave model analysis of one-step process in proton inelastic scattering to continuum

Y. Watanabe and M. Kawai*

A paper on this subject will be published in Nuclear Physics A with the following abstract:

The semiclassical distorted wave model of one-step inelastic scattering recently developed is extended to include the effects of non-locality of distorting potentials and energy and angle dependence of two-nucleon scattering cross sections, and is applied to calculation of (p,p'x) cross sections for target nuclei ranging from ^{54}Fe to ^{209}Bi at incident energies ranging from 62 to 200 MeV. The model reproduces experimental cross sections, including the absolute magnitude, at forward angles and high energies of the outgoing protons. The effects of the corrections on the calculated cross sections, and comparisons with other models are discussed.

1

As the next stage, an extended version[1)] of this model considering multistep direct process is now being implemented for calculations of nucleon inelastic scattering as well as charge-exchange reaction such as (p,n) and (n,p) reactions, in order to check the applicability of the model to nuclear data evaluation at intermediate energies.

References:

1) M. Kawai and H.A. Weidenmüller, Phys. Rev. C 45, 1856 (1992)

* Department of Physics, Kyushu University

IV-B-6 Study of ^{12}C Breakup Processes and Carbon Kerma Factors

H. Kashimoto, Y. Watanabe, Y. Koyama, H. Shinohara, and S. Chiba*

A paper on this title was presented at the 1992 Symposium on Nuclear Data, and published in JAERI-M 93-046, with the following abstract:

Recent studies of ^{12}C breakup processes in nucleon-induced reactions are reported with the following subjects: (i) analyses of spectra of protons and a-particles emitted from proton-induced reactions at 14, 16, and 26 MeV, (ii) development of a Monte Carlo computer code to simulate successive sequential breakup decay from reactions with ^{12}C induced by nucleons, and (iii) application of the results to calculations of carbon kerma factors at incident energies ranging from 10 to 20 MeV.

In addition, the above-mentioned Monte Carlo (SCINFUL/DDX) code has recently been extended as so to include kerma factor calculations. A preliminary result of ^{12}C-kerma factors gives good agreement with recent experimental data[1)] at high neutron incident energies. Improvement on the code is now in progress to apply this code to evaluation of DDXs of all emitted particles including some recoil nuclei and total and partial kerma factors for interaction of neutrons with ^{12}C.

Reference:

1) U.J. Schrewe et al., Proc. of Int. Conf. on Nuclear Data for Science and Technology, Jülich, Germany, 13-17 May, 1991 (Springer-Verlag, 1992), pp.586

* Japan Atomic Energy Research Institute

IV-B-7 FKK analysis of proton-induced reactions on medium-heavy nuclei in the 10-30 MeV region

Y. Watanabe, M.B. Chadwick* and P.E. Hodgson**

The quantum-mechanical theory of Feshbach, Kerman and Koonin[1] has been used extensively by various authors to analyze preequilibrium nucleon emission data. Recently, it has been recognized that there is an appreciable MSD contribution even at low incident energies through some analyses of (n,n') data[2,3]. In order to confirm this, it is also desirable to analyze proton-induced reactions which are complementary to neutron-induced reactions. This analysis is useful to obtain more reliable conclusions because the proton data is usually more precise than the neutron data.

In the present work, the codes[2,3] based on the FKK theory are applied to analyze recent experimental (p,p') data[4] for ^{98}Mo and ^{106}Pd at incident energies from 12 to 26 MeV and also (p,n) data[5] for the same targets at 26 MeV only. The aim of the work is to derive the fraction of MSD and MSC processes at low incident energies and to investigate whether a consistent description of (p,p') and (p,n) data is possible by using the same approximation and parameters in the FKK calculation. The result is also compared with the analysis of (n,n') and (n,p) reactions at similar incident energies in order to obtain a unified understanding of preequilibrium nucleon emission from nucleon-induced reactions.

So far, the sensitivity of MSD cross sections to the optical model potential (OMP) parameters has been investigated in a preliminary analysis, and the importance of a suitable choice of OMP parameter sets is indicated. Further detailed analysis of (p,p') and (p,n) reactions is now in progress.

References:

1) H. Feshbach, A. Kerman and S. Koonin, Ann. Phys. **125**, 429 (1980)
2) M.B. Chadwick and P.G. Young, Phys. Rev. C **47**, 2255 (1993)
3) H.B. Olaniyi, P. Kanjanarat and P.E. Hodgson, J. Phys. G, **19**, 1029 (1993)
4) Y. Watanabe et al, Z. Phys. A **336**, 63 (1990); JAERI-M 92-027, pp.330 (1992) and JAERI-M 93-043, pp.297 (1993)
5) E. Mordhorst et al., Phys. Rev. C **34**, 103 (1986); S. Hölbling et al., Z. Phys. A **338**, 11 (1991)

Work performed in part under the auspices of the US Department of Energy by the Lawrence Livermore National Laboratory under contact W-7405-ENG-48.

* Lawrence Livermore National Laboraory, Livermore, California, U.S.A.
** Nuclear Physcis Laboratory, Physics Department, Unversity of Oxford, U.K.

V. NAGOYA UNIVERSITY

A. Department of Nuclear Engineering

V-A-1 Measurement of Formation Cross Sections producing Short-lived Nuclei by 14 MeV Neutrons

Y. Kasugai, A. Tanaka, M. Asai, H. Yamamoto, T. Iida* and K. Kawade

Eighteen neutron activation cross sections for (n,2n), (n,p), (n,n'p), (n,t) and (n,α) reactions producing short-lived nuclei with half-lives between 42 s and 42 d have been measured in the energy range of 13.4 to 14.9 MeV for Mg, S, Ga, Y, Mo, Pd, Sn, Ta and W. The d-T neutrons were generated by an intense 14 MeV neutron source facility (OKTAVIAN) of Osaka University. Measured reactions: (n,2n); $^{181}Ta^{g}$, $^{186}W^{g}$, (n,p); $^{119}Sn^{m}$, ^{181}Hf, $^{182}W^{m}$, ^{184}W, ^{186}W, (n,n'p); ^{26}Mg, $^{98}Mo^{m}$, $^{100}Mo^{m}$, $^{106}Pd^{m}$, $^{181}Ta^{m}$, (n,t); ^{32}S, (n,α); $^{71}Ga^{m}$, $^{181}Ta^{m}$, 184W, 186W. Here [(n,2n); $^{181}Ta^{g}$] means $^{181}Ta(n,2n)^{180g}Ta$.

Half-lives of ^{107m}Pd and ^{107m}Ag produced by 14 MeV neutron bombardments were measured with Ge detectors in the spectrum multi-scaling mode; 20.78±0.09 s for ^{107m}Pd and 43.03±0.28 s for ^{107m}Ag.

* Osaka University

V-A-2

Measurement of Formation Cross Section of Short-lived Nuclei by 14 MeV Neutrons - Ru, Pd, Cd, Sn -

Y. Kasugai, A. Tanaka, M. Asai, H. Yamamoto, T. Katoh, T. Iida*, A. Takahashi* and K. Kawade

A paper on this subject was published in JAERI-M 93-124(1993).

Abstract

Eighteen neutron activation cross sections for (n,2n), (n,p), (n,n'p) and (n,α) reactions producing short-lived nuclei with half-lives between 21 s and 21 min have been measured in the energy range of 13.4 to 14.9 MeV for Ru, Pd, Cd and Sn.

Half-lives of ^{105m}Rh, $^{120m1}In$ and $^{120m2}In$ produced by 14 MeV neutron bombardments were measured with Ge detectors in the spectrum multi-scaling mode.

* Osaka University

V-A-3 Decay Scheme of Mass-separated ^{152}Nd

M. Shibata, M. Asai, T. Ikuta, H. Yamamoto, J. Ruan[1], K. Okano[2], K. Aoki[3], and K. Kawade

A paper on this subject was published in Appl. Radiat. Isot. 44.923(1993).

Abstract

Gamma-rays and internal conversion electrons in the decay of 1.6-min ^{152}Nd were measured. The radioactive sources were separated from the fission products of ^{235}U(n,f) with an on-line isotope separator (KUR-ISOL). A precise decay scheme of ^{152}Nd involving 35 γ-rays and 12 levels has been established. The 25 γ-rays and 7 levels were observed for the first time.

[1] Rikkyo University
[2] Research Reactor Institute, Kyoto University
[3] Himeji Institute of Technology

V-A-4 Low-Lying Levels in ^{147}Nd in the Decay of ^{147}Pr

M. Shibata, A. Taniguchi, H. Yamamoto, K. Kawade, J. Ruan[1], T. Tamai[2], Y. Kawase[2] and K. Okano[2]

A paper on this subject was published in J. Phys. Soc. Jpn. 62, 87(1993).

Abstract

The level structure of ^{147}Nd has been studied from the decay of ^{147}Nd. The radioactive sources of ^{147}Pr were separated from the fission products of ^{235}U using the on-line isotope-separator KUR-ISOL and chemical separation techniques. A decay scheme has been constructed involving 93 γ-rays and a newly observed 126.1 keV level. The half-lives of 49.9, 127.8 and 214.6 keV levels were determined to be 1.0±0.3 ns, 0.4±0.1 ns and 4.53±0.06 ns, respectively. Conversion coefficients of 15 transitions were determined. The parities for the levels at 49.9, 127.8, 214.6, 314.7 and 463.5 keV are deduced to be odd. Spins and parities for the 769.3 and 792.6 keV levels are deduced to be $3/2^+$. The properties of transition probabilities between the low -lying triplet hole states are similar to that of three particle states in the N=85 isotones.

[1] Rikkyo University
[2] Research Reactor Institute, Kyoto University

VI. OSAKA UNIVERSITY

A. Department of Nuclear Engineering

VI-A-1 Measurement of DDX Charged Particle Cross Sections With 14.1 MeV Incident Neutrons

A. Takahashi, Y. Murakami and H.Nishizawa

A charged particle spectrometer based on the two-dimensional E-TOF analysis was developed[1] to measure DDX charged particle cross sections with a pulsed D-T neutron source OKTAVIAN. The pulse shape discrimination technique applied to signals from a CsI(TI) scintillation detector was quite effective to eliminate background signals and measure separately proton and alpha-particle events.

DDX data of proton emission were obtained for iron, nickel and cobalt at 5 angle points[2][3]. The theoretical model calculations, currently being applied in the evaluation works, reproduced successfully the measured proton DDX data for three elements and the α-praticle DDX data for iron.

DDX data of α-particle emission were also measured for iron, Be-9 and C-12[3][4]. A model calculation for Be based on the competing process of sequential and multi-body breakup processes of particle emissions could consistently reproduce both the neutron and α-particle DDX data by experiments. The ENDF/B-VI evaluation for Be-9 is satisfactory.

1) Ogino,S.,Takahashi, A.:JAERI-M 90-025(1990)
2) Ogino,S.,et al.:OKTAVIAN Rep.A91-01(1991)
3) Takahashi,A.et al.:"Measurement of DDX charged particle cross sections with 14.1MeV incident neutrons",preprint presented at Int.WS. Nuclear Data for Fusion Reactor Technology,Del Mar Cal.USA,May3-6,1993
4) Murakami,Y.,et al.:JAERI-M 93-046(1993)324

VII. RIKKYO (St. Paul's) UNIVERSITY

A. Department of Physics

VII-A-1 Measurements of the Neutron Scattering Cross Sections for ^{12}C, ^{16}O, ^{40}Ca and ^{56}Fe at 14.2 MeV

S. Shirato, T. Nishio and Y. Ando

Double differential cross sections (DDX) for elastic and inelastic neutron scattering from ^{12}C, ^{16}O, ^{40}Ca and ^{56}Fe at 14.2 MeV, which were measured at forward angles from 10° to 70° in 10° increments using the neutron time-of-flight (TOF) facility of the 300 kV Cockcroft-Walton accelerator of Rikkyo University, have been preliminarily analyzed.

Neutron TOF spectra were obtained from the signals of scattered neutrons and the associated α-particles produced in the $^{3}H(d,n)^{4}He$ reaction at 165 keV, using an NE213 liquid scintillator of 10 cm ϕ x 30 cm for the neutron detector and a thin (50 μm) NE102A plastic scintillator for the α-particle detector[1]. The characteristics of the cylindrical scatterers in this experiment using ^{nat}C, CH_2, ^{nat}Fe, ^{nat}Ca and ^{nat}CaO are given in Table 1. Cross sections were obtained absolutely using the neutron detection efficiency calculated by the Kurz code[2] and also checked in relative to the absolute ones measured with the 2 in ϕ x 2 in neutron detector[3,4] for ^{nat}C, CH_2 and ^{nat}Fe.

Measured energy spectra (DDX) of scattered neutrons should be reported in the near future[5] in comparison with the theoretical curves[6] based on the evaluated data JENDL-3.

In general, measured angular distributions for elastic scattering[5] are in agreement with optical model calculations using the parameters[7-10] given in Table 2 and with JENDL-3. However, small discrepancies (< 30%) between the optical model and the JENDL-3 predictions are found in a CM angular region around 50° for ^{12}C, ^{16}O and ^{56}Fe. The present elastic data on ^{40}Ca are in good agreement with the JENDL-3 prediction rather than the optical model one which gives larger (< 2 times) cross sections.

Measured differential cross sections for inelastic neutron scattering from the first excited states (0^+) of ^{12}C and ^{56}Fe and the second exited states (3^-) of ^{16}O and ^{40}Ca[5] are in fair agreement with the predictions of the exact finite-range DWBA and of JENDL-3, using the deformation parameters $\beta_L(0^+ \rightarrow J^\pi)$ given in Table 2. The values of $\beta_L(0^+ \rightarrow J^\pi)$ are consistent with those of other authors for ^{12}C[11], ^{40}Ca[9] and ^{56}Fe[10]. The present data on $^{12}C(n,n')^{12}C^*(1st)$ are expressed in terms of Legendre polynomials $P_l(z)$ as follows[7]:

$$d\sigma(\theta_{CM})/d\Omega = 17.20 + 15.34P_1(z) + 25.40P_2(z), \text{ (mb/sr)} \qquad (1)$$

where $z = \cos\theta_{CM}$. Eq. 1 gives larger (< 2 times) cross sections than JENDL-3 at $\theta_{CM} < 40^{o}$. The data on $^{16}O(n,n')^{16}O^*(2nd)$ agree with JENDL-3 rather than DWBA, while the data on $^{40}Ca(n,n')^{40}Ca^*(2nd)$ do with DWBA rather than JENDL-3. The data on $^{56}Fe(n,n')^{56}Fe^*(1st)$ agree with both predictions.

The details of discrepancies mentioned above are investigating experimentally (in statistics) and theoretically (in parameters) at present.

References:

1) S. Shirato, S. Shibuya, Y. Ando, T. Kokubu and K. Hata: Nucl. Instr. Methods A278, 477 (1989).

2) R. J. Kurz: UCRL-11339 (1964) unpublished.

3) K. Hata, S. Shirato and Y. Ando: JAERI-memo 02-308 (1990).

4) K. Hata, S. Shirato and Y. Ando: JAERI-M 91-032, 328 (1991).

5) S. Shirato, T. Nishio and Y. Ando: Report (in Japanese) written by summarizing the effort implemented under the Research-in-Trust in 1991 - 1992 fiscal years from the Japan Atomic Energy Research Institute (JAERI); T. Nishio, S. Shirato and Y. Ando: in proceedings of the 1993 symposium on nuclear data (JAERI).

6) T. Fukahori and I. Tazaki, JAERI-memo 62-453 (1988).

7) K. Gul, M. Anwar, M. Ahmad, S. M. Saleem and N. A. Khan: Phys. Rev. C24, 2458 (1981).

8) J. S. Petler, M. S. Islam, R. W. Finlay and F. S. Dietrich: Phys. Rev. C32, 673 (1985).

9) G. M. Honore et al.: Phys. Rev. C3, 1129 (1986).

10) M. Hyakutake et al.: J. Phys. Soc. Japan 38, 606 (1975).

11) N. Olsson, B. Trostell and E. Ramstrom: Nucl. Phys. A496, 505 (1989).

Table 1 Specifications of the scatterer samples used in this experiment.

SCATTERER	WEIGHT* (g)	SIZE (cm)	PURITY (%)	FORM	VESSEL
^{nat}C	34.840	3.0ϕ x 3.0	99.9	SOLID	NON
CH_2	19.597	3.0ϕ x 3.0	99.9	SOLID	NON
^{nat}Fe	166.020	3.0ϕ x 3.0	99.9	SOLID	NON
^{nat}Ca	92.440	4.8ϕ x 6.0	99.5	GRAIN	CH_2**
^{nat}CaO	74.618	4.8ϕ x 6.0	99.9	POWDER	CH_2**

* Weight error of ± 0.005 g.

** 13.891 g (the outer size of 5.0 cm ϕ x 6.6 cm).

Table 2 Optical potential [U(r)] and deformation [$\beta_L(0^+\to J^\pi)$] parameters at 14.2 MeV. [$U_C(r) = 0$]

	V (MeV)	W_s* (MeV)	V_{so}** (MeV)	r_0 (fm)	r_0' (fm)	a (fm)	b (fm)	c_{so} (fm)	$\beta_L(0^+\to J^\pi)$	Ref.
^{12}C	Entrance channel (g.s., 0^+):									
	46.5	8.88	4.39	1.28	0.86	0.39	0.39	0.39		7)
	Exit channel (1st e.s., 2^+):									
	55.0	2.60	4.39	1.20	0.86	0.39	0.39	0.39	0.65(2^+)	
^{16}O	Entrance channel (g.s., 0^+):									
	49.32	4.35	4.31	1.15	1.38	0.646	0.473	0.45		8)
	Exit channel (2nd e.s., 3^-):									
	51.13	2.46	4.31	1.15	1.38	0.646	0.473	0.45	0.33(3^-)	
^{40}Ca	Entrance channel (g.s., 0^+):									
	46.52	6.26	5.08	1.25	1.25	0.65	0.58	0.50		9)
	Exit channel (2nd e.s., 3^-):									
	47.5	5.52	5.22	1.25	1.25	0.65	0.58	0.50	0.33(3^-)	
^{56}Fe	Entrance channel (g.s., 0^+):									
	43.55	10.24	6.00	1.25	1.242	0.673	0.47	0.673		10)
	Exit channel (1st e.s., 2^+):									
	43.55	10.24	6.00	1.25	1.242	0.673	0.47	0.673	0.23(2^+)	

The potential form is given by the following expression:

$$U(r) = U_C(r)-V/(1+f_V(r))-i[W_V/(1+f_W(r))+W_G/f_G(r)+4W_S f_W(r)/(1+f_W(r))^2]$$
$$-(\hbar/m_\pi c)^2 V_{so}(1/rc_{so})f_{so}(r)(1+f_{so}(r))^{-2}\underline{L}*\underline{S},$$

where $f_V(r) = \exp[(r-r_0A^{1/3})/a]$, $f_W(r) = \exp[(r-r_0'A^{1/3})/b]$,

$f_{so}(r)= \exp[(r-r_0A^{1/3})/c_{so}]$, $f_G(r) = \exp[(r-r_0'A^{1/3})^2/b^2]$.

* Note $W_s = V_I/4$ using the DWUCK4 notation.

** Note $V_{so} = V_{LS}/4$ in the $\underline{l}$-$\underline{\sigma}$ form using the DWUCK4 notation.

VIII. TOHOKU UNIVERSITY

A. Department of Nuclear Engineering

VIII-A-1 Measurements of Double-differential Neutron Emission Cross Sections of Mo, Ta and W

S.Matsuyama, T.Ohkubo, M.Baba, T.Ito, T.Akiyama, N.Ito and N.Hirakawa

A paper on this subject was published in JAERI-M 93-046 (1993) p.345-355 with the following abstract:

Double-differential neutron emission cross sections (DDXs) of Mo, Ta and W have been measured for 14 MeV incident neutrons using Tohoku University Dynamitron time-of-flight spectrometer.

DDX data were obtained at 8-10 angles for secondary neutron energy range down to 0.7 MeV. Furthermore we deduced angle-integrated spectra and angular distributions of continuum neutrons.

The present results of DDXs for these nuclides are in good agreement with other experimental data. On the other hand, they show discrepancies from the data derived from the evaluated nuclear data of JENDL-3 and ENDF/B-VI. The angular distribution of continuum neutrons are compared with the systematics proposed by Kalbach-Mann and Kalbach.

VIII-A-2 Measurement of Double-differential α-particle Production Cross Sections of Fe and Ni Using Gridded Ionization Chamber

N.Ito, M.Baba, S.Matsuyama, I.Matsuyama, N.Hirakawa
S.Chiba*, T.Fukahori*, M.Mizumoto* and K.Hasegawa*

A paper on this subject was published in JAERI-M 93-046 (1993) p.334-344 with the following abstract:

Double-differential α-particle production cross sections of Fe and Ni were measured for neutron energy region between 4 and 14 MeV using a gridded ionization chamber. The method applied in this work enables us to measure the double-differential cross sections at various incident neutron energies because of the high efficiency and background suppression capability of the gridded ionization chamber. The double-differential cross sections, the energy-differential cross sections and the excitation functions were obtained for (n,xα) reactions of Fe and Ni, and are compared with the previous experiments and evaluated data.

---

* Japan Atomic Energy Research Institute, Tokai Research Establishment

VIII-A-3

Production of 7.7 and 11.5 MeV Neutrons by the $^{14,15}N(d,n)$ Reactions

M.Baba, N.Ito, I.Matsuyama, S.Matsuyama and N.Hirakawa

Monoenergetic neutrons in the 7-13 MeV region which are indispensable for measurements of fusion related nuclear data are usually obtained by the D(d,n) and T(p,n) reactions. These reactions are very useful owing to large cross sections and few spurious components. However, they are not applicable with a low energy accelerator in a few MeV range like our 4.5 MV Dynamitron electrostatic accelerator.

The $^{14}N(d,n)^{15}O$ (Q=9.885 MeV) and $^{15}N(d,n)^{16}O$ (Q=5.12 MeV) reactions are promising as the source of 7-12 MeV neutrons in our facility because of large positive Q-values[1]. While these reactions are not monoenergetic sources, the first-excited state is well separated from the ground-state in both ^{15}O and ^{16}O (5.27 and 6.06 MeV, respectively). Therefore, they will be useful for studies of thresholds reactions and neutron scattering from low lying levels although the reaction cross sections are much smaller than the D(d,n) and T(p,n) reactions[1].

We have studied the emission spectra and intensities of neutrons produced by the $^{14,15}N(d,n)$ reactions to exploit the applicability as the source of 7-12 MeV neutrons in the 4.5 MV Dynamitron accelerator. The emission spectra were measured using the time-of-flight technique as a function of deuteron energy to evaluate the excitation function and relative intensity of the neutrons to the excited states. We employed a gas cell filled with elemental nitrogen or enriched ^{15}N (99.9% ^{15}N) for a neutron production target.

The measurement indicated that neutrons of 11.5 MeV and 7.7 MeV are obtained by the $^{14}N(d,n)$ and $^{15}N(d,n)$ reactions, respectively, at the deuteron energy with cross section maximum. The energy spread was around 400 keV for the gas pressure of about 80 kPa, and these neutrons were separated from contaminant ones as expected with no serious backgrounds. Test experiments applying the sources were carried out on (n,α) reactions using a gridded ionization chamber[2] and on neutron scattering. Both results revealed the applicability of the sources for nuclear cross section studies in both energy points. In the case of (n,α) reaction, the neutrons from the excited states do not introduce serious interference because of high "threshold" energy of (n,α) reactions except for light elements. For efficient use of the sources, however, the neutron intensity should be increased substantially by developing a target withstanding higher beam current.

References:

1) J.L.Weil and K.W.Jones: Phys. Rev., 112(6) (1958) 1975
2) M.Baba et al.: Proc.Int.Conf. on Nuclear Data for Science and Technology, Jülich 1991, p.477

B. Cyclotron and Radioisotope Center

VIII-B-1 Measurement of $^{137}Cs(\gamma,n)$ Cross Section by Nuclear Recoil Separation Method

Akira Yamadera, Yoshitomo Uno, Takashi Nakamura,
Ichiro Fujiwara*, Seiichi Shibata** and Takeshi Kase***

A paper on this subject was published in Nucl. Instrum. Methods in Phys. Research, A329, 188 (1993) with the following abstract:

The average cross section of $^{137}Cs(\gamma,n)$ reaction in the giant dipole resonance region was measured by using the nuclear recoil separation method. Thin ^{137}Cs targets on aluminum supports were prepared by evaporating a $^{137}CsCl$ solution which was diluted with certain amounts of natural $^{133}CsCl$ in a vacum chamber. Six targets having different ^{137}Cs activities and ^{133}Cs carrier concentrations backed by aluminum catcher foils were irradiated in a vacuum cell with bremsstrahlung having maximum energy of 60 MeV and 45 MeV. The ^{136}Cs and ^{132}Cs activities, recoiled from the target foil by the (γ,n) reaction were measured with a pure Ge detector. The (γ,n) cross section ratios of $^{137}Cs(\gamma,n)^{136}Cs$ and $^{133}Cs(\gamma,n)^{132}Cs$ were 1.10±0.05 and 1.22±0.11 for 45 MeV and 60 MeV bremsstrahlung respectively, by using the internal standard method. The average cross sections of the $^{137}Cs(\gamma,n)^{136}Cs$ reaction could be estimated to be 135±8 mb/eq.q. and 157±15 mb/eq.q. for 45 MeV and 60 MeV bremsstrahlung respectively.

---

* Ottemon University

** University of Tokyo

*** Power Reactor and Nuclear Fuel Development Corporation

VIII-B-2

Measurement of Neutron Activation Cross Sections in the $^{7}Li(p,n)^{7}Be$ Monoenergetic Neutron Field for Neutron Energy Range of 15 MeV to 40 MeV.

Titik S. Soewarsono, Y. Uwamino* and T. Nakamura

I. Introduction

Neutron activation cross section data for neutron energy above 20 MeV are very scarce[1-3] and discrepant and no evaluated data files are currently available. In order to fulfill this data need for dosimetry, radiation safety and material damage studies, we have estimated neutron activation cross sections for fifteen isotopes of natural and enriched samples in the energy range of 15 to 40 MeV.

The intense neutron field for sample irradiation has ever been developed using the semi-monoenergetic neutrons produced by the $^{9}Be(p,n)^{9}B$ reaction[4,5]. The neutron spectrum was however rather broad monoenergetic peak, which required the unfolding technique to get the excitation functions. We therefore developed more monoenergetic neutron field produced by $^{7}Li(p,n)^{7}Be$ reaction[6]. This aimed to avoid the ambiguity coming from the unfolding method.

Samples were irradiated in the $^{7}Li(p,n)$ neutron field at the SF cyclotron of Institute for Nuclear Study (INS), while the neutron spectrum was measured with the TOF method at the AVF cyclotron of CYRIC, Tohoku University. The neutron fluence during irradiation at INS was obtained by connecting the yield of ^{7}Be produced in the target to the measured neutron spectrum at CYRIC via the angular-differential cross sections[7,8]. For these irradiations, two types of targets were employed, 2 mm thick of 99.98% enriched ^{7}Li target backed with 12 mm thick carbon, as a proton beam stopper, and the only 12 mm thick carbon target.

The cross sections at the peak neutron energy, E_{peak} were estimated by taking into account the low-energy component of neutron spectrum, as the following formula :

$$\sigma(E_{peak}) = \frac{A - \int_{E_{th}}^{E_1} \sigma(E)\,\Phi(E)\,dE}{N\,\Phi(E_{peak})} \qquad (1)$$

where A is the reaction rate, $\Phi(E)$ the neutron spectrum, $\sigma(E)$ the neutron cross section, E_{th} the threshold energy for neutron reaction, and E_1 the minimum energy at the peak of neutron spectrum.

II. Experiment

Neutron spectra produced from the two targets were measured with a liquid scintillation detector NE213 of 127 mm diam. x 127 mm long which was placed at about 12 m behind the target. The protons of 20, 25, 30, 35 and 40 MeV bombarded these two targets at 0 deg, and the angular distributions of produced neutrons were measured using the beam -swinger system from 0 to 125 deg.

The enriched samples of ^{24}Mg, ^{25}Mg, ^{28}Si, ^{29}Si, ^{54}Fe, ^{56}Fe, ^{63}Cu, ^{65}Cu, ^{64}Zn, and ^{66}Zn , and natural samples of ^{12}C, ^{23}Na, ^{27}Al, ^{55}Mn, and ^{197}Au were activated

by the $^{7}Li(p,n)$ neutrons produced by protons of 20, 25, 30, 35, and 40 MeV. The activities of irradiated samples were measured with the HP Ge detector. The gamma-ray peak counts were analyzed with the KEI-11EF[9] and corrected to the sum-coincidence effect and self-absorption effect[10].

III. Results

The neutron energy spectrum measured for 40 MeV proton bombardment is shown in Fig.1, for the two types of ^{7}Li+C and C targets. The dominant peak of $^{7}Li(p,n)^{7}Be$ at the neutron energy of 38 MeV comes from the ground state and the first excited state (0.429 MeV) that can not be separated due to 1.2 MeV energy loss in the target of 40 MeV proton energy. Smaller peak at 33 MeV neutron energy corresponds to the second excited state (4.57 MeV). The low-energy continuous spectrum corresponds to the higher energy state of ^{7}Be, and the $^{12}C(p,n)$ and $^{13}C(p,n)$ neutrons. The spectrum obtained from carbon backing shows the sharp decrease at neutron energy around 22 MeV, due to the Q-value of $^{12}C(p,n)$, -18.1 MeV.

As examples, Figures 2, 3 and 4 show the neutron activation cross sections for $^{12}C(n,2n)^{11}C$, $^{23}Na(n,2n)^{22}Na$ and $^{197}Au(n,2n)^{194}Au$ reactions, respectively. The present results of $^{12}C(n,2n)$ cross section show good agreement with the data obtained by Brill et al.[11], except for result at 38 MeV neutron energy. The same tendency is seen in Fig.3 for $^{23}Na(n,2n)$ cross section in the present data. The result of $^{197}Au(n,4n)^{194}Au$ cross section lies in between the data by Uwamino et al.[5], and calculated data by Greenwood[12].

References

1. McLane V. et al., BNL-NCS-17541 (1988).
2. Handbook on Nuclear Activation Data, Tech. Rep. Series No. 273, IAEA (1987).
3. ENDF B-VI, National Cross Section Center, BNL (1990).
4. Uwamino Y. et al., Nucl. Sci. and Eng. 111 (1992) 391.
5. Uwamino Y. et al., Nucl. Inst. and Meth. A271 (1988) 546.
6. Soewarsono T.S. et al., JAERI-M 92-027 (1992) 354.
7. Schery S.D. et al., Nucl. Inst. and Meth. 147 (1977) 399.
8. Orihara H. et al, Nucl. Inst. and Meth. A257 (1987) 189.
9. Komura K., Inst. for Nuclear Study Report INS-TCH-7, Univ. of Tokyo, 1972.
10. Nakamura T., Nucl. Inst. and Meth. 105 (1972) 77.
11. Brill O.D. et al, DOK 136, Inst. Atom. En. I.V. Kurchatova, Moscow (1961) 55.
12. Greenwood L.R., ANL/FPP/TM-115, Argonne Nat. Lab., 1978.

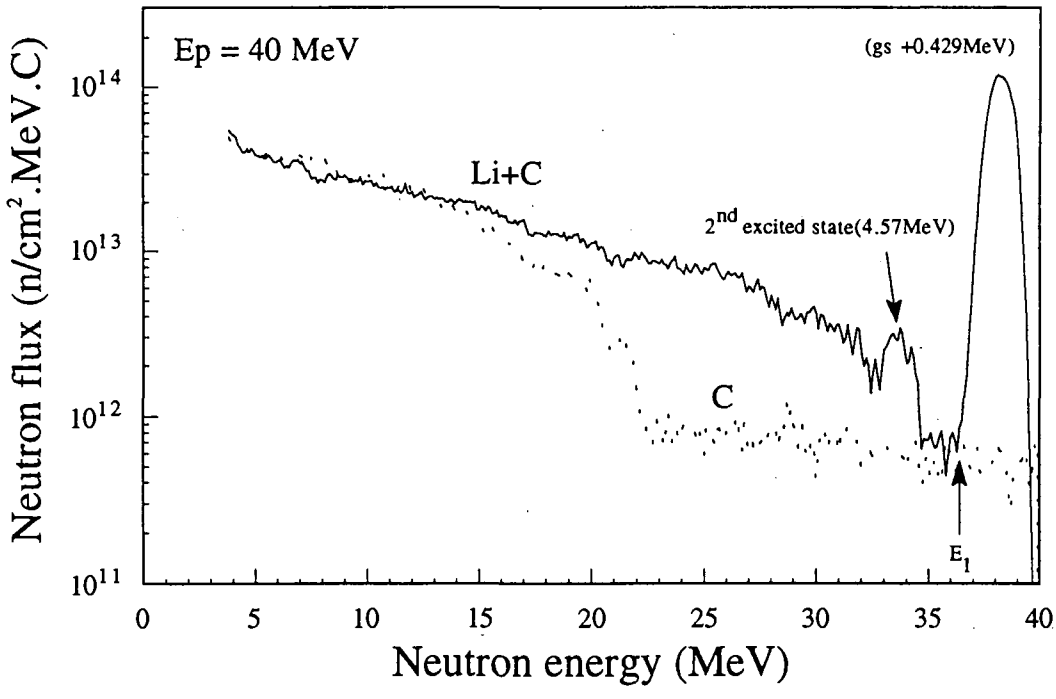

Fig.1 Normalized neutron energy spectra of Li backed with carbon and the only carbon target for proton energy of 40 MeV.

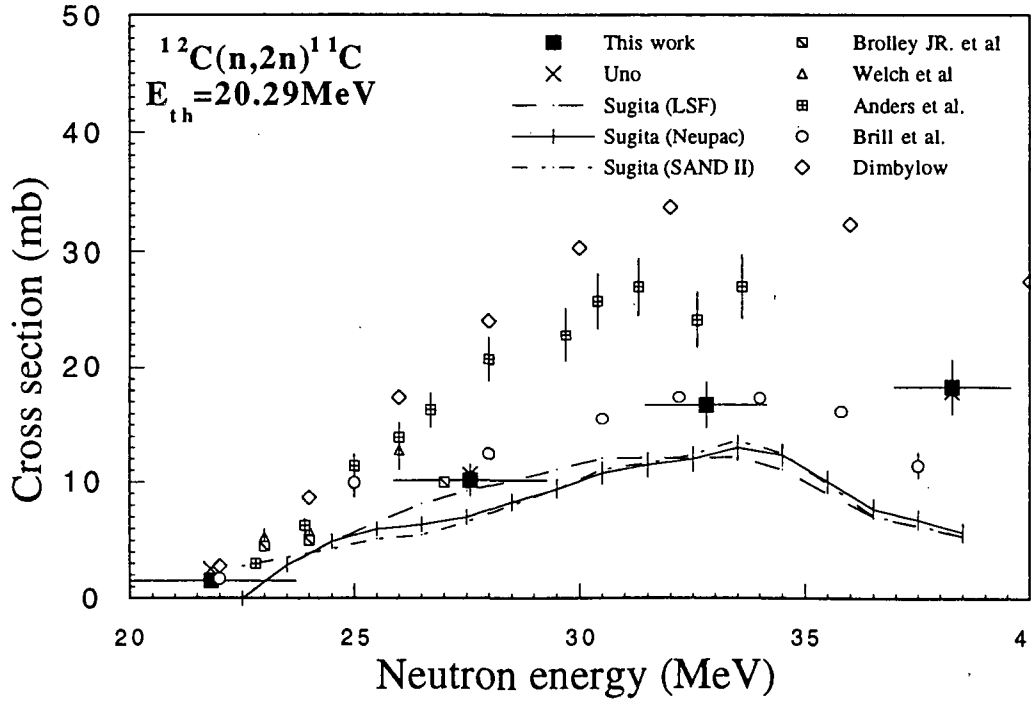

Fig. 2 Neutron activation cross sections of $^{12}C(n,2n)^{11}C$

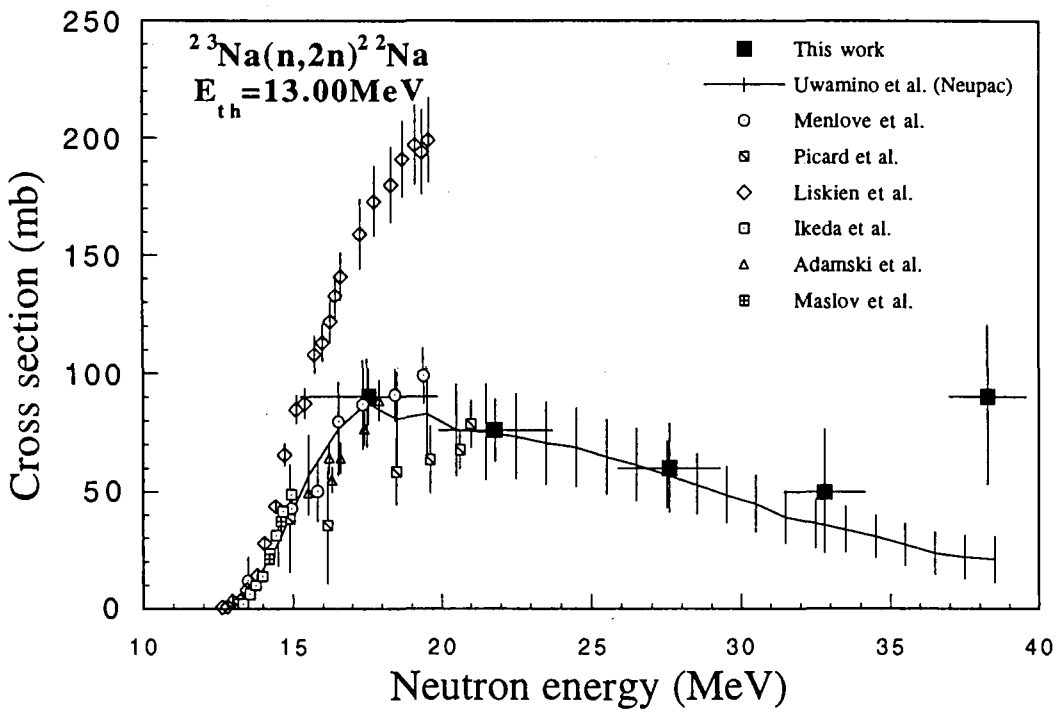

Fig.3 Neutron activation cross sections of $^{23}Na(n,2n)^{22}Na$

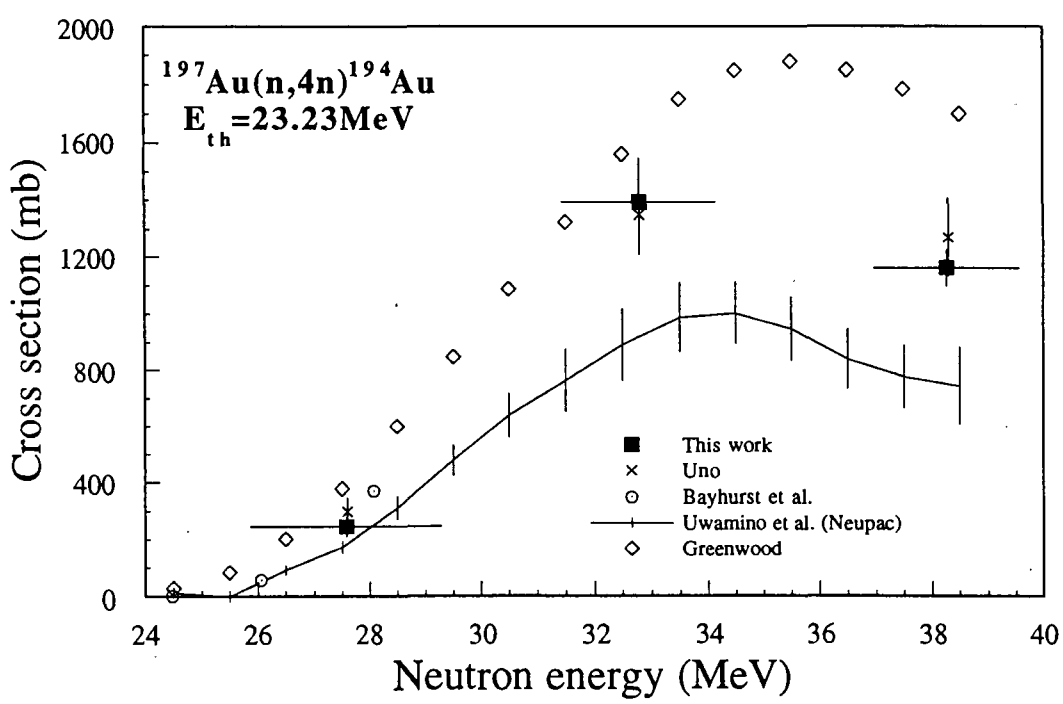

Fig.4 Neutron activation cross sections of $^{197}Au(n,2n)^{194}Au$.

C. Laboratory of Nuclear Science

VIII-C-1 The reactions ^{6}Li(e,e'p) and ^{6}Li(e,e't)

T. Hotta, T. Tamae, T. Miura, H. Miyase*, M. Sugawara, T. Tadokoro,
A. Takahashi, E. Tanaka and H. Tsubota*

In order to investigate the properties of excited states, the cluster structure and the electrodisintegration reaction mechanism in ^{6}Li, ^{6}Li(e,e'p) and ^{6}Li(e,e't) cross sections have been measured using a 134MeV continuous electron beam at energy transfer between 27MeV and 37MeV and momentum transfer of 61MeV/c on an average. Scattered electrons were measured at 26° with a magnetic spectrometer. Charged particles emitted from the target were detected with Si-solid-state detectors arranged out of the scattering plane ($\phi_X = -45°$ and $\phi_X = -135°$). Good particle identification was achieved by the ΔE-E method. Events corresponding to different final states were identified from missing-energy spectra.

Measured angular distributions fitted with Legendre polynomials for the (e,e'p) reactions are shown in Fig.1. No remarkable difference is seen between two angular distributions corresponding to protons emitted from the p-shell (E_m= 2-8MeV) and s-shell (E_m= 20-23MeV). There exists a large component of $P_3(\cos\theta_X)$ in both cases. The result of Legendre fitting suggests that higher multipoles than E1 contribute to this reaction. Existence of a longitudinal-transverse interference term which is much larger than the PWIA prediction is also a common feature of these reactions. We can see the difference between the p-shell and s-shell in the excitation functions shown in Fig.2.

In the (e,e't) reaction, the angular distribution and the excitation function have been measured for events corresponding to the two-body t-^{3}He final state. The fitting result of the angular distribution (Fig.3) shows a strong E1 contribution to this reaction. There is little $P_3(\cos\theta_X)$ component in the polynomials. The interference between E1 and C0 or M1 components makes the angular distribution asymmetric. It is expected that the multipolarity of this reaction is sensitive to different cluster model description of the ground state of ^{6}Li. We have carried out ^{6}Li(e,e't) measurement at different energy and momentum transfer regions. Data analysis is now underway.

---

*Department of Physics, Tohoku University

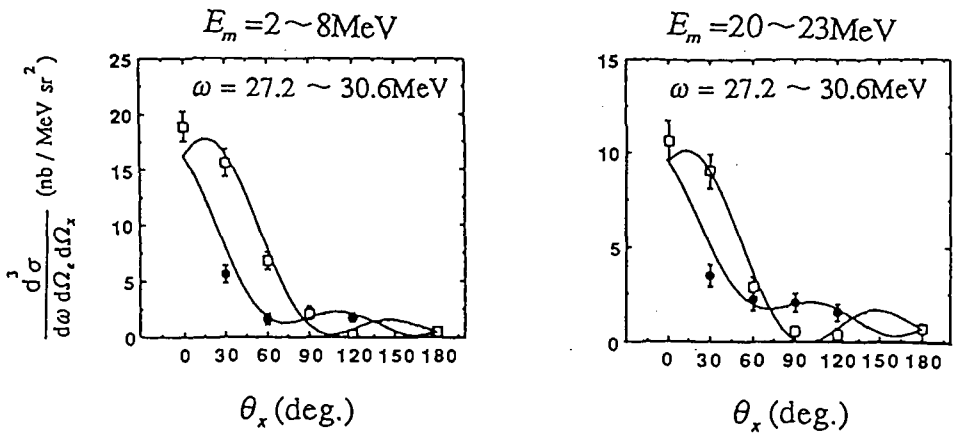

Fig.1 Angular distributions for the ^{6}Li(e,e'p) reactions. Solid circles and open squares represent cross sections at ϕ_X=−45°, and ϕ_X=−135° respectively. Data are fitted with Legendre polynomials.

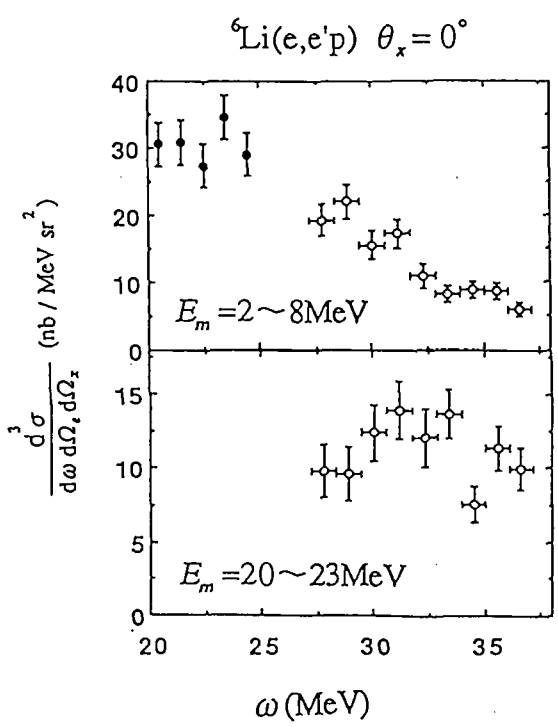

Fig.2 Excitation functions for the ^{6}Li(e,e'p) reactions. Solid circles are results of previous measurement.

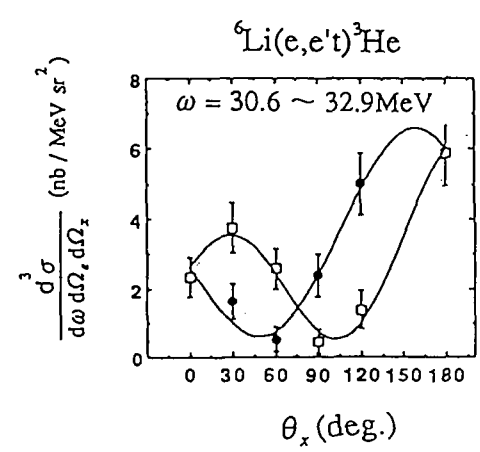

Fig.3 Angular distribution for the ^{6}Li(e,e't)^{3}He reaction, same as Fig.1.

VIII-C-2

Out of Plane Measurement for the $^{12}C(e,e'n_0)^{11}C$ reaction in the GR region

M. Oikawa, T. Saito, K. Takahisa*, Y. Suga, T. Tohei**, T. Nakagawa**,
K. Abe*** and H.Ueno****

The out-of plane measurement for the $^{12}C(e,e'n_0)^{11}C$ reaction has been carried out at various excitation energies from 22 to 26 MeV and momentum transfer of 0.412 fm^{-1} (at the excitation energy of 22.5 MeV). Decay neutrons were detected by eleven NE-213 liquid-scintillator detectors placed at following combinations of the polar angle q and the azimuthal angle ϕ: (0°,180°), (30°,180°), (60°,180°), (90°,180°), (150°,180°), (180°,180°), (30°,135°), (60°,135°), (90°,135°) and (30°,90°) .

The angular distributions in this experiment (Fig.1) are asymmetric about q = 90°. Especially the angular distribution at the excitation energy 22.5 MeV has a far larger peak at the forward angle of q than at the backward angle and is very different from the result of Cavinato's calculation[1)]. The parameters obtained by fitting the angular distributions in this experiment were converted to those in photonuclear reaction so that we could compare those with the parameters in $^{12}C(\gamma, n)^{11}C$ experiment[2)](Fig.2). We can find a significant difference in the a_1 parameter at the excitation energy 22.5 MeV. This shows that, in the $^{12}C(e,e'n_0)^{11}C$ reaction, the interference between E1 and other components appears strongly at the excitation energy 22.5 MeV.

From the ϕ dependence of the differential cross section, the interference and non-interference terms were separated (Table.1). From the present work it was confirmed that the strength of the interference and non-interference terms could be evaluated each other by out-of-plane measurement of the (e,e'n) reaction in the GR region. However, quantitative argument will require a experiment with higher statistical precision.

References:

1) M. Cavinato et al. : Nucl. Phys. A444, 13 (1985).
2) J. A. Rawlins et al. : Nucl. Phys. A122, 128 (1968).

*Present Address: RCNP, Osaka University
**Department of Physics, Tohoku University
***Department of Nuclear Engineering, Tohoku University
****Department of Physics, Yamagata University

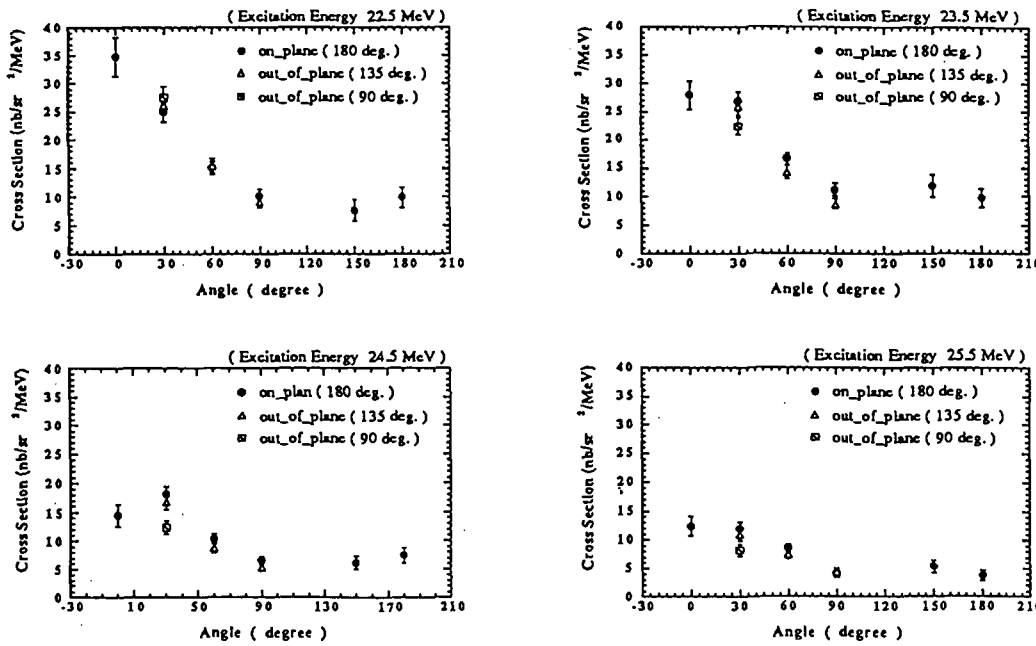

Fig.1 Angular distributions of the differential cross section for the $^{12}C(e,e'n_0)^{11}C$ reaction.

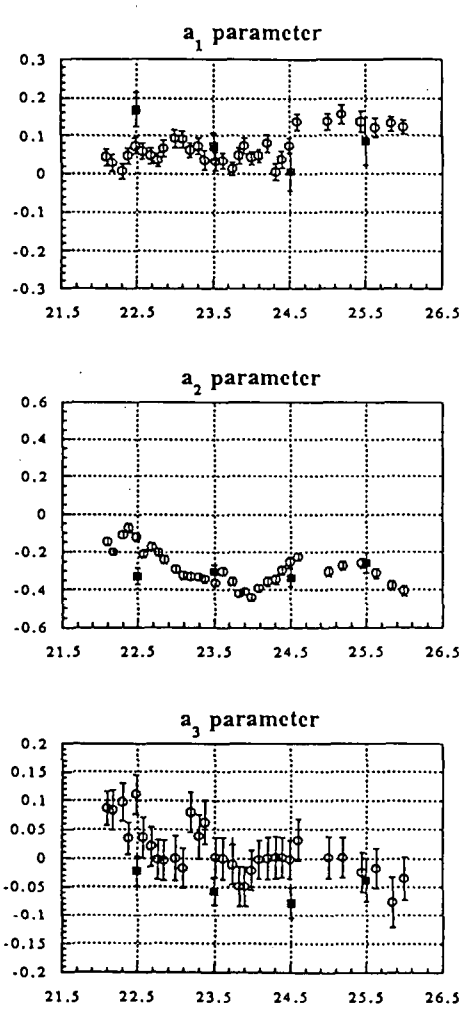

Table.1 Interference (LT and TT) and non-interference (L+T) terms at the each excitation energies. L+T term represents the sum of longitudinal and transverse terms, LT term longitudinal-transverse interference term and TT term transverse-transverse interference term.

Excitation Energy (MeV)	L+T term (nb/sr²/MeV)	LT term (nb/sr²/MeV)	TT term (nb/sr²/MeV)
22.5	26.3 (±6.3)	0.10 (±11)	1.25 (±5.3)
23.5	21.7 (±5.6)	6.09 (±9.7)	0.85 (±5.1)
24.5	11.4 (±4.5)	7.68 (±7.8)	0.99 (±4.1)
25.5	7.99 (±3.6)	4.22 (±6.3)	0.27 (±3.3)

Fig.2 Fitting parameters in photonuclear reaction. Closed squares represent parameters converted from fitting parameters of the angular distributions in the present work and open circles fitting parameters of the angular distributions in $^{12}C(\gamma,n)^{11}C$ experiment[2].

VIII-C-3 Measurement of $^{31}P(\gamma,p)$ Reaction at E_γ= 55 - 88 MeV

H. Matsuyama*, H. Itoh, S. Ito, O. Konno, K. Maeda**, T. Sasaki***, T. Suda**
T. Terasawa and M. N. Thompson****

Photoprotons from the $^{31}P(\gamma,p)$ reaction were measured at the tagged photon energies ranging from 55 to 88 MeV. The cross sections were obtained at proton emission angles of 30°, 45°, 60°, 75° and 90°. The proton spectrum was fitted by a sum of six Gaussians centered at E_x= 0.0 (0^+), 2.2 (2^+), 5.2 (3^+), 7.6 (2^+), 10.6 and 13.6 MeV states in ^{30}Si residual nucleus. Since the proton energy resolution was about 3 MeV, these partitions must contain contributions from near-by levels. In the $^{31}P(e,e'p)$ experiment[1] performed recently at NIKHEF, populations to levels at 3.5, 6.8, 8.1, 9.6, 10.2 and 11.2 MeV were also observed separately.

The momentum distributions of protons inside the nucleus were deduced from the data by assuming a direct proton knockout process[2] of the (γ,p) reaction. Fig.1 shows comparisons of the momentum distributions deduced from the (γ,p) data with the DWIA calculations in which the bound state wave functions and spectroscopic factors were employed from the (e,e'p) results[1].

As one can see from the figure, the (γ,p) results exceed the DWIA results based on the (e,e'p) by 10 to 100 times, except for the ground state transition. The differences might be attributed to a possible presence of multi-nucleon processes in the (γ,p) reaction.

References:

1) J. Wesseliny et al.: Nucl. Phys. A545, 519 (1992).
2) J. Londergan and G. Nixon: Phys. Rev. C 19, 998 (1979).

* Present Address: Toshiba Corporation
** Department of Physics, Tohoku University
*** Present Address: Fuji Electric Co., Ltd.
**** School of Physics, The University of Melbourne

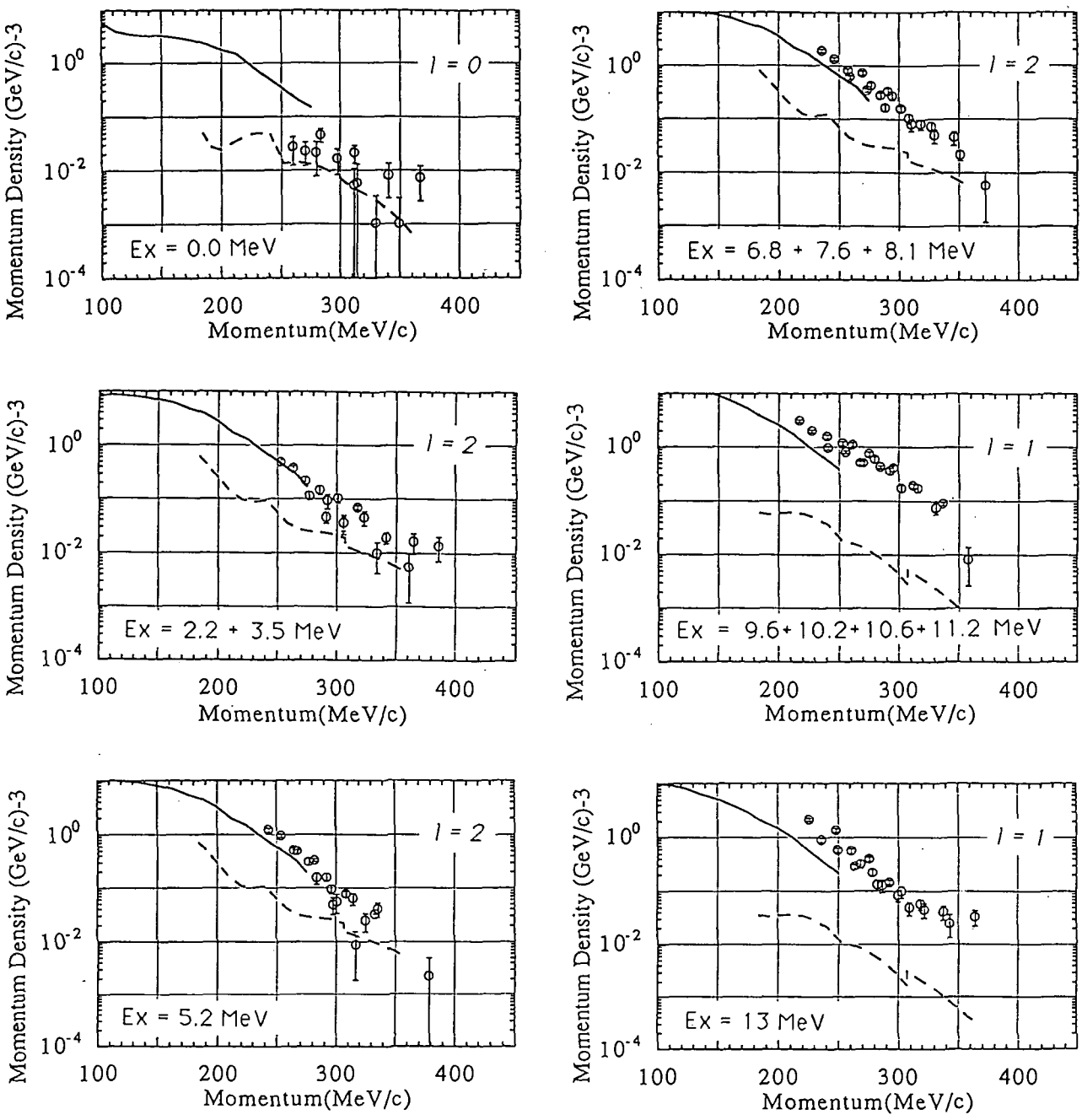

Fig.1 The momentum distributions of protons in ^{30}Si deduced from the $^{31}P(\gamma,p)$ experiment. Also shown are the (e,e'p) results[1)](solid line), and its DWIA extrapolations to the (γ,p) experimental kinematics (dashed line).

VIII-C-4 Large Volume Liquid Scintillator Neutron Detector

S. Ito, O. Konno, M. Takeya*, T. Terasawa, K. Maeda**, T. Suda** and T. Fukuda***

A large volume liquid scintillator (13.3 *l* of NE213) neutron detector made of a long cylindrical aluminum tube has been developed (Fig.1). The difficulties in light collection have been overcome by employing an aluminized plastic film (TS-100 Toyo Metalizing Co.) having more than 90% reflection factor as the mirror reflector inside the tube.

The absolute neutron detection efficiencies of the detector were measured using the neutron beam provided by the Cyclotron and Radioisotope Center of Tohoku University. The results are shown in Fig.2. The performances of the time resolution and the n-γ discrimination were checked by the photoneutron measurement of the $^{13}C(\gamma,n)$ reaction using the tagged photon facility of the Laboratory of Nuclear Science. The detector was placed at 2.5 m apart from the target. The time resolution of 0.7 ns (FWHM) was obtained from the prompt γ-ray peak in the TOF spectrum. The PSD time distributions for the two photomultipliers are plotted in Fig.3. A good n-γ separation of the order of 10^3 γ-rejection rate has been achieved.

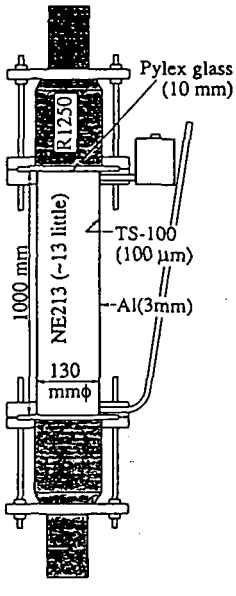

Fig.1 Out-look.

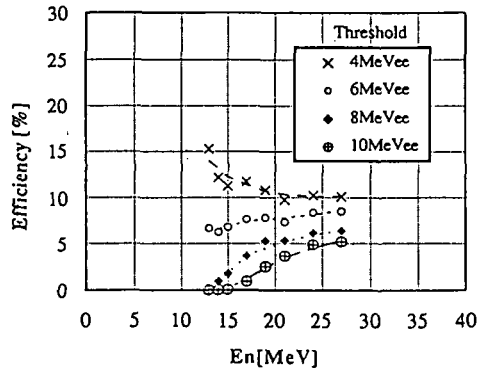

Fig.2 Neutron detection efficiencies.

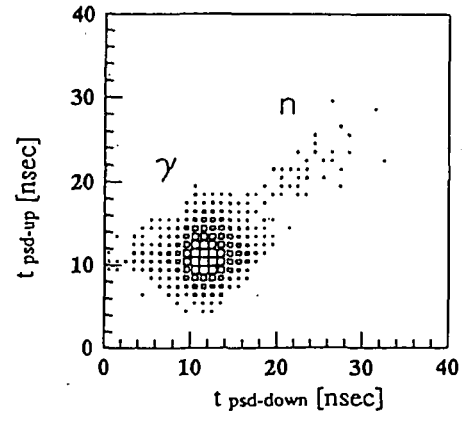

Fig.3 PSD time distributions.

* Present Address: Alps Electric Co., Ltd.
** Department of Physics, Tohoku University
*** Institute for Nuclear Study, University of Tokyo

VIII-C-5 New Beam Line for Parasitic Experiment

H. Itoh, S. Ito, O. Konno, M. Muto, M. Oikawa, T. Saito, Y. Suga, M.Sugawara
T. Tamae and T. Terasawa

The construction of a new beam transport system connecting the two experimental hall in the Laboratory of Nuclear Science has been completed (Fig. 1). The feasibility of the beam quality for parasitic tagged photon experiments at the 1st experimental hall has been examined by transporting a 130 MeV continuous electron beam from the pulsed beam stretcher (SSTR) in the 2nd experimental hall. A photon tagging spectrometer with Au radiator of 10^{-3} r.l. thick was placed at the end of the beam line. The results are as follows.

electron beam intensity : several nA (SSTR : 100 nA)
electron beam emittance : 1 mm.mrad (SSTR : 20 mm.mrad)
duty cycle : 50 % (SSTR : 80 %)
spurious electron rates : 0.1 - 0.3 % (2nd hall : 3 - 10 %)
tagging efficiency : 60 %

Actual measurements of $^{12}C(e,e')$ and $^{12}C(\gamma,p)$ have been performed at the 2nd and 1st hall, respectively, using the same electron beam from the SSTR. Good results have been obtained. The new beam line is concluded as feasible for the parasitic tagged photon experiment.

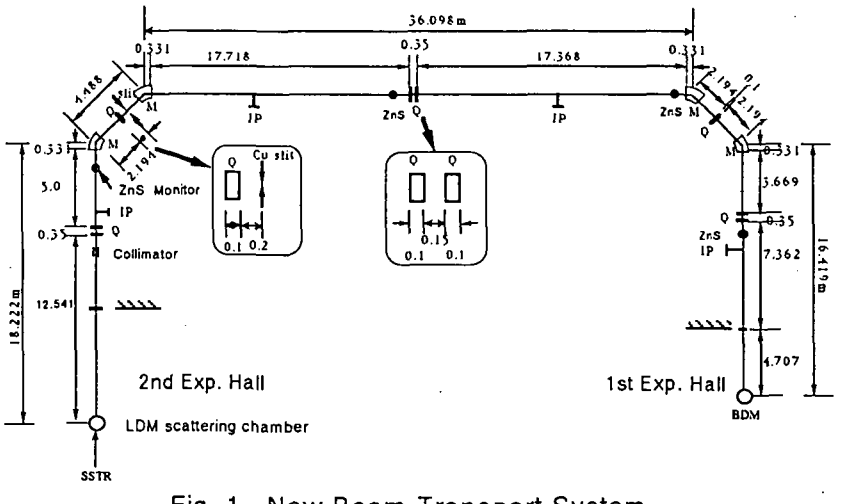

Fig. 1 New Beam Transport System

IX. Tokyo Institute of Technology

A. Research Laboratory for Nuclear Reactor

IX-A-1

Electromagnetic Transitions from Broad Neutron Resonance in Nuclei with A < 40 and Resonance Structure

H.Kitazawa and M.Igashira

For the last decade we have observed primary electromagnetic transitions from broad spd-wave neutron resonances in p-shell (^{9}Be, ^{13}C, ^{14}N, ^{16}O) and sd-shell (^{19}F, ^{24}Mg, ^{28}Si, ^{32}S) nuclei, in expectation that those resonances would possess a simple configuration and therefore the resonance structure would be revealed through the observation of a well-known electromagnetic interaction with the nuclei. As a consequence we found many single-particle E1 transitions from resonances in the even-even[1-3] and even-odd[4] nuclei. In those transitions, the s→p and p→s transitions can be satisfactorily explained by the valence-capture model of Lane and Mughabghab, while the p→d and d→p transitions are considerably retarded due to coupling between the single-particle transitions and the giant E1 resonance excitation in the target nuclei. Moreover, the valence-capture model was found to meet with little success for E1 transitions from broad resonances in the odd-even and odd-odd nuclei.[5] The disagreement with model predictions might be due to an essential participation of the p-n correlation between the incident neutron and the extra (unpaired) proton in the target nucleus. Certain evidence was also found for E1 transitions to show the 2^+ and 3^- one-phonon core excitation in p-wave resonances in ^{28}Si and ^{32}S[6,7] and the 2^+ and 4^+ rotational core excitation in p-wave resonances in ^{24}Mg.[1] In the transitions from s-wave resonances in the even-even nuclei, strong M1 transitions to the final states with single-particle character have been observed. This enhancement of M1 transitions would result from the excitation of collective isovector M1 states in the core nucleus.[3]

A paper on this subject will be submitted to the International Symposium on Capture Gamma-Ray Spectroscopy and Related Topics, Fribourg (1993).

References:

1) T.Uchiyama, M.Igashira, and H.Kitazawa: Phys. Rev. **C41**, 862, (1990).
2) M.Igashira, H.Kitazawa, and K.Takaura: Nucl. Phys. **A536**, 285, (1992).

3) H.Kitazawa, M.Igashira, M.Shimizu, K.Muto, T.Oda, Y.Achiha, Y.-H.Lee, and N.Mukai: Phys. Rev. **C46**, 2364, (1992).
4) S.Raman, M.Igashira, Y.Dozono, H.Kitazawa M.Mizumoto, and J.E.Lynn: Phys, Rev, **C41**, 458, (1990).
5) M.Igashira, H.Kitazawa, S.Kitamura, H.Anze, and M.Horiguchi: Proc. Int. Conf. on Capture Gamma-Ray Spectroscopy, Pacific Grove, California, 1990 (AIP Conference Proceedings No.**238**, New York, 1991) p.624.
6) H.Kitazawa, M.Ohgo, T.Uchiyama, and M.Igashira: Nucl. Phys. **A464**, 61, (1987).
7) H.Kitazawa, M.Igashira, Y.Achiha, N.Mukai, F.Uesawa, T.Andoh, and S.Shibata: Nucl. Phys. **A536**, 109, (1992).